8-2000

Characterization of chloroplast transit peptides and the major stromal Hsp70, CSS1 : implications for an ATP-dependent chloroplast protein import molecular motor

Robert Alvin Ivey

To the Graduate Council:

I am submitting herewith a dissertation written by Robert Alvin Ivey entitled "Characterization of chloroplast transit peptides and the major stromal Hsp70, CSS1 : implications for an ATP-dependent chloroplast protein import molecular motor." I have examined the final electronic copy of this dissertation for form and content and recommend that it be accepted in partial fulfillment of the requirements for the degree of Doctor of Philosophy, with a major in Biochemistry and Cellular and Molecular Biology.

Barry D. Bruce, Major Professor

We have read this dissertation and recommend its acceptance:

Jeffrey Becker, Beth Mullin, Gary Stacey, Wesley Wicks

Accepted for the Council:

Carolyn R. Hodges

Vice Provost and Dean of the Graduate School

(Original signatures are on file with official student records.)

To the Graduate Council:

I am submitting herewith a dissertation written by Robert A. Ivey, III, entitled "Characterization of Chloroplast Transit Peptides and the Major Stromal Hsp70, CSS1: Implications for an ATP-dependent Molecular Motor Mechanism of Chloroplast Protein Import." I have examined the final copy of this dissertation for form and content and recommend that it be accepted in partial fulfillment of the requirements for the Degree of Doctorate of Philosophy, with a major in Biochemistry and Cellular and Molecular Biology.

Barry D. Bruce, Major Professor

We have read this dissertation
and recommend its acceptance:

Jeffrey Becker

Beth Mullin

Beth Mullin

Gary Stacey

Wesley Wicks

Characterization of Chloroplast Transit Peptides and the Major Stromal Hsp70, CSS1: Implications For an ATP-dependent Chloroplast Protein Import Molecular Motor

A Dissertation

Presented for the

Doctorate of Philosophy

Degree

The University of Tennessee, Knoxville

Robert Alvin Ivey, III

August 2000

This dissertation is dedicated

to my wife

Shannon Rebecca Mellichamp Ivey, DVM

and

to my parents

Robert Alvin Ivey, Jr.

and

Rachel Cheryl Steele Ivey

ACKNOWLEDGMENTS

I would like to thank my advisor, Dr. Barry Bruce, for the good he has done in the difficult task of training me as a scientist. It is my fervent wish that he look back on my graduate tenure and appreciate the good that we did together. I would also like to thank those members of my laboratory and department who have remained loyal to me. Those people have supported me when I needed it most and has challenged me to read, learn, do, and even be more than I am. I consider each of them a friend for life and am proud to have shared my graduate school experience with them.

I would also like to thank my advisory committee–Drs. Jeffrey Becker, Beth Mullin, Gary Stacey, and Pete Wicks--for their time, efforts, and patience while working with me. I would especially like to acknowledge a recently departed dear friend and mentor, Dr. Jorge Churchich. His tireless efforts in scientific excellence and high academic standards will remain an inspiration to me. Additional thanks go to my undergraduate mentor, Dr. Jessup Shively, of Clemson University, who showed by example how to be a scientist, and who has probably forgotten more about being one than I will ever learn.

I would like to thank the organizations who have funded my research and travels: the National Science Foundation, the American Society of Plant Physiologists, StressGen Biotechnologies, Inc., the University of Tennesse, Knoxville, the Science Alliance, and my own Department of Biochemistry.

Finally, I am indebted beyond measure to my wife Shannon for her love, companionship, and support, and for bringing such happiness to my life.

ABSTRACT

Chloroplast protein import is a relatively poorly understood protein trafficking system. In other protein import systems, the translocation "machinery" has been identified and well studied, including the mechanism by which proteins are unidirectionally transported across the importing membrane. In the chloroplast, no such "molecular motor" is acknowledged. The work described in this dissertation is a preliminary attempt to assign that role to the major stromal Hsp70, CSS1. We have shown, through a variety of *in vivo* and *in vitro* techniques, interaction between a chloroplast transit peptide and two members of the Hsp70 class of molecular chaperones, DnaK and CSS1. We have also mapped this specific interaction to the N-terminus of one transit peptide and generallized this N-terminal bias to all transit peptides through statistical analyses. Futhermore, we have generated a recombinant form of CSS1 and have developed a novel chromatographic technique to purify it in an active form. Finally, we have biochemically characterized CSS1, relating its place within the Hsp70 protein family and describing its catalytic and chaperone activities in detail. This work provides the basis for further *in vivo* and *in vitro* studies which our data predict will prove that CSS1 is the chloroplast protein import molecular motor.

PREFACE

Since his first introduction to intracellular signal transduction as an undergraduate, the author of this study has been enthralled by the concept of "higher order" design found throughout biology. Not only are the biomolecules which make up living systems constructed to fulfill their immediate chemical functions, they are also built to coordinate with each other within the larger context of the cell, the organ, and ultimately, the organism. Multiple layers of information necessary for potential functions, laid out in a hierarchical manner, are contained within systems which seem much simpler at first glance. For example, relatively simple side chains of individual amino acids, which in turn make up proteins, carry out most of the biochemistry we study. However, these same functional groups can simultaneously help or prevent proteins from folding, help maintain or diminish protein stability, respond to extrinsic chemical stimuli and alter the protein's activity or chemical makeup, and even direct proteins to different locations within the cell like a postal address on an envelope. This latter topic especially intrigued the author and directed him to explore the question of protein trafficking using the relatively unexplored chloroplast as a model system.

Chapter One provides a brief and general literature review of two topics: chloroplast protein import, which includes some general concepts of cell compartmentalization, and molecular chaperones, with special emphasis on Hsp70's. Given the relative novelty of the chloroplast import system and the difficulties of working with higher plants, much of the material discussed is of a speculative nature.

While the field of molecular chaperones, especially the Hsp70 class, is more established, applying that knowledge base to chloroplasts must be done conservatively.

Chapter Two is adapted from a published manuscript and is the copyrighted property of the journal *Cell Stress & Chaperones*. In this study, we used *in vivo* and *in vitro* techniques to show a specific interaction between the prokaryotic Hsp70, DnaK, and a chloroplast targeting sequences, transit peptide. We observed co-purification of Dnak with the transit peptide using an overexpression system in *E. coli*. We then purified both the chaperone and the transit peptide to homogeneity. After demonstrating conformational changes in the chaperone upon transit peptide binding and the transit peptide's ability to compete for chaperone binding, we used mild cell lysis conditions to purify the entire Hsp70 chaperone machine.

Chapter Three is also adapted from a published manuscript and is the copyrighted property of the journal *Plant Physiology*. In this study, we used two statistical analyses to generalize the Hsp70-transit peptide interaction to all stromally targeted transit peptides of higher plants in a published database. We predicted strongest affinity at the N-terminus of transit peptides and then biochemically mapped this interaction to the N-terminus of the transit peptide from the precursor of the small subunit of rubisco. We also showed that the transit peptide similarly interacts with the physiologically relevant stromal Hsp70 homolog, CSS1, and could protect Hsp70's from proteolytic degradation and stimulate the chaperone's weak ATPase activity.

Chapter Four is primarily methodological in nature. To further manipulate the CSS1 system, we generated a recombinant form of the protein from a precursor gene

construct supplied as a gift. Purification was problematic to say the least. We were forced to contend with impurities which shared almost all the chemical properties conventionally used to separate proteins. In addition, at least one impurity bound to recombinant CSS1, and maintaining solubility of the chaperone required extensive trial-and-error benchwork. However, we ultimately succeeded in purifying a soluble, functional recombinant chaperone by developing a novel denaturation/renaturation chromatography protocol.

Chapter Five continues CSS1 biochemical characterization, but only with the biochemically purified form. We conducted homology analyses of prokaryotic, algal, and higher plant Hsp70's to demonstrate the prokaryotic evolutionary origin of the plastid. We also analyzed the relative homologies of higher plant Hsp70's from different cellular locations to further emphasize the point. After calling into question the methods used to predict the stromal processing site for CSS1 and other proteins imported into the chloroplast, we performed a series of classical, comparative *in vitro* experiments to characterize CSS1's ability to autophosphorylate hydrolyze ATP, and be ATPase-stimulated by peptide substrates and heterologous co-chaperones. Finally, we demonstrated CSS1's ability to refold a denatured protein and a transit peptide's ability to compete with the denatured protein for CSS1 binding.

Chapters Two through Five each contain introductory material specific to the respective topics. The data in this study are discussed extensively within each chapter as well. Therefore, Chapter Six summarizes the work in toto without belaboring the

arguments reviewed previously. Chapter Six also identifies criticisms of the project and offers an outline for several directions of continuing the research.

TABLE OF CONTENTS

LIST OF FIGURES

LIST OF ABBREVIATIONS

^{125}I-RCMLA – RCMLA radiolabeled with ^{125}I

ADP- adenosine-5'-diphosphate

AtE1 – *A. thaliana* Hsp20

ATP- adenosine-5'-triphosphate

BCIP – 5-bromo-4-chloro-3-indolyl phosphate

BiP – ER Hsp70 homolog

CBPS – cellulose bound peptide scanning

CcHsp70 – cyanobacterial chloroplast Hsp70

CHLPEP – a chloroplast transit peptide database

Com70 – chloroplast outer envelope-associated Hsp70

Cpn10 – chloroplast Hsp10

Cpn60 – chloroplast Hsp60

CRAG - A 31-kDa fusion protein which contains 12 residues of cro repressor, truncated protein A, and 14 residues of beta-galactosidase

CSS1 – chloroplast stress seventy, homolog one

DnaK – *E. coli* Hsp70

DnaJ – *E. coli* Hsp40

DTT - dithiothriotol

ER – endoplasmic reticulum

FPLC – fast performance liquid chromatography

GroEL – *E. coli* Hsp60

GroES – *E. coli* Hsp10

GrpE – *E. coli* Hsp20

GST – glutathione-*S*-transferase

GST-SStp – fusion protein of GST and SStp

GTP – guanosine-5'-triphosphate

His-S – dual epitope tag; His_6-Tag fused to the RNAse S peptide

His-S-CSS1 – fusion protein of His-S and CSS1

His-S-SStp – fusion protein of His-S and SStp

Hsc70 – heat shock cognate, 70 kDa class

Hsp10 – heat shock protein , 10 kDa class

Hsp100 – heat shock protein, 100 kDa class

Hsp20 – heat shock protein, 20 kDa class

Hsp40 – heat shock protein, 40 kDa class

Hsp60 – heat shock protein, 60 kDa class

Hsp70 – heat shock protein, 70 kDa class

IAP70 – intermembrane space-associated Hsp70

IPTG – isoproponyl-thiogalactoside

kDa – kilodaltons

MgADP – magnesium coordinated with ADP

MgE1 – *S. cerevisiae* mitochondrial Hsp20

MSF – mitochondrial import stimulation factor

MWCO – molecular weight cut-off

NBT – Nitro Blue Tetrazolium

NTP – purine-5'-triphosphate

PBF – precursor binding factor

PBS – phosphate-buffered saline

prSSU – precursor of the small subunit of rubisco

PTP99 – CHLPEP update in 1999

RCMLA – reduced, carboxymethylated α-lactalbumin

RBP – Rubisco binding protein

RPPD – random peptide phage display

rubisco – ribulose-1,5-bisphosphate carboxylase/oxygenase

SDS – sodium dodecylsulfate

SDS-PAGE – SDS polyacrylamide gel electrophoresis

SPP – stromal processing peptidase

SRP – signal recognition particle

SSC1 – stress 70 cognate; mitochondrial Hsp70

SStp – transit peptide from prSSU

$SStp_{GST}$ – SStp derived from GST-SStp

$SStp_{HIS}$ – SStp derived from His-S-SStp

TbATP – terbium coordinated with ATP

Tic – translocator at the inner envelope of the chloroplast

Tim – translocator at the inner membrane of the mitochondria

Toc – translocator at the outer envelope of the chloroplast

Tom – translocator at the outer membrane of the mitochondria

Chapter 1 – General Introduction

CELLULAR COMPARTMENTALIZATION

General concepts

Eukaryotic cells are defined by their diverse membrane systems which compartmentalize their cells into distinct intracellular environments. The advantages of partitioning cells are many fold and have led to several evolutionary advantages (Alberts et al., 1994). First, eukaryotic cells are spatially organized to allow for more efficient metabolism by separating and channeling intermediate metabolites between active metabolic centers. Second, the ability to generate membrane potentials and specifically separate metabolites increases the diversity of metabolic possibilities available to the cell. Third, eukaryotic cells can sequester harmful or potentially toxic compounds from the rest of the cell or allow two mutually exclusive metabolic pathways to function simultaneously in different compartments. Fourth, multiple membrane systems allow for a transport system alternative to metabolite transport, vesicular transport, which leads to further advantages including metabolite customization en route to its ultimate destination. Finally, membrane diversification and asymmetric design have ultimately lead to the evolution of multicellular organisms. Without all of the advantages conferred by compartmentalization listed above, plants and animals could not chemically function.

Protein sorting

As important as membrane systems are in eukaryotes, all of the diverse biochemistry is ultimately carried out by proteins. In order to benefit the cell, certain proteins must function in a particular manner in a specific location at a predetermined time or developmental stage. Although virtually all proteins are synthesized in the cytosol, most function in a different cellular compartment (Schatz and Dobberstein, 1996). Herein lies the problem of protein sorting, which is summarized in diagrammatical form in Figure 1-1. Each eukaryotic cell needs a sorting system which can work fast enough to keep up with protein synthesis and exacting enough to prevent harmful, or at least wasteful, mistargeting of proteins synthesized in the cytosol.

To solve this problem, the eukaryotic cell has evolved a proficient sorting system which relies on five sets of components to ensure delivery of proteins to their proper destinations (Schatz and Dobberstein, 1996): 1) targeting information contained within each newly synthesized precursor protein, 2) targeting factors on the *cis* (cytosolic) side of the translocating membrane which direct the precursor to that membrane, 3) a translocation apparatus with a receptor and a translocation channel to transport the precursor in an extended conformation, 4) a mechanism to generate vectorial movement of the precursor through the channel, and 5) a processing/folding system on the *trans* (lumenal) side of the membrane to produce the functional protein in its native environment.

Figure 1-1. Protein trafficking in eukaryotic cells. The solid black line indicates gated transport; the dotted black lines, transmembrane transport; and the solid gray lines, vesicular transport.

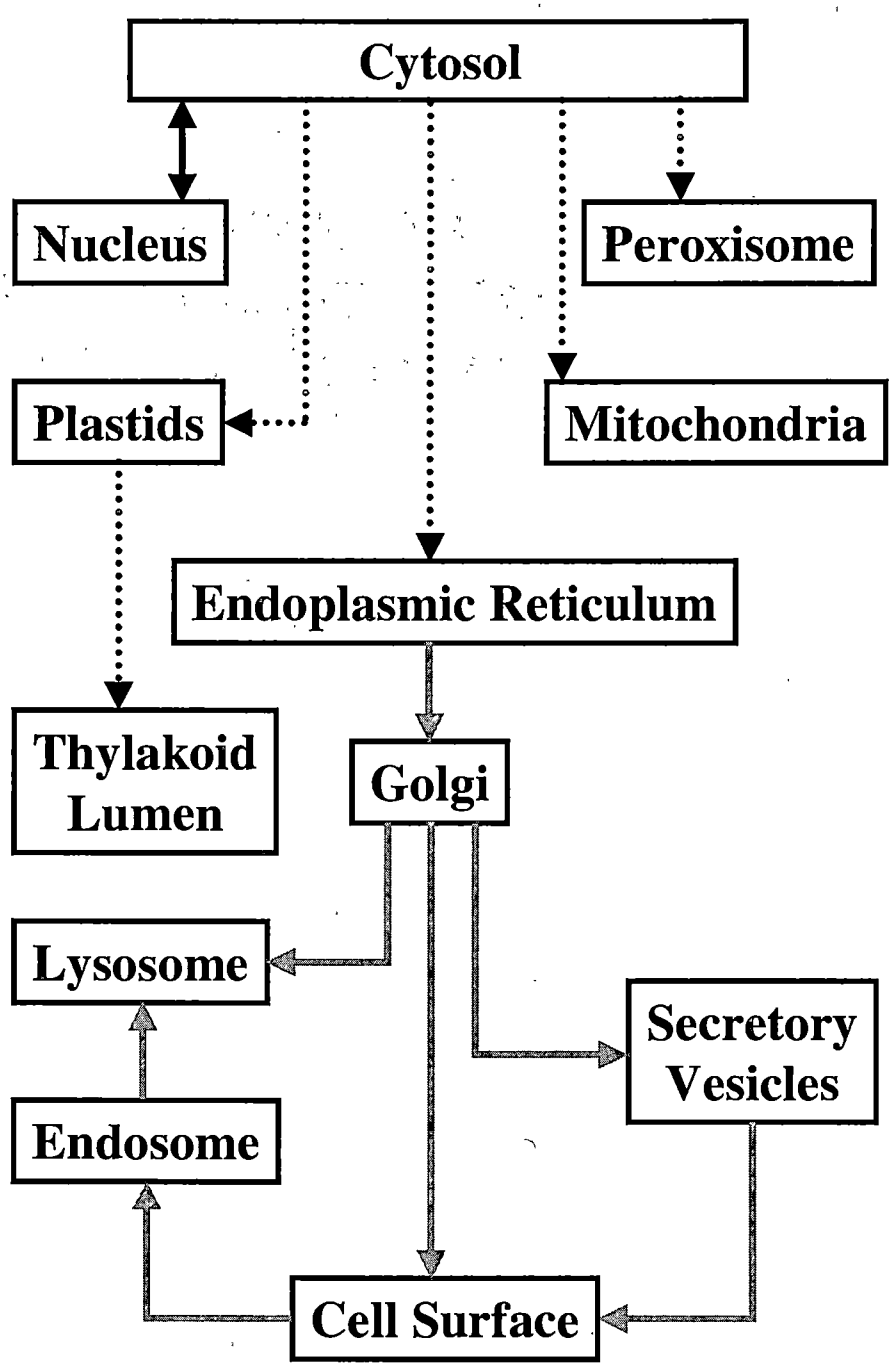

Figure 1-1. Protein trafficking in eukaryotic cells.

Targeting signals

Every protein that functions in a non-cytosolic location contains sequence information necessary and sufficient to initiate the targeting and translocation processes. Although most targeting signals are cleavable N-terminal extensions, some are C-terminal or even internal and remain as part of the functional protein post translocation. Since ER, mitochondrial, and plastid protein import involves N-terminal, cleavable transit peptides, this discussion will be limited to those targeting signals and their respective cytosolic targeting factors.

In general, targeting sequences themselves share little homology among different precursors, even those which utilize the same import pathway. Variations in length and amino acid composition preclude all but the most rudimentary comparisons for similarity. However, some relationships within each class of targeting signal can be surmised from analyzing many precursors. For example, ER signals, called signal peptides because of their similarity to bacterial secretory sequences, are generally 20-70 amino acids in length and contain three loosely defined domains: 1) the N-terminus usually contains several basic residues, 2) the middle region is generally hydrophobic, and 3) the C-terminus has the potential to form an amphipathic α-helix in a membrane-mimetic environment (von Heijne, 1984; von Heijne, 1985).

In contrast, mitochondrial and plastid signals contain many hydroxylated residues throughout their sequences (von Heijne et al., 1989). However, the similarity between presequences (mitochondrial) and transit peptides (plastid) ends there. Presequences are much shorter (17-42 residues), have basic N-termini, and hydrophobic C-termini (von

Heijne et al., 1989). Mitochondrial presequences have also been shown to form amphipathic α-helices when exposed to lipids found in mitochondrial membranes (Tamm and Bartoldus, 1990). Transit peptides, on the other hand, range from 25 to 125 residues in length and have hydrophobic N-termini, basic middle regions, and helix forming C-termini (Bruce, 1998; von Heijne et al., 1989), yet have little to no secondary structure in aqueous solution (von Heijne and Nishikawa, 1991). The latter two observations are supported by recent work in which the C-terminal third of a transit peptide interacted with the non-bilayer forming lipids monogalactosyldiacylglycerol and digalactosyldiacylglycerol in liposomes resembling the chloroplast outer envelope (Pinnaduwage and Bruce, 1996).

Because of the third membrane system in green plastids (chloroplasts), the thylakoid, precursors destined for the thylakoid lumen have bipartite transit peptides (Cline and Henry, 1996; Weisbeek et al., 1989). These precursors are imported into the stroma of the chloroplast by the common import pathway and then "exported" into the thylakoid via a variety of newly described pathways (reviewed in Keegstra and Cline, 1999). Thus, chloroplasts have a total of six targeted destinations for protein trafficking: 1) the outer envelope, 2) the intermembrane space between envelopes, 3) the inner envelope, 4) the stroma, 5) the thylakoid membrane, and 6) the thylakoid lumen. The great majority of the precursors targeted to the latter five locations are initially imported by a common pathway, regardless of ultimate destination or transit peptide sequence. Given the complex arrangement of the chloroplast and the fact that transit peptides are

the most divergent set of all targeting signals known, discovering the mechanisms of the initial sorting of chloroplast precursors remains a fundamental challenge today.

Cytosolic Targeting Factors

In the ER, one form of the initial sorting is carried out by a cytosolic factor known as the signal recognition particle (SRP), which binds to the nacent signal sequence and recruits the precursor, ribosome and all, to the ER membrane for co-translational translocation into the ER lumen (Sanders and Schekman, 1992; Waters et al., 1986). In the mitochondrial system, two cytosolic factors have been identified which enhance the targeting and import efficiency of mitochondrial precursors. First, the presequence binding factor (PBF) was purified and shown to bind a presequence and stimulate precursor import *in vitro* (Murakami and Mori, 1990). Interestingly, when Hsp70 was added to the PBF/precursor complex, import was enhanced even further. Second, the mitochondrial import stimulation factor (MSF) was shown to maintain precursor import competence by preventing folding prior to import (Hachiya et al., 1993). MSF also rescues aggregated precursors in an ATP-dependent manner and is inhibited by treatment with *N*-ethylmaleimide. Therefore, Hachiya and co-workers concluded that MSF is a multifunctional, mitochondrial-specific molecular chaperone.

Although an early study describes the possibility of molecular chaperones as cytosolic targeting factors in the chloroplast import system (Waegemann et al., 1990), only recent work makes this hypothesis seem probable. The transit peptide of the precursor of the small subunit of Rubisco (SStp) can be phosphorylated by a cytosolic

kinase (Waegemann and Soll, 1996). This phosphorylated transit peptide resembles the phosphopeptide binding motif for 14-3-3 proteins. When phosphorylated SStp is exposed to wheat germ lysate, specific 14-3-3 proteins and a cytosolic Hsp70 homolog form a complex with the transit peptide in an ATP-dependent manner (May and Soll, 2000). This interaction is especially significant since 14-3-3 proteins can act in both recruitment of Hsp70s (Ballinger et al., 1999; Hohfeld et al., 1995) and in phosphorylation-mediated signal transduction pathways (Aitken et al., 1992; Dubois et al., 1997). Additionally, protein import using this complex proceeds four-fold faster than with precursor alone. It is important to note, however, that cytosolic factors are not required for either mitochondrial or chloroplast protein import *in vitro*.

ER VS. MITOCHONDRIAL PROTEIN IMPORT SYSTEMS

The reports of cytosolic factors in chloroplast protein import discussed above are preliminary, originating from the same laboratory. Much more study in this and other areas are needed before the entire process can be properly delineated. To gain insight into the chloroplast system, a brief review of other, better characterized protein import systems is helpful.

The ER contains an evolutionarily conserved heterotrimeric central membrane channel, Sec61 (Panzner et al., 1995). Although capable of co-translational translocation without Hsp70 participation (Hamman et al., 1998), Sec61 associates with a tetrameric Sec62/63p complex (Panzner et al., 1995), which is required for lumenal Hsp70 recruitment (Lyman and Schekman, 1997), during post-translational translocation. Of

these components, only BiP, the lumenal Hsp70 homolog, consumes ATP, a means to provide directionality to the translocation process (Matlack et al., 1999).

Because mitochondria and chloroplasts are thought to have prokaryotic origins, the mitochondrial system is perhaps a better model system for studying chloroplast protein import than the ER. Still, protein translocation into mitochondria shares many characteristics of ER protein import. Both systems form tight, aqueous channels to post-translationally import nuclear-encoded precursor proteins in response to activation by targeting signals contained within the precursors (Plath et al., 1998), and both use *trans*-localized Hsp70s, to consume ATP in order to achieve translocation (Panzner et al., 1995; Ungermann et al., 1994). In fact, both systems use proteins with J-domains similar to that in bacterial DnaJ (ER, Sec63; mitochondria, Tim44) to recruit their respective Hsp70s to the *trans* side of the translocating membrane (Bomer et al., 1997; Lyman and Schekman, 1997).

However, mitochondrial import occurs across two membranes instead of one. Therefore, its import machinery and conditions are inherently more complicated. For example, the mitochondria has two membrane channel complexes, one in the outer membrane and one in the inner membrane. During import, these complexes form contact sites between the membranes so that translocation occurs across both membranes simultaneously (Schatz and Dobberstein, 1996). Also, mitochondrial precursor proteins can associate with cytosolic targeting factors which guide their post-translational import processes (Hachiya et al., 1994; Murakami and Mori, 1990). Furthermore, mitochondrial import requires a membrane potential to drive translocation across the Tim (Translocon

at the Inner membrane of Mitochondria) components (Martin et al., 1991; Ungermann et al., 1996).

Depending on the presentation of the precursor to the mitochondrial outer membrane, the precursor is bound by a complex of either Tom70/Tom37 (Haucke et al., 1995) or Tom22/Tom20 (Haucke et al., 1996). The bound precursor is then delivered to the outer membrane translocation channel, which consists of at least five proteins: Tom40, Tom38, Tom7, Tom6, and Tom5. Tom40 forms the central channel (Vestweber et al., 1989), while the other proteins are not essential for translocation (Alconada et al., 1995). Once the precursor has moved across the outer membrane, the electrochemical potential of the inner membrane engages the precursor to the Tim complex (Ungermann et al., 1996). Eight proteins (Tim33, Tim23, Tim17, Tim14, Tim11, Tim44, SSC1{mitochondrial Hsp70}, and Mge1) provide the channel and drive translocation into the matrix in an ATP-dependent manner (Berthold et al., 1995; Kronidou et al., 1994; Rassow et al., 1994; Schneider et al., 1994).

CHLOROPLAST PROTEIN IMPORT APPARATUS AND MODEL

Unlike the mitochondrion or other organelles, the chloroplast is the metabolic workhorse of the plant cell. The chloroplast carries out everything from energy production and carbon assimilation during photosynthesis to starch, lipid, amino acid, protein, and nucleotide biosynthesis to ion homeostasis to nitrogen and sulfur assimilation (Alberts et al., 1994). Given the diverse metabolic properties of chloroplasts, the fact that Rubisco accounts for half of the protein in every leaf, and the number of

chloroplasts per cell (as many as 1000), chloroplast protein import is the most active form of protein translocation in all of biology.

The chloroplast import system has been studied for over 20 years (Chua and Schmidt, 1978; Highfield and Ellis, 1978), yet most of the progress made so far has been in identifying catalytic requirements and participating proteins (reviewed in Keegstra and Froehlich, 1999). Little evidence of component stoichiometries or ratios of bound:freely diffusable Tic (Translocator at the Inner envelope of the Chloroplast) and Toc (Translocator at the Outer envelope of the Chloroplast) components exists. Also, no one has demonstrated functions for most of these participants or analyzed the structure/function relationships between the import machinery and the diverse precursor proteins.

The following, which is summarized in Figure 1-2, is a brief overview of our current state of knowledge concerning the chloroplast protein import system, its components, and their proposed roles in the transport process. Unlike the mitochondrial system (Schleyer et al., 1982), initiation of protein import into the chloroplast does not require an electrochemical gradient (Fluegge and Hinz, 1986). Energetically, the chloroplast import process can be divided into four steps: 1) an energy-independent, reversible interaction between the precursor, the outer envelope lipids, and the docking protein/receptor, 2) a Toc complex formation step requiring ~50-100 μM cytosolic ATP or GTP, 3) a translocating step requiring 250-350 μM ATP in the intermembrane space, and 4) a translocating step requiring 500 μM to 1 mM ATP in the stroma (reviewed in Keegstra and Cline, 1999). Many protein components of the outer envelope are protease-

Figure 1-2. Transit peptide-mediated protein import into chloroplasts. Graphical representation of the suggested order of events, energetic requirements, and participating proteins of the outer and inner chloroplast envelopes.

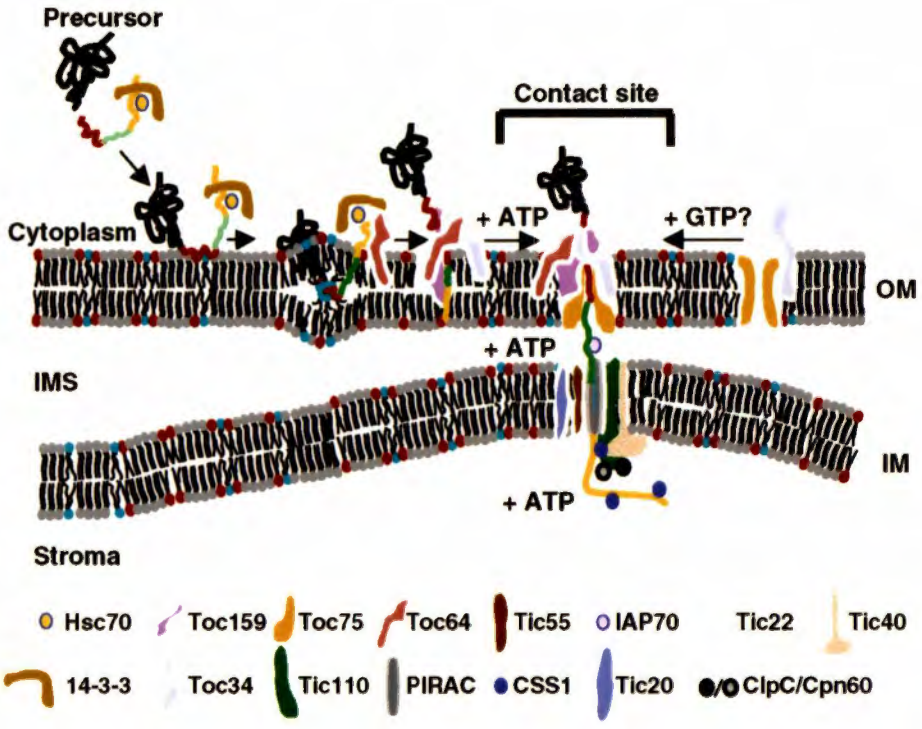

Figure 1-2. Transit peptide-mediated import into the chloroplast

sensitive (Cline et al., 1985), and precursor proteins are thought to translocate in an unfolded conformation (Pilon et al., 1992). The latter topic will be discussed later.

Early stages of import

The role of transit peptide-lipid interactions is well established (van't Hof et al., 1991; van't Hof et al., 1993) and is generally viewed as the initial interaction between a precursor protein and the chloroplast (Bruce, 1998; Pinnaduwage and Bruce, 1996). This interaction is sequence specific and lipid class dependent. The C-terminus of SStp inserts, to some degree, into bilayers containing the non-bilayer forming lipid monogalactosyldiacylglycerol, which comprises about 17% of the lipid content in the outer envelope (Pinnaduwage and Bruce, 1996).

After this initial targeting event, the proteinaceous Toc complex performs three necessary functions in the protein import process: 1) specific transit peptide recognition, 2) precursor translocation initiation, and 3) contact site formation with the inner envelope (reviewed in Keegstra and Froehlich, 1999), see Figure 1-2). As mentioned earlier, phosphorylated transit peptides bind 14-3-3 proteins and cytosolic Hsc70 from wheat germ, enhancing their import competence (May and Soll, 2000; Waegemann and Soll, 1996). A likely docking site for this ternary complex is the newly identified Toc64, peripheral membrane protein which contains 14-3-3 motifs itself and co-purifies and crosslinks with other Toc and Tic components in the presence of precursor proteins (Sohrt and Soll, 2000). For the purposes of this discussion, "integral" membrane proteins

are membrane proteins which contain functional domains on both sides of a membrane, while "peripheral" membrane proteins do not.

Several laboratories have independently identified three other Toc components--Toc159, Toc 75, and Toc 34--through crosslinking, co-purification, or both (Akita et al., 1997; Ma et al., 1996; Nielsen et al., 1997). In the earliest stages of protein import prior to the first NTP energy requirement, the precursor interacts with Toc64, Toc159 and (indirectly) Toc34 (Kouranov and Schnell, 1997; Perry and Keegstra, 1994), the latter two containing GTP binding domains (Kessler et al., 1994; Seedorf et al., 1995). The role(s) of GTP in the import process is not understood, but regulation of early transport intermediates and initiation of contact site formation with the inner envelope have been proposed (Keegstra and Froehlich, 1999).

Toc159, another peripheral membrane protein, was originally identified as Toc86 (Hirsch et al., 1994; Perry and Keegstra, 1994), which was proven to be a proteolytic fragment of Toc159 (Bolter et al., 1998). It is believed that Toc159 contains contains a precursor binding site because Toc159 antibodies block precursor binding (Hirsch et al., 1994) and precursors readily crosslink to this putative receptor (Kouranov and Schnell, 1997; Ma et al., 1996). On the other hand, no evidence exists of precursor binding directly to the peripheral protein, Toc34, although it may regulate precursor binding to Toc159 (Kouranov and Schnell, 1997). The fourth Toc component, Toc 75, is the only integral membrane protein in the Toc complex and is therefore most likely a protein conducting channel. In addition to binding transit peptides in an NTP-dependent manner (Kouranov and Schnell, 1997; Ma et al., 1996), Toc75--when reconstituted into

liposomes--also exhibits voltage sensitive ion conductance properties which are specifically regulated by transit peptides (Hinnah et al., 1997).

Late stages of import

The best characterized Tic protein is Tic110, which was first identified by immunoprecipitation (Kessler and Blobel, 1996) and crosslinking (Lubeck et al., 1996) studies. Tic110 is an integral membrane protein with the majority of its sequence exposed to the stroma (Jackson et al., 1998), a topology which may allow Tic110 to recruit molecular chaperones to the inner envelope in a manner similar to that of Tim44, which recruits SSC1 (Stress Seventy Cognate 1) to the inner mitochondrial membrane during protein import (Rassow et al., 1994; Schneider et al., 1994). Chaperone recruitment to the inner envelope will be discussed in detail later.

Tic22 and Tic20 were originally identified and characterized by crosslinking strategies and shown to interact with each other and the Toc complex (Kouranov and Schnell, 1997). While Tic22 is a peripheral membrane protein which is exposed to the intermembrane space and contains no nucleotide or peptide binding motifs, Tic20 is integrated into the inner envelope, extending a hydrophilic domain into the intermembrane space and a basic domain into the stroma. Based on these observations, Tic22 is proposed to facilitate contact site formation with the Toc complex while Tic20 serves to anchor Tic22 to the inner envelope.

Tic55, which has only been identified by one lab via blue-native polyacrylamide gel electrophoresis (Caliebe et al., 1997), is the least well characterized Tic component

and contains a Reiske-type iron-sulfur center whose function is unknown. If Tic55 is confirmed as a chloroplast protein import component, any role of the redox center would be a novel phenomenon in organellar protein trafficking.

A possible protein conducting channel was also discovered recently, but hasn't been purified or given a "Tic" designation (van den Wijngaard and Vredenberg, 1997). Instead, the 50-picosiemens anion channel is called the protein import related anion channel, or PIRAC. Associating with Tic110 (van den Wijngaard and Vredenberg, 1999), the channel is gated by 100 μM ATP coupled with a chloroplast precursor protein (Dabney-Smith et al., 1999; van den Wijngaard et al., 1999; van den Wijngaard and Vredenberg, 1997). Processed or truncated precurusor proteins have no effect on the channel.

The very recent discovery of Tic40, which also associates with Tic110, may ultimately have the greatest significance with respect to molecular chaperone involvement in chloroplast protein import (Stahl et al., 1999). Tic40 was originally described as Tic/Toc40—simultaneously occupying both the outer and inner envelopes—by generating partially translocated intermediate precursor proteins *in vitro* (Ko et al., 1995; Wu et al., 1994). After refining the chloroplast fractionation process, crosslinking Tic40 to Tic110, and performing detailed immunohistochemical studies, Stahl and co-workers (1999) proved that Tic 40 is a peripheral membrane protein and resides exclusively in the inner envelope with the majority of its sequence exposed to the stroma. When Tic40's amino acid sequence was analyzed, the only homology observed was with the Hsp70 interacting protein (Hip), which is a 14-3-3 protein. A Tic40/CSS1

interaction would be a directly parallel to the Tim44/SSC1 interaction in the mitochondrial import system (Rassow et al., 1994; Schneider et al., 1994). Although Tic40 and CSS1 have not been crosslinked or co-purified to date, these findings described above, taken together with the transit peptide-Hsp70 interaction studies from our laboratory (Ivey and Bruce, 2000; Ivey et al., 2000), provide a strong case for Hsp70 involvement as a molecular motor in chloroplast protein import.

The last step in the import process involves cleaving the transit peptide and folding the processed protein into its native structure. The stromal processing peptidase (SPP) cleaves the targeting sequences from most precursor proteins upon import into the stroma. SPP must recognize and cleave hundreds, perhaps thousands, of structurally unrelated precursors. Although a loose consensus for proteolytic cleavage (V/I-X-A/C$^{\blacktriangledown}$A.) has been identified based on 32 non-homologous precursors with known cleavage sites (Gavel and von Heijne, 1990), most precursors lack one or more features of this consensus. After cleavage, mature proteins are folded/assembled in the stroma by molecular chaperones as they would be in the cytosol (Hemmingsen et al., 1988). CSS1 and other chaperone activity in the import process will be discussed after a brief introduction to molecular chaperones.

HSP70 INVOLVEMENT IN CHLOROPLAST PROTEIN IMPORT

General concepts concerning molecular chaperones

From early studies of the spontaneous, reversible folding properties of ribonuclease A *in vitro*, Anfinsen (1973) proposed that all of the information necessary

for a protein to fold and achieve its native structure is contained within its primary amino acid sequence. In principle, this paradigm continues to be true. However, in shaping the study of protein folding, the unchallenged dogma eventually led to the idea that protein folding *in vivo* occurs through a similar process. This mistaken notion has been completely amended in the last 15 years primarily because of the discovery of several proteins which control the processes by which proteins attain their native structures in the cell. These proteins include specialized "foldases", such as protein disulfide isomerase and peptidyl prolyl isomerase, as well as the ubiquitous and more familiar molecular chaperones (reviewed in Gething and Sambrook, 1992, and Hendrick and Hartl, 1993).

Several years ago, the working definition for a molecular chaperone was "...a protein that binds to and stabilizes an otherwise unstable conformer of another protein—and by controlled binding and release of the substrate protein, facilitates its correct fate *in vivo*; be it folding, oligomeric assemby, transport to a particular subcellular compartment, or controlled switching between active/inactive conformations" (Hendrick and Hartl, 1993). Today, we know that chaperones are also involved in a whole host of other cellular activities, such as replicative enzyme activation, targeting of proteins for degradation, force generation for protein translocation, antigen delivery, and apoptosis inhibition, just to name a few (reviewed in Lund, 1995, and Mallouk et al., 1999).

As the definition implies, molecular chaperones function primarily by forming noncovalent interactions with unfolded or incorrectly folded polypeptide chains, thus stabilizing them and preventing or reversing the formation of aggregates. Given the high

protein concentration *in vivo*, such unproductive reactions would be strongly preferred with non-native polypeptides over the correct folding pathway. Therefore, molecular chaperones protect new or stressed proteins from the cellular millieu, most often by interacting with solvent-exposed, hydrophobic regions of protein substrates which would normally be buried in the native state. Although mechanistically unclear, repeated cycles of binding and release by the chaperones result in a functional conformation of the newly folded protein without covalent modification to it or the molecular chaperones involved. Energy is required for these processes, usually in the form of ATP (Bukau and Horwich, 1998).

From a thermodynamic perspective, the non-native protein is bound by the chaperone(s) at a low energy state, or thermodynamic minimum, in which it is "trapped" and lacks sufficient activation energy to achieve a transition state and possibly assume a different conformation. As a result of binding and release by the chaperone(s), the non-native protein is transferred to a higher energy state in which other conformations may result. A subset of these newly possible conformations, particularly those resembling the lowest possible energy state, are usually classified as "native" (Todd et al., 1996).

Although first described in reference to their specific induction during cellular stress response (Craig, 1985; Lindquist, 1986), molecular chaperones are expressed constitutively and are essential for cell viability and growth (Craig, 1989; Fayet et al., 1989). Therefore, the common abbreviation "Hsp", which stands for "heat shock protein", is sometimes substituted with the more accurate "Hsc", for "heat shock constitutive" or "heat shock cognate". The numbers after the textual abbreviations, such

as "70" in "Hsp70", signify the molecular weight in kilodaltons of that particular chaperone or chaperone class.

The Hsp70 chaperone machine

Hsp70s may function alone in the cell, but usually in conjunction with Hsp40 and, in prokaryotic and organellar systems, Hsp20 (reviewed in Bukau and Horwich, 1998). These three proteins, which are evolutionarily conserved throughout biology, interact with more proteins than any other cellular machinery. The *E. coli* chaperone machine, which is by far the best characterized, consists of DnaK (Hsp70), DnaJ (Hsp40), and GrpE (Hsp20).

The molecular basis for DnaK's peptide affinity has been studied using *in vitro* and crystallographic techniques (Gragerov et al., 1994; Rudiger et al., 1997; Schmid et al., 1994; Zhu et al., 1996). Substrates are short, contiguous polypeptide segments of 5 amino acids in length. These peptides are generally hydrophobic in nature, with leucine and isoleucine prevalent as the central residue. Basic residues are preferred to flank this central region, but do not contribute to the direct interactions between DnaK and its substrate. In contrast, acidic residues are excluded from the central binding core and the flanking regions almost without exception. Such sequences occur approximately every 36 residues in proteins and preferentially localize to buried β strands (Gragerov et al., 1994; Rudiger et al., 1997; Schmid et al., 1994).

A high affinity peptide, which must be extended such that it is separated from the rest of the protein by at least 10 Å, binds in a β sandwich motif in the C-terminal peptide

binding domain (Figure 1-3A). The sandwich consists of four β strands, whose loops act to "cradle" the peptide, followed by a flexible hinge region and then two α helices which fold over the peptide like a "lid" during peptide binding. The binding channel, which is 7 Å long and 5 Å wide, maintains seven H-bonds with the five central residues of the substrate through main chain atoms in the chaperone's β turns (Zhu et al., 1996).

DnaK's other globular domain at it's N-terminus harnesses energy derived from ATP through hydrolysis (Figure 1-3B). The tertiary structure is nearly identical to that of hexokinase, another ATP-binding enzyme (DeLuca-Flaherty et al., 1988). Two subdomains are divided by a deep cleft which contains the nucleotide binding pocket. The mechanistic basis by which ATP hydrolysis leads to the mechanical work necessary to change the conformation of the peptide substrate is not known. Although the ATPase domain can function alone, significant conformational changes in this domain during ATP hydrolysis are only observed in the intact chaperone (Buchberger et al., 1995).

Stimulation of ATP hydrolysis, probably through other conformational changes, is the primary function of the co-chaperone, DnaJ (Karzai and McMacken, 1996; Szabo et al., 1996; Wall et al., 1994). Interaction with DnaK is accomplished by a hallmark, N-terminal "J-domain" which contains a conserved His-Pro-Asp motif in a loop between two helices (Wall et al., 1994). The C-terminal domain can also bind peptide substrates, which will be discussed shortly.

In addition to exhibiting weak ATP hydrolysis activity, DnaK alone also releases ADP and P_i too slowly for physiological processes. This problem is remedied by GrpE (Dekker and Pfanner, 1997; Liberek et al., 1991; Miao et al., 1997). Crystallographic

Figure 1-3. X-ray crystal structures of Hsp70s. α-helices are shown in read; β-sheets, in yellow; coils, in white. (**A**) The C-terminal peptide binding domain of *E. coli* DnaK. (**B**) The N-terminal ATPase domain of bovine cytosolic Hsc70.

A.

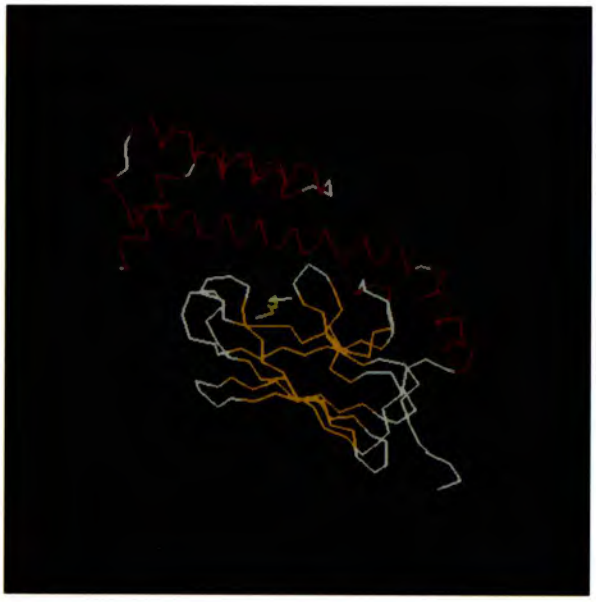

B.

Figure 1-3. X-ray crystal structures of Hsp70s.

studies of the stable complex between a GrpE dimer and a DnaK monomer show that one of the GrpE subunits opens DnaK's nucleotide binding cleft, rotating subdomain IIB by 14° relative to its ADP-bound conformation (Harrison et al., 1997).

ATPase cycle

The ATPase cycle of DnaK, which is summarized in Figure 1-4, is essentially DnaK's alternation between two states (McCarty et al., 1995; Palleros et al., 1993; Schmid et al., 1994). First, DnaK's ATP-bound state exhibits low affinity and fast exchange rates for peptide substrates, and the peptide binding pocket is open. Second, the ADP-bound state displays high affinity and slow exchange rates for peptide substrates with the peptide binding pocket closed.

At the start of the cycle, ATP is bound by the chaperone. After a slow structural rearrangement (Ha and McKay, 1995; Theyssen et al., 1996), hydrolysis can be kinetically coupled to release or exchange of any previously bound peptide. Thus, the ADP-bound form is stabilized with respect to a new peptide substrate. This transition is the key regulatory point in the entire cycle and is controlled by DnaJ, which binds and stimulates DnaK's ATPase activity (Liberek et al., 1991; McCarty et al., 1995). Coupling of energy expenditure to productive peptide substrate binding by DnaK ensures a stable interaction with the incoming peptide substrate and prevents futile ATPase cycles in the absence of substrate. This hypothesis is supported by the fact that DnaJ-mediated ATPase stimulation is always greater when substrates are present. After hydrolysis and peptide binding, DnaK's affinity for DnaJ is reduced, and DnaJ dissociates (Gamer et al., 1996).

Figure 1-4. ATPase cylce of *E. coli* DnaK. Diagrammatic representation of the prototypical Hsp70 ATPase reaction cycle including interaction by the co-chaperones DnaJ and GrpE, and binding of an unfolded peptide substrate.

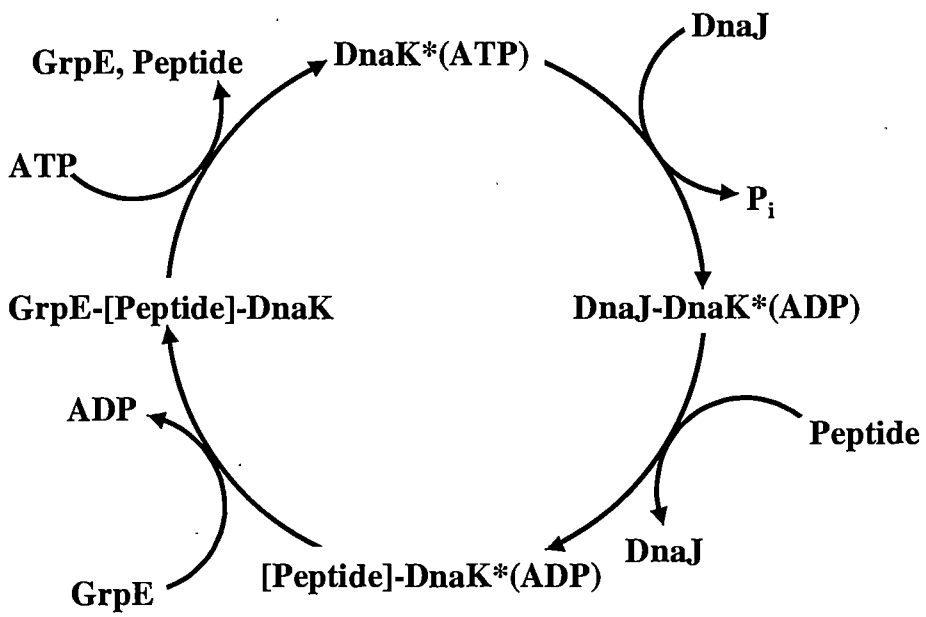

Figure 1-4. ATPase cylce of *E. coli* DnaK.

GrpE then binds the ternary complex of DnaK/ADP/peptide and induces release of the nucleotide. ATP quickly binds DnaK again, causing dissociation of both GrpE and the now folded peptide substrate, bringing the cycle full circle.

Further regulation of Hsp70s in the eukaryotic cytosol seems probable since no GrpE homologs have been found to date. In yeast, the cytosolic DnaJ homolog, Ydj1p, stimulates both ATP hydrolysis and nucleotide exchange (Ziegelhoffer et al., 1995). Even more diverse forms of regulation in eukaryotic systems seem to exist in the forms of two newly discovered cytosolic proteins which bear no resemblance to any other co-chaperones. Hip is proposed to stabilize the Hsp70/ADP/peptide ternary complex, essentially displaying an anti-GrpE activity (Hohfeld et al., 1995), while Hop stimulates nucleotide exchange in a manner similar to that of GrpE (Frydman and Hohfeld, 1997; Hohfeld and Jentsch, 1997).

Hsp70 involvement in organellar protein import

Hsp70 chaperones play key roles in post-translational protein translocation in prokaryotic systems (Wild et al., 1992), as well as in the endoplasmic reticulum (Vogel et al., 1990), mitochondria (Kang et al., 1990), and probably the chloroplast (Ivey and Bruce, 2000; Ivey et al., 2000; Kourtz and Ko, 1997; Waegemann et al., 1990). While evidence for Hsp70 involvement in the bacterial, mitochondrial, and ER systems is definitive, we are much less certain in the case of the chloroplast. Less work has been done with plant systems because of the historical inability to perform genetic knockout

studies. To better understand what might be occurring in the chloroplast, we look to the better characterized systems of the ER and mitochondria for insight.

Ratchet vs. motor

In the posttranslational protein import pathways of the ER, mitochondria, and chloroplast, precursor proteins are generally thought to traverse the envelopes in an extended, unfolded conformation (reviewed in Schatz and Dobberstein, 1996). This condition requires maintaining a multitude of precursors in import competent conformations before and during import, providing an energy-dependent mode for physically moving the proteins across the membranes, and finally refolding and assembling the precursors once import is complete. The only known class of molecules able to function in all these capacities is that of molecular chaperones.

How do they achieve precursor translocation? To date, evidence exists for two divergent but not mutually exclusive models which may provide a possible translocation mechanism. The Brownian Ratchet Model (Simon et al., 1992) describes Hsp70s binding to precursors emerging from the membrane during import to serve as "anchors" which passively prevent retrograde motion into the cytosol. Random thermal fluctuations allow for small portions of the extended precursors to move further into the interior of the organelle, which allows Hsp70s to bind at more interior positions, trapping more and more of the protein in the organelle until import is complete.

The more recent Molecular Motor Model (Glick, 1995) also involves direct chaperone interaction with the precursor, but here, the organellar Hsp70 itself is anchored

to the membrane. ATP-dependent conformational changes in Hsp70 allow for the precursors to be actively "pulled" across the membrane in repeated cycles of precursor binding and release until the entire precursor is imported. In the ER, the "anchor protein" is Sec63 (Sanders et al., 1992); in mitochondria, Tim44 (Schneider et al., 1994). Both Sec63 and Tim44 have homology to the co-chaperone DnaJ (reviewed in Brodsky, 1996), which functions in combination with Hsp70 and GrpE to form the DnaK chaperone sytem (reviewed in Hendrick and Hartl, 1993).

Potential Hsp70 involvement in the chloroplast protein import system

The chloroplast actually contains three Hsp70 homologs (Marshall et al., 1990). While one is associated with the outer envelope (Ko et al., 1992), two are soluble in the stroma (Marshall et al., 1990). Of the latter, the major form, Chloroplast Stress Seventy 1 (CSS1; not to be confused with the mitochondrial Hsp70, SSC1), has been cloned (Marshall and Keegstra, 1992). Despite one report of Hsp70 interaction with a precursor (Waegemann et al., 1990) and several of Hsp70s involved in translocation complexes (Nielsen et al., 1997; Schnell et al., 1994; Waegemann and Soll, 1991), the potential role of this chaperone in chloroplast protein import has not been characterized, although the obvious post import role of protein folding is apparent (Madueno et al., 1989; Tsugeki and Nishimura, 1993).

Although CSS1 is the only organellar chaperone shown to directly interact with a physiological targeting sequence (Ivey and Bruce, 2000; Ivey et al., 2000), and chloroplastic homologs of DnaJ and GrpE have been identified (Schlicher and Soll,

1997), no putative membrane anchor protein had been found in the chloroplast inner envelope until recently (Stahl et al., 1999). Because specific Hsp70 affinity for the tetratricopeptide (14-3-3) repeat sequences is well documented (Irmer and Hohfeld, 1997; Prapapanich et al., 1996), Tic40 is a prime candidate for CSS1 recruitment.

Given the chloroplast import machinery's robust protein unfolding ability (America et al., 1994; Guera et al., 1993) and apparent capacity to import very small folded proteins (Clark and Theg, 1997), the simplest forms of the models described above may not adequately portray what is happening in the chloroplast. Mitochondria, on the other hand, cannot import partially folded protein domains (Wienhues et al., 1991). Unlike the ER and mitochondria, the translocation machinery of the chloroplast is thought to contain several other nucleotide triphosphate hydrolases besides Hsp70: Toc86 and Toc34, part of the initial receptor complex at the surface of the chlorplast (Kessler et al., 1994; Seedorf et al., 1995); IAP70/Com70, the Hsp70 associated with the inner surface of the outer envelope (Kourtz and Ko, 1997; Schnell et al., 1994), which could explain a separate ATP-dependent step in the intermembrane space (Scott and Theg, 1996); and ClpC, an hsp100 homolog originally described in prokaryotes as a regulatory subunit for the ClpP housekeeping protease (reviewed in Squires and Squires, 1992).

Potential ClpC and Cpn60 involvement

ClpC is also an abundant soluble, stromal protein (Moore and Keegstra, 1993; Shanklin et al., 1995), although it adsorbs nonspecifically to membranes and surfaces (Shanklin et al., 1995). Like Hsp70, ClpC also associates with translocation complexes

(Akita et al., 1997; Caliebe et al., 1997; Nielsen et al., 1997), though not in a precursor-dependent fashion (Nielsen et al., 1997). However, ClpC/hsp100's chaperone properties are evident: hsp100's ATPase activity is activated by its substrates, hsp100 can protect proteins from heat denaturation, disaggregate proteins, and assist in protein-DNA complex assembly (Wawrzynow et al., 1995). Hsp100 can also substitute for the DnaK chaperone system in some roles during replication (Wickner et al., 1994). However, this causes some targeting to the ClpP protease. In fact, the yeast mitochondrial hsp100 homolog interacts posttranslocationally with newly imported precursor proteins in the absence of mitochondrial Hsp70 (Schmitt et al., 1995) and targets abnormal precursors to an as-yet-unidentified protease for degradation.

The primary obstacle for ClpC serving to drive chloroplast protein import is the concept of specificity. Unlike Hsp70s, which are known to bind many, many proteins (Hendrick and Hartl, 1993), hsp100's are characterized by relationships with specific cellular targets (Squires and Squires, 1992; Wickner et al., 1994), most of which are marked for degradation. The ssrA-tag, a C-terminal sequence motif (Ala-Ala-Asn-Asp-Glu-Asn-Tyr-Ala-Leu-Ala-Ala) added to damaged proteins prosttranslationally in prokaryotes, conveys hsp100 affinity for any protein, regardless of its folding status (Keiler et al., 1996; Tu et al., 1995). In these cases, binding to hsp100 signals proteolysis by ClpP. The highly conserved region of hsp100 responsible for this function is the PDZ-like domain, a non-linear amino acid sequence which is repeated in some hsp100 homologs (Levchenko et al., 1997). These PDZ domains, found in the C-terminal regions of all PDZ-containing proteins, confer specific protein-protein interaction properties to

all members of the family (reviewed in Fanning and Anderson, 1996). However, not all known hsp100 targets have homologously tagged C-termini. In a recent study, another potential recognition factor--the sequence LD(A/L) at or near an a-helix--common to all observed hsp100 binding proteins was identified (Wawrzynow et al., 1996).

Therefore, ClpC's more likely role in chloroplast protein import involves protein turnover. Degradation in the stroma is ATP-dependent, or at least ATP-stimulated (Malek et al., 1984; Shanklin et al., 1995). Unassembled (Liu and Jagendorf, 1984; Schmidt and Mishkind, 1983) and mistargeted chloroplast (Halperin and Adam, 1996) proteins are also degraded in the stroma in an ATP-dependent manner. Since the abundant ClpC/ClpP protease system is the only ATP-dependent protease system identified to date, it is a strong candidate for a general housekeeping enzyme. This system could possibly serve at a branch point immediately following import to determine whether or not to allow the newly imported precursor to proceed with folding and assembly or to be degraded. ClpC's two nucleotide binding domains, which are common to prokaryotic permeation proteins (Squires and Squires, 1992), provide another possibility for ClpC function. ClpC most likely interacts directly with Tic110 (Akita et al., 1997; Caliebe et al., 1997; Nielsen et al., 1997) because, in isolated complexes which lack Tic110 (Schnell et al., 1994; Waegemann and Soll, 1991), ClpC is not present either.

Likewise, Cpn60 is also present in translocation complexes which contain Tic110 (Kessler and Blobel, 1996). Cpn60 is a Hsp60 chaperonin homolog which was originally described as the Rubisco binding protein (RBP) because of its ability to assemble the hexadecameric holoenzyme (Hemmingsen et al., 1988). Cpn60/Cpn10 are functional

homologs of the bacterial GroEL/GroES chaperonin system. Whether Cpn60 acts to aid in protein insertion into the inner envelope, promote translocation of precursor proteins, and/or fold newly imported proteins is not known.

SUMMARY

As this discussion has shown, the two disparate fields of research, molecular chaperones and protein trafficking, have been joined in recent years. That Hsp70s serve as molecular ratchets and motors in organellar translocation systems is now well established. Our laboratory is currently attempting to show that CSS1 drives protein import into the chloroplast in a similar manner. The following chapters are the initial groundwork en route to proving that thesis.

Chapter 2-*In vivo* and *in vitro* interaction between DnaK and a chlorpolast transit peptide

ABSTRACT

Chloroplast transit peptides have been proposed to function as substrates for Hsp70 molecular chaperones. Although many models of chloroplast protein import depict Hsp70's as the translocation motor that drives protein import into the organelle, no direct evidence has demonstrated that transit peptides function either *in vivo* or *in vitro* as substrates for the chaperone. In this report, we demonstrate that DnaK binds SStp *in vivo* (the full-length transit peptide for the precursor to the small subunit of Rubisco) when fused to either glutathione-*S*-transferase (GST) or to a His_6-S-peptide tag (His-S) via an ATP-dependent mechanism. Three independent biophysical and biochemical assays confirm the ability of DnaK and SStp to interact *in vitro*. The co-chaperones, DnaJ and GrpE, were also associated with the DnaK/SStp complex. Therefore, both GST-SStp and His-S-SStp can be used as affinity-tagged substrates to study chaperone/transit peptide interactions, as well as providing a novel, functional probe to study the dynamics of DnaK/DnaJ/GrpE interactions *in vivo*. The combination of these results provides the first experimental support of a transit peptide-dependent interaction between a chloroplast precursor and an Hsp70. These results are discussed in light of a general mechanism for protein translocation into chloroplasts and mitochondria.

INTRODUCTION

Although the chloroplast contains its own genome, the vast majority of chloroplast localized proteins are nuclear-encoded and synthesized as larger molecular weight precursors. These precursors contain an amino-terminal extension known as a transit peptide that is both necessary and sufficient to direct the targeting and translocation of precursors into the chloroplast with high fidelity (reviewed in Bruce and Keegstra, 1994). This transit peptide enables the productive interaction of precursors with the translocation apparatus of the chloroplast envelope. Early sequence analysis of transit peptides suggested the existence of three loosely conserved domains (Karlin-Neumann and Tobin, 1986). However, only recent work, combining both *in vitro* (Pilon et al., 1995; Pinnaduwage and Bruce, 1996; Bruce, 1998) and *in vivo* (Kindle, 1998; Rensink et al., 1998) approaches, has demonstrated that different regions of the transit peptide perform different functions in the import process. A persistent problem with this quasi-modular organization is that little to no homology exists between different transit peptides. This degeneracy is particularly difficult to explain and argues either for some unknown common secondary structure and/or for the involvement of an interaction which intrinsically requires low amino acid sequence specificity.

Although precursors targeted for different organelles lack homology in their targeting sequences mos current models of protein translocation across a membrane include a peripherally attached Hsp70 that functions as molecular motor (Craig et al., 1989; Ostermann et al., 1990; Scherer et al., 1990; Brodsky et al., 1995; Schatz and Dobberstein, 1996) Since the Hsp70 chaperones are known to have degenerate peptide substrate specificity, they are able to bind a diverse set of precursor proteins during import into these organelles. Although

not supported by direct evidence, current models of chloroplast protein transport assume a direct interaction between the transit peptide of the incoming precursor and the peptide binding domain of the molecular chaperone (Gray and Row, 1995; Keegstra et al., 1995; Heins et al., 1998). Consistent with these models, it has been the proposal that one of the functional properties of chloroplast transit peptides is as a substrate for Hsp70 chaperones. This proposal has been supported by a statistical analysis indicating that transit peptides are flexible structures enriched in sequences that are predicted to exist as a random coil (von Heijne and Nishikawa, 1991). Yet, to date there has been no evidence either for a direct interaction of transit peptides with Hsp70, nor is there clear agreement on the involvement of Hsp70 in the chloroplast protein import process (Soll and Waegemann, 1992; Nielsen et al., 1997).

In this study, we demonstrate the first direct interaction between a chloroplast transit peptide and the prokaryotic Hsp70 homologue, DnaK. Although not the physiological chaperone involved in chloroplast protein import, DnaK is highly homologous (>74 similarity) to the major chloroplast Hsp70, CSS1 (Marshall and Keegstra, 1992), and DnaK has been recently shown as a valid model chaperone for studying interactions between mitochondrial precursors and the mitochondrial Hsp70, SSC1 (Zhang et al., 1999). *In vivo* and *in vitro* evidence establish that the full length transit peptide for the precursor to the small subunit of Rubisco contains one or more sequences that function as a high affinity, ATP dependent substrate for DnaK. The implications of these findings on the interactions between precursors and molecular chaperones are discussed for chloroplast and mitochondrial protein import.

MATERIALS AND METHODS

Construction of vectors for expression of SStp

The pea prSSU gene in pSP65 (Promega) was digested with BamHI/SphI to release a 220 bp fragment which lacked the codons for the first five amino acids, MASMI, and the last two amino acids at the C-terminus, QY. This fragment was ligated into a BamHI/SphI digested pGEM-7Zf (Promega) to yield pGEM-7Zf-SStp[1]. To rebuild the C-terminus of SStp, pGEM-7Zf-SStp[1] was digested with SphI/ApaI and a linker was inserted which added codons encoding QY at the C-terminus. This linker also engineered a SmaI site to enable cloning into pGEX-2T (Pharmacia). This construct, pGEM-7Zf-SStp[2], was then digested with BamHI/EcoRV and a second linker was inserted which rebuilt the N-terminal MASMI sequence. This construct, pGEM-7Zf-SStp[3], was then digested with BamHI/SmaI to liberate a 188 bp fragment, which was inserted into a BamHI/SmaI digested pGEX-2T vector to form pGEX-2T-SStp. Primers corresponding to regions flanking the SStp-encoding region were used to amplify the insert via standard PCR protocols which engineered BamHI and EcoRI restriction sites at the 5' and 3' ends of the amplified product, respectively. The amplified product was digested and ligated into pET30a vector (Novagen) to yield pET30a-SStp. Both constructs were confirmed by DNA sequencing.

E. coli protein expression

The first construct (pGEX-2T-SStp), which placed the sequence encoding SStp in frame at the C-terminus of glutathione-S-transferase, was transformed into *E. coli* [BL(21)]. The cells were grown to a cell density corresponding to an OD_{600} of 0.6, induced with 100

μM isopropylthio-β-D-galactoside [IPTG] for one hour, pelleted, resuspended, and lysed by sonication on ice in PBS, pH 8.0 containing 1% (v/v) Triton X-100, 1 mM DTT, 5 mM EDTA, 2 mM leupeptin, 2 mM pepstatin, 1 mM PMSF, 5 mM 1,10-phenanthroline, and 3 mM ADP. The second construct (pET30a-SStp), which placed the SStp sequence at the C-terminus of the dual His-S tag, was transformed into *E. coli* [BL(21)(DE3)]. The cells were grown to a cell density corresponding to an $O.D._{600}$ of 0.6, induced with 1 mM IPTG for three hours, pelleted, resuspended, and lysed by sonication on ice according to a pET Manual protocol (Novagen).

Stepwise purification of DnaK, $SStp_{GST}$, and GST

The lysate was centrifuged at 25,000 x g for 30 min at 4 °C. The resulting supernatant was then loaded at 4 °C onto a 5 ml column of glutathione-Sepharose (Pharmacia). The column was first washed with 10 column volumes of PBS containing 1% Triton, then equilibrated with DnaK elution buffer (PBS, pH 8.0 containing 2 mM $MgCl_2$ and 50 mM KCl). DnaK was eluted with 3 mM ATP in the same buffer. Next, the column was equilibrated with thrombin buffer (PBS, pH 8.0 containing 2.5 mM $CaCl_2$). Thrombin (5 units) was then added onto the column in the same buffer and allowed to digest the fusion protein for 4-6 hours. After $SStp_{GST}$ elution in thrombin buffer, glutathione-S-transferase was eluted by equilibrating the column with PBS containing 5 mM reduced glutathione.

The lysate was centrifuged at 25,000 x g for 30 min at 4 °C. The resulting supernatant was then loaded at 4 °C onto a 5 ml column of glutathione-Sepharose (Pharmacia). The column was first washed with 10 column volumes of PBS containing 1% Triton, then

equilibrated with DnaK elution buffer (PBS, pH 8.0 containing 2 mM $MgCl_2$ and 50 mM KCl). DnaK was eluted with 3 mM ATP in the same buffer. Next, the column was equilibrated with thrombin buffer (PBS, pH 8.0 containing 2.5 mM $CaCl_2$). Thrombin (5 units) was then added onto the column in the same buffer and allowed to digest the fusion protein for 4-6 hours. After $SStp_{GST}$ elution in thrombin buffer, glutathione-S-transferase was eluted by equilibrating the column with PBS containing 5 mM reduced glutathione.

Purification of $SStp_{HIS}$

Purification of $SStp_{HIS}$ was carried out, unless otherwise noted, under denaturing conditions in urea according to a pET Manual protocol (Novagen). The fusion protein was digested with enterokinase after removing the urea with a linear gradient until the column was equilibrated with wash buffer (Novagen). Eluted $SStp_{HIS}$ was separated from the protease by ultra-filtration through a 30 kDa MWCO membrane and concentrated using a 1 kDa MWCO membrane. The peptide was then dialyzed into buffer A [25 mM Tris, 20 mM HEPES (pH 7.15), 47.5 mM KCl and 2.25 mM $Mg(OAc)_2$], aliquoted, and frozen at -85 °C.

Purification of $SStp_{HIS}$ was carried out, unless otherwise noted, under denaturing conditions in urea according to a pET Manual protocol (Novagen). The fusion protein was digested with enterokinase after removing the urea with a linear gradient until the column was equilibrated with wash buffer (Novagen). Eluted $SStp_{HIS}$ was separated from the protease by ultra-filtration through a 30 kDa MWCO membrane and concentrated using a 1 kDa MWCO membrane. The peptide was then dialyzed into buffer A [25 mM Tris, 20

mM HEPES (pH 7.15), 47.5 mM KCl and 2.25 mM $Mg(OAc)_2$], aliquoted, and frozen at -85 °C.

Circular dichroism, Tb^{+3} luminescence, and tryptophan fluorescence measurements

Circular dichrosim spectrometry was performed on a Jasco J-40A Spectropolarimeter at 20°C using circular quartz cells with pathlengths of 0.1 cm and a sensitivity setting of 1 x 10^{-5} to 5 x 10^{-6}. Upon addition of SStp, the complex was allowed to equilibrate at 20°C for 10 min. The CD spectra are reported in millidegrees optical rotation after baseline correction for the buffer (TBS plus Mg-ADP). Measurements of the DnaK/SStp complex were also corrected by substraction of the contribution of the transit peptide alone.

Intrinsic flourescence measurements of DnaK's single tryptophan were performed on a Perkin Elmer LS 50 B Luminescence Spectrometer. Samples were excited at 290nm with a slit with of 1 nm. DnaK (1 μM) was added to TBS in the presence of 3 mM MgADP. Purified SStp was added to yield a molar ratio of SStp : DnaK from 0-10. Upon addition of SStp the complex was allowed to equilibrate for 10 min at 20°C for 10 min. Spectra were read at 20°C at a scan rate of 1 nm/sec. All spectra were initially corrected by baseline subtraction (TBS plus MgADP).

Sensitized luminescence, arising from the resonance energy transfer from tryptophan to Tb^{+3}, was performed on a Perkin-Elmer LS 50 B Luminescence Spectrometer. For excitation of the tryptophan chromophore, the sample was excited using a pulsed xenon flash lamp with a pulse width at half-peak height of 10 μs. The decay time was 1 ms; the gate time was 10 ms. Excitation was at 290 nm; both the excitation and emission slit widths were set

at 5 nm. For phosphorescence measurements, equimolar concentrations of terbium chloride and disodium ATP were added to solutions containing either SStp, DnaK, or a mixture of both SStp and DnaK. Terbium's absorption spectrum overlaps tryptophan's emission spectrum, allowing non-radiative transfer upon excitation of tryptophan at 290 nm. The phosphorescence spectra of these solutions due to terbium emission were then collected from 450 to 650 nm.

Native gel shift competition assay with ^{125}I-RCMLA

DnaK binding competition studies with reduced, carboxymethylated α-lactalbumin radiolabeled with iodine (^{125}I-RCMLA)--similar to those performed by Freeman and co-workers (Freeman et al., 1995)--were carried out by incubating ^{125}I-RCMLA, DnaK, and the competing peptide (SStp) for 30 minutes at 37°C in Buffer A. Native Sample Buffer [100 mM Tris-HCl, pH 6.8 containing 10% (v/v) glycerol and 0.04% (w/v) bromphenol blue] was added and the samples were resolved by electrophoresis on a 6% native acrylamide gel: gel buffer, 400 mM Tris-HCl, pH 8.6; stacking gel, 4.5% (w/v) acrylamide with an acrylamide:bis-acrylamide ratio of 30:0.8 in 120 mM Tris-HCl, pH 6.8; running buffer, 25 mM Tris-HCl, pH 8.3 containing 192 mM glycine. The proteins were then fixed with acetic acid, the gels were dried, and autoradiograms developed. Quantitative scanning densitometry was performed with a Molecular Dynamics Model 3000 Series Computing Densitometer.

Glutathione-agarose affinity precipitation of *E. coli* chaperones

Small cell cultures (10 ml) were grown and induced normally but lysed by sonication in buffers contains different detergent and/or salt concentrations. The crude lysates were spun at 16,000 x g. Aliquots of each of the supernatants were added to microfuge tubes containing 100 µl of glutathione-Sepharose and mixed gently for five minutes at 4 °C. After washing the glutathione-Sepharose in batch three times with 1 ml of the same lysis buffer, SDS sample buffer was added directly to the glutathione-Sepharose to elute the bound proteins.

Electrophoresis, western blotting, and far-western blotting

All appropriate samples were boiled in reducing SDS-PAGE sample buffer, run on 10-20% gradient SDS-PAGE, and stained with coommassie brilliant blue (C.B.B.). Appropriate samples were electroblotted to polyvinyl difluoride [PVDF] membrane, and Western blots were performed with α-DnaK, α-DnaJ, α-GrpE, and α-GST antibodies. Secondary antibodies were conjugated to alkaline phosphatase. Far Western blots were performed on samples containing His-S-SStp with the RNAse S protein conjugated to alkaline phosphatase. All blots were developed with 5-bromo-4-chloro-3-indolyl phosphate [BCIP] and Nitro Blue Tetrazolium [NBT]. All appropriate samples were boiled in reducing SDS-PAGE sample buffer, run on 10-20% gradient SDS-PAGE, and stained with coommassie brilliant blue (C.B.B.). Appropriate samples were electroblotted to polyvinyl difluoride [PVDF] membrane, and Western blots were performed with α-DnaK, α-DnaJ, α-GrpE, and α-GST antibodies. Secondary antibodies were conjugated to alkaline phosphatase. Far Western blots were performed on samples containing His-S-SStp with the RNAse S

protein conjugated to alkaline phosphatase. All blots were developed with 5-bromo-4-chloro-3-indolyl phosphate [BCIP] and Nitro Blue Tetrazolium [NBT].

RESULTS

Association of DnaK with SStp fusion proteins in *E. coli*

The full-length transit peptide for the pea small subunit of Rubisco was cloned into pGEX-2T to generate a GST-SStp fusion (32 kDa) and into pET30a to produce a His-S-SStp fusion (11.5 kDa). The organization and sequence of the resulting SStp from both of these vectors is shown in Figures 2-1A and 2-1B. Both fusion peptides contain protease cleavage sites which allow the separation of SStp from the respective fusion partner. Routinely, 1-2 mg of the purified peptide was recovered per liter of *E. coli* culture using the pGEX expression system, whereas the pET system yielded 60-80 mg of purified peptide per liter of *E. coli* culture. Part of the discrepancy in yield may be due to the difference in solubility of the GST-SStp (highly soluble) and His-S-SStp (majority forms inclusion bodies) fusion proteins *in vivo*. GST-SStp is highly susceptible to cellular proteases in as little as 40 minutes after induction, as shown in Figure 2-2A, whereas His-S-SStp, a much smaller peptide with less overall structure, remains intact after three hours of induction (Figure 2-2B). The full-length transit peptide for the pea small subunit of Rubisco was cloned into pGEX-2T to generate a GST-SStp fusion (32 kDa) and into pET-30a to produce a His-S-SStp fusion (11.5 kDa). The organization and sequence of the resulting SStp from both of these vectors is shown in Figures 2-1A and 2-1B. Both fusion peptides contain protease cleavage sites which

Figure 2-1. Design of SStp fusion constructs. (A) Expression of SStp in pGEX-2T yields a 32.6 kDa fusion product with SStp attached to the C-terminus of glutathione-S-transferase. Upon cleavage with thrombin, the resulting $SStp_{GST}$ contains two additional N-terminal amino acids, glycine and serine. Also, both fusion proteins contain the first two amino acids (MQ) of the mature domain of small subunit and a tyrosine at the C-terminus of SStp. (B) Expression of SStp in pET-30a yields a 12.1 kDa fusion product with SStp attached to the C-terminus of the S-Tag epitope sequence. Upon cleavage with enterokinase, the resulting $SStp_{HIS}$ contains seven additional N-terminal amino acids, AMADIGS.

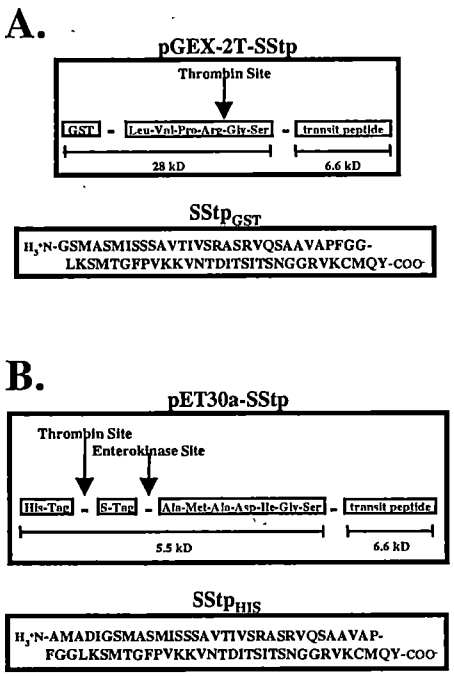

Figure 2-1. Design of SStp fusion constructs.

Figure 2-2. GST-SStp and His-S-SStp expression. (A) Western blot of *E. coli* whole cell extract with α-GST antibody at various stages of induction of GST-SStp expression. (B) Far western blot of *E. coli* whole cell extract with S-protein alkaline phosphatase conjugate during induction of His-S-SStp expression.

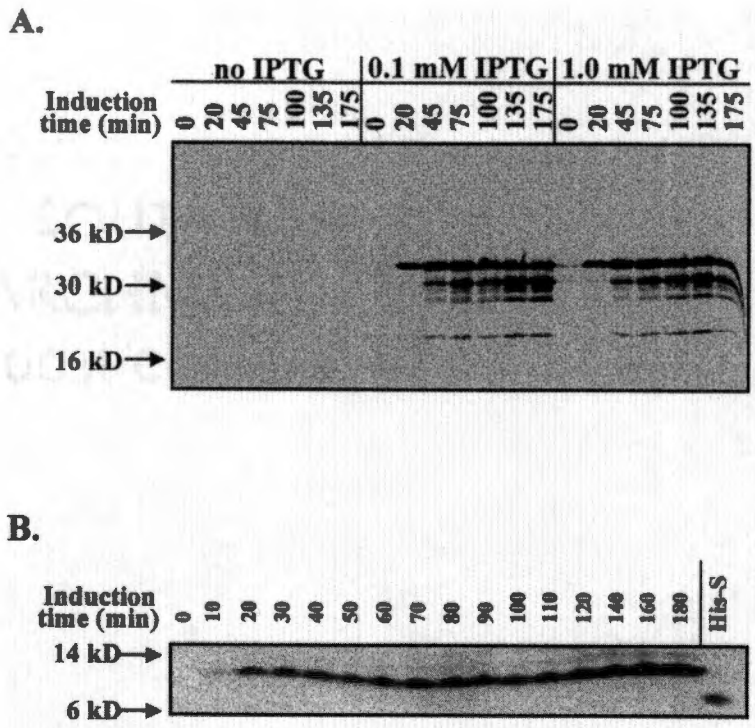

Figure 2-2. GST-SStp and His-S-SStp expression.

allow the separation of SStp from the respective fusion partner. Routinely, 1-2 mg of the purified peptide was recovered per liter of *E. coli* culture using the pGEX expression system, whereas the pET system yielded 60-80 mg of purified peptide per liter of *E. coli* culture. Part of the discrepancy in yield may be due to the difference in solubility of the GST-SStp (highly soluble) and His-S-SStp (majority forms inclusion bodies) fusion proteins *in vivo*. GST-SStp is highly susceptible to cellular proteases in as little as 40 minutes after induction, as shown in Figure 2-2A, whereas His-S-SStp, a much smaller peptide with less overall structure, remains intact after three hours of induction (Figure 2-2B).

When the GST-SStp fusion protein was eluted from the glutathione-Sepharose column, two major bands were routinely observed: GST-SStp with a molecular weight of ~32 kDa and a second protein with an apparent molecular weight of 70 kDa. The 70 kDa protein was strongly associated with GST-SStp, as extensive washing with 1% Triton and 1 M NaCl did not disrupt the complex (data not shown). Thrombin cleavage of the bound GST-SStp released $SStp_{GST}$ from GST, and the 70 kDa protein co-eluted with $SStp_{GST}$ from the glutathione-Sepharose column (Figure 2-3A). Attempts to separate $SStp_{GST}$ from this 70 kDa protein via ultra-filtration through a 30 kDa MWCO membrane yielded no protein in the flow-through (data not shown), further indicating the existence of a high molecular weight complex. Western blotting identified the 70 kDa protein as DnaK, the prokaryotic Hsp70 homologue (Figure 2-3B). This interaction was mediated through $SStp_{GST}$ since isolation of GST from cells containing the control pGEX-2T plasmid did not contain DnaK (discussed later).

Figure 2-3. Co-purification of DnaK and SStp. (A) C.B.B. stained SDS gel of the elution profile from a glutathione-Sepharose column after thrombin treatment. A 70 kDa contaminant protein (DnaK) co-elutes with $SStp_{GST}$. The minor band at 26 kDa, which is constant in every fraction, shows column leakage of cleaved GST. The 4 kDa band is an *in vivo* degradation product of SStp after 16 hours of induction. (B) Western blot of the fractions in (A) probed with α-DnaK confirmed that the contaminating protein is the molecular chaperone DnaK interacting *in vivo* with $SStp_{GST}$. (C) The imidazole elution profile from a Ni-Sepharose column was probed with α-DnaK (upper panel) in a western blot and with the S-protein-alkaline phosphatase conjugate (lower panel) in a far western blot. The cells were lysed under native conditions (without denaturant).

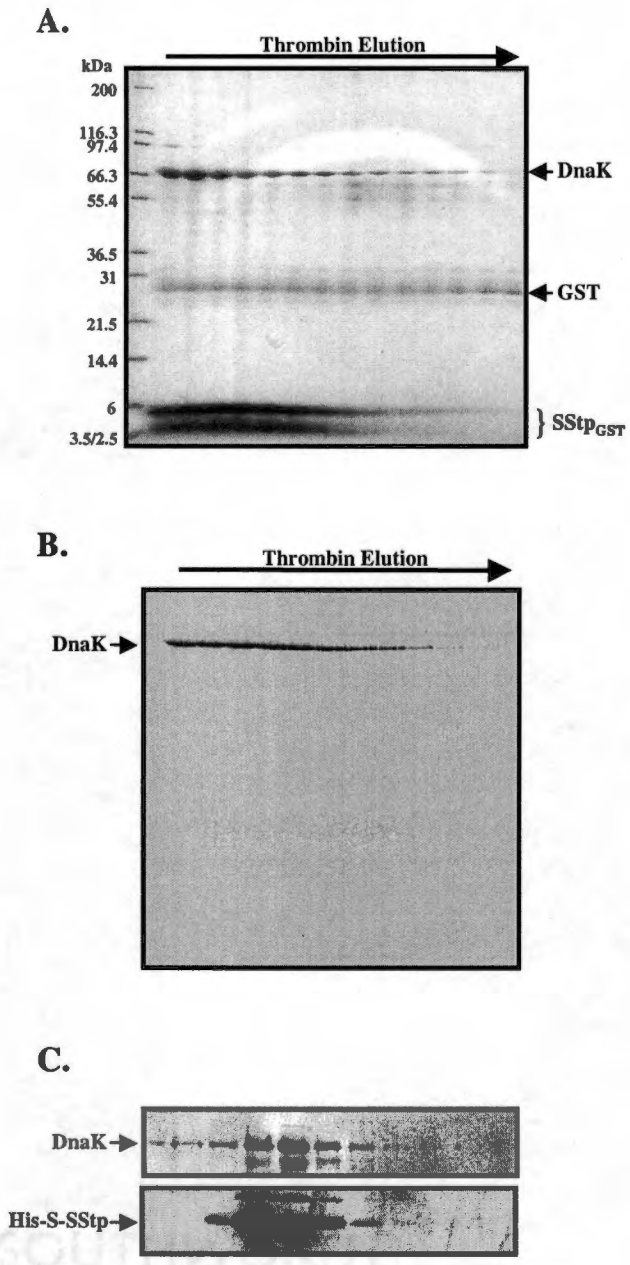

Figure 2-3. Co-purification of DnaK and Sstp.

To verify that the sequences responsible for DnaK interaction were localized in Sstp, a second fusion protein, His-S-SStp, was expressed in *E. coli*. When "native" lysate from these cells was applied to a Ni-Sepharose column, His-S-SStp and DnaK co-purified in the same fractions. This fusion protein allows the S-peptide epitope to be detected via its interaction with an alkaline phosphatase conjugate of S-Protein (Kim and Raines, 1993). Figure 2-3C shows a duplicate western and a far-western analysis of imidazole elution fractions, using an α-DnaK antibody in the former and an S-protein/alkaline phosphatase conjugate in the latter. Again, DnaK co-eluted with His-S-SStp. DnaK did not co-elute with the vector-encoded control peptide containing both the His-tag and the S-tag epitopes (data not shown). Taken together, these data strongly indicate that SStp contains sequences recognized by DnaK when expressed in *E. coli*. This DnaK/SStp association is independent of SStp's fusion partner and is seen for both moderate and strong levels of expression.

Purification of DnaK, $SStp_{GST}$ and GST

Binding and/or hydrolysis of ATP induces Hsp70s to undergo a conformation change which results in the release of their peptide substrates (Liberek et al., 1991; Szabo et al., 1994). Therefore, after sample loading and column washing, 3 mM ATP was used to elute pure DnaK from the glutathione-Sepharose column (Figure 2-4A). Subsequent thrombin digestion of the remaining protein on the column yielded pure $SStp_{GST}$ (Figure 2-4B), and finally, GST was eluted with 5 mM glutathione (Figure 2-4C). Thus, three proteins were sequentially purified from a total *E. coli* lysate utilizing a single chromatography step. That

Figure 2-4. Purification of $SStp_{GST}$. (A) C.B.B. stained SDS gel of the elution profile from a glutathione-Sepharose column after incubation with 3 mM ATP. DnaK elutes alone, leaving GST-SStp bound to the matrix. (B) C.B.B. stained SDS gel of the elution profile from the same glutathione-Sepharose column in (A) after subsequent thrombin treatment. Pure $SStp_{GST}$ elutes from the column. (C) GST elutes after subsequent equilibration with 5 mM glutathione.

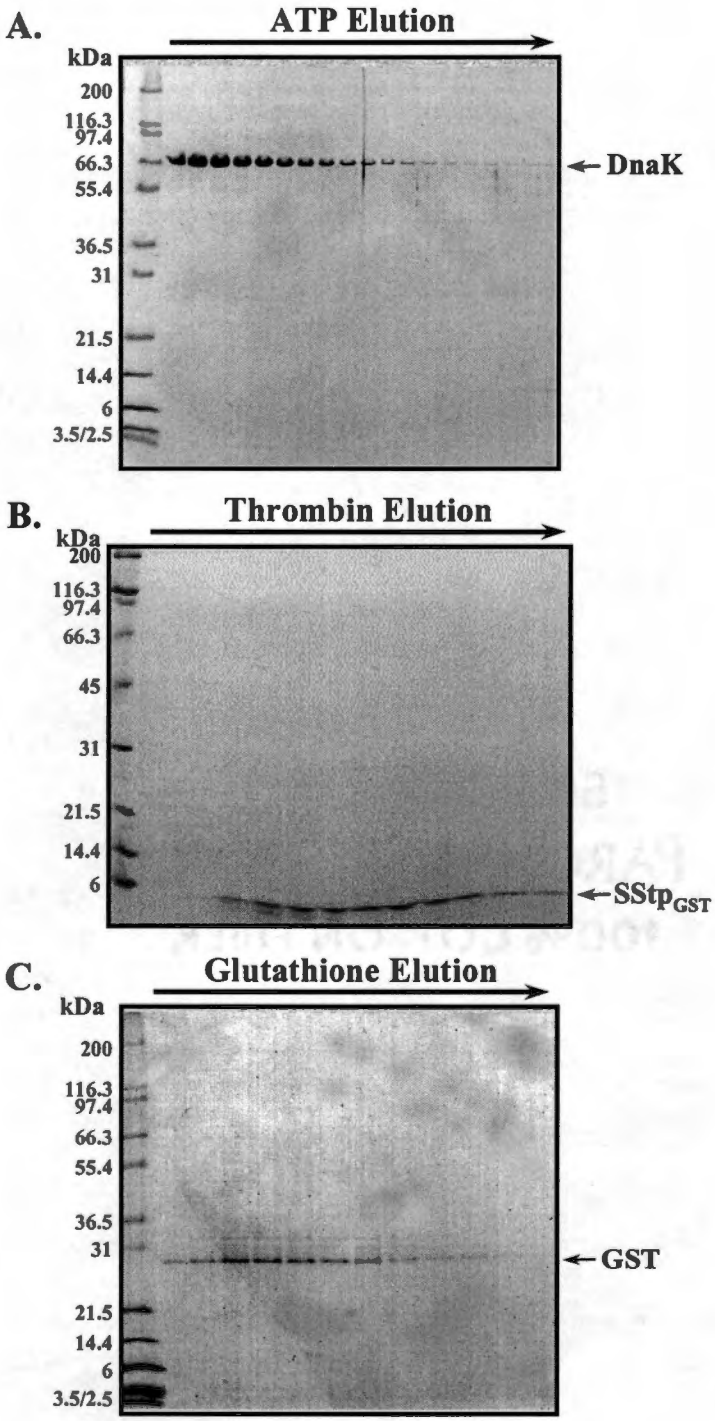

Figure 2-4. Purification of $SStp_{GST}$

$SStp_{GST}$ dissociated from DnaK in an ATP-dependent fashion indicated that it was bound via the peptide binding domain of DnaK, similar to other DnaK substrate

In vitro analyses of the DnaK-SStp interaction

To explore the ability of DnaK and SS-tp to interact *in vitro*, we conducted several biophysical and biochemical analyses to detect conformational changes in DnaK upon addition of SStp.

Initially, for a global average of possible peptide binding-induced secondary changes in DnaK, circular dichroism was performed in the presence and absence of SStp (Figure 2-5A). The increase in magnitude of the negative peak at 211 nm upon addition of SStp is similar to spectra previously observed for Hsc70/peptide complexes in which β-turn content increased (i.e., stabilized) while β-sheet content decreased (Park et al., 1993). Because conformationally extended peptide substrates bind to β-turns in DnaK's substrate binding domain (Zhu et al., 1996). This further shows SStp's authenticity as an *in vitro* DnaK substrate.

Next, analysis of DnaK's tryptophan fluorescence spectrum was utilized to determine if a secondary structural change at position 102 occurred upon SStp binding. Upon excitation at 290 nm, purified DnaK exhibited an emission peak at ~347 nm (Figure 2-5B), indicating that W102 resides in a relatively hydrophilic region of the native protein. Addition of SStp, even up to 10 times the molar ratio of DnaK, did not significantly affect the quantum yield or emission wavelength maximum; therefore, W102 remains in a hydrophilic environment when DnaK is bound to SStp. Given that W102 is positioned at the surface of DnaK,

Figure 2-5. *In vitro* analyses of DnaK/SStp interaction. (A) Circular dichroism spectra of DnaK (500 nM) in the presence and absence of SStp (500 nM). (B) Tryptophan fluorescence emission spectra of DnaK (1 μM) in the presence and absence of SStp. (C) Stimulated luminescence spectra of Tb^{+3} (300 μM) complexed to ATP (300 μM) in the presence and absence of DnaK (1 μM) and/or SStp (1 or 2 μM as indicated). (D) Native gel shift competition assay with ^{125}I-RCMLA (7 μM), DnaK (0.7 μM), and SStp (70 μM). *Putative $DnaK_{dimer}$: ^{125}I-RCMLA complex; **Putative $DnaK_{monomer}$: ^{125}I-RCMLA complex; ***unbound ^{125}I-RCMLA.Peptide #1 = GKGDDIFVHRKGDGND; Peptide #2 = DGNDIITDSDGNDKLSFS.

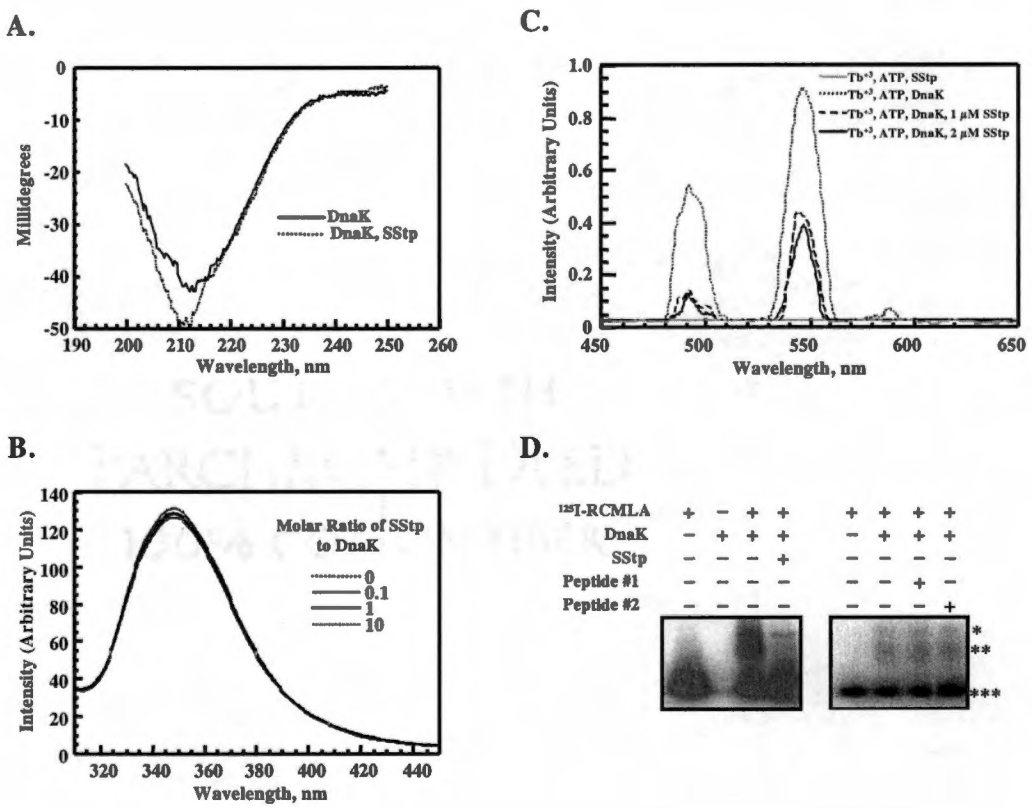

Figure 2-5. *In vitro* analyses of the DnaK-SStp interaction.

specifically at the "tip" of subdomain 2 of the ATPase domain (Harrison et al., 1997), these findings are not surprising.

To demonstrate that SStp binding *in vitro* affects DnaK's ATPase domain as well, energy transfer experiments were conducted to observe any distance changes between W102 and the ATP binding site at the opposite end of DnaK's subdomain 2 (Harrison et al., 1997) upon addition of SStp. Terbium(III) complexed to ATP at DnaK's ATP binding site allowed for a specific luminescence labelling strategy to observe this phenomenon. Upon addition of TbATP to purified DnaK and initial excitation of W102 at 290 nm, Tb^{+3} exhibited characteristic sensitized luminescence dependent on excitation by W102 emission at 320 nm (Figure 2-5C). When an equimolar amount of SStp was added, the luminescence intensity decreased, indicating an increased distance between W102 and Tb^{+3} upon SStp binding. The affect was also saturatable, because doubling the amount of SStp did little to change the luminescence signal; therefore, SStp interacts with DnaK in a 1:1 stoichiometric ratio, consistent with current evidence and models for other peptides. SStp alone did not stimulate Tb^{+3} luminescence. Because the R_0 value for tryptophan (donor) and Terbium (acceptor) (Kwok and Churchich, 1994) is many fold less than the distance between W102 and the ATP-binding site (Harrison et al., 1997), no specific distance calculations were attempted. However, the smaller peak values were caused by conformational changes and not ATP hydrolysis because nucleotide exchange, not hydrolysis, is the limiting step in the ATP cycle of DnaK (see Chapter 1 for discussion).

Finally, to show that SStp can competitively bind DnaK, native gel shift assays were performed with ^{125}I-RCMLA and purified DnaK. Several studies have previously shown that

the permanently unfolded nature of RCMLA allows it to function as a model substrate for DnaK and other Hsp70 homologues (Cyr et al., 1992; Freeman et al., 1995). By co-incubating DnaK with both ^{125}I-RCMLA and a competing non-labeled substrate, the relative affinities for the two substrates can be evaluated. The autoradiograph in the left panel of Figure 2-5D shows two new bands of lower electrophoretic mobility when ^{125}I-RCMLA was incubated with DnaK (lane 3). These two bands probably reflected ^{125}I-RCMLA association with a monomer and dimer form of DnaK similar to what has been observed in other reports (King et al., 1995; Schonfeld et al., 1995). When purified SStp was added to the incubation at a 3.6-fold mass excess relative to ^{125}I-RCMLA, the two bands with lower mobility were disrupted and RCMLA regained its original mobility. Scanning densitometry of these bands indicated that less than 10% of the original radiolabeled complex persisted in the presence of SStp, indicating that SStp successfully competed as an alternative substrate for DnaK. In fact, SStp prevented the formation of both $DnaK_{monomer}$:^{125}I-RCMLA and $DnaK_{dimer}$:^{125}I-RCMLA complexes. The right panel of Figure 2-5D shows two competitor peptides with sequences unrelated to SStp and which failed to compete with ^{125}I-RCMLA for DnaK binding.

Purification of a cellular DnaK/DnaJ/GrpE chaperone complex

Glutathione-Sepharose affinity precipitation was used to evaluate the ability of $SStp_{GST}$ to associate simultaneously with not only DnaK but also other members of the *E. coli* DnaK chaperone machine. When the *E. coli* cells were lysed under mild conditions (Figure 2-6; no detergent, NaCl at low, medium, and high concentrations) DnaK, DnaJ, and GrpE

Figure 2-6. Co-Chaperones are affinity-precipitated with DnaK and GST-SStp. Western blots of purified complexes using various cell lysis conditions (see Materials and Methods). **U** = uninduced cells (no IPTG) and **I** = induced cells (100 mM IPTG). The blot in the top panel was probed with α-DnaK; the second panel, α-DnaJ; the third panel, α-GrpE; and the bottom panel, α-GST. Note the *in vivo* proteolytic degradation of GST-SStp under all lysis conditions.

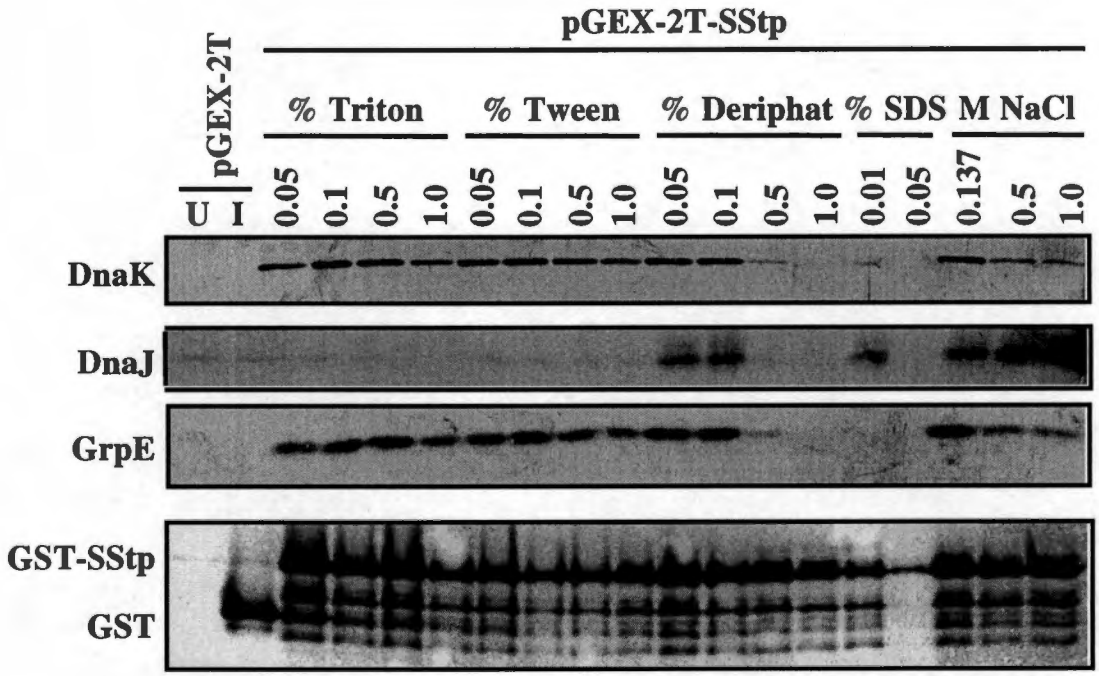

Figure 2-6. Co-Chaperones are affinity-precipitated with DnaK and GST-SStp.

all co-precipitated with GST-SStp. Neither DnaK, DnaJ, nor GrpE were co-precipitated from lysates of cells transformed with the control plasmid pGEX-2T (Figure 2-6, pGEX-2T). Consistent with results described above, these findings indicate that sequences contained within $SStp_{GST}$ mediates the interaction with chaperones. Interestingly, the interaction between DnaK and GrpE is quite stable and is detected under all of the lysis conditions except high concentrations of the zwitterionic detergent, Deriphat-160, and the anionic detergent, SDS. Conversely, DnaJ co-precipitated only with low concentrations of Deriphat-160 and SDS, or with no detergent (NaCl only). Whether DnaJ's association with the complex was mediated via direct interaction with $SStp_{GST}$ or, alternatively, by its association with the other chaperones, has not been determined. Nonetheless, co-purification of the entire DnaK chaperone complex provides further direct evidence that $SStp_{GST}$ serves as an Hsp70 substrate in a cellular environment, albeit a microbial one.

DISCUSSION

A direct interaction between the Hsp70 class of molecular chaperones and chloroplast transit peptides has been proposed previously (von Heijne and Nishikawa, 1991). Although several recent studies have attempted to identify the linear peptide sequences recognized by Hsp70s (Blond-Elguindi et al., 1993; Gragerov et al., 1994; Rudiger et al., 1997), none have directly analyzed precursor proteins or their targeting sequences. However, it has been shown recently that by applying results on the peptide binding preference for DnaK to a group of mitochondrial presequences, that, as a rule, they are are predicted to contain sequences which function as good substrates for DnaK binding (Zhang et al., 1999). The validity of this

observation is strengthened by molecular modeling data that suggests that the peptide binding cavity of the mitochondrial chaperone, SSC1, is very similar to the binding site on DnaK that has been solved by crystallography (Zhu et al., 1996). In this report, we demonstrate the first direct interaction between the Hsp70 class of molecular chaperones and a full-length targeting sequence. Specifically, the chloroplast transit peptide, SStp, was observed to co-purify with DnaK under all but the harshest buffer conditions, indicating a tightly bound complex. This DnaK/SStp interaction is independent of SStp's fusion partner and is specific for sequences in the transit peptide since DnaK failed to associate with either GST or the dual epitope tag, His-S alone. This interaction is mediated through the DnaK peptide-binding domain and like other high affinity substrates, SStp's association is modulated by the status of nucleotide binding.

The stability of the DnaK/SStp interaction was sufficient to allow purification of the entire DnaK/DnaJ/GrpE chaperone complex. This represents the first demonstration of an affinity-tagged substrate able to recover the in vivo assembled chaperone complex. An artificial substrate, CRAG, was shown to be recognized by DnaK when expressed in E. coli (Sherman and Goldberg, 1991). However, this substrate was also found to bind large quantities of GroEL (E. coli Hsp60) as well as lower amounts DnaK. In addition, the La protease and several other unidentified proteins were also observed to bind CRAG. These additional interactions plus the fact that a significant amount of DnaK (~30%) could not be released from the CRAG protein with ATP, argue for more than one mode of chaperone interaction and suggest possible non-specific interactions. In contrast, our work has shown that SStp is specific for DnaK and can be readily removed by ATP treatment. For these

reasons, we propose that SStp is an ideal DnaK substrate that can be used to explore the reaction dynamics of the DnaK chaperone cycle both in vivo and in vitro. Expression of SStp could also be used to monitor the effects of cellular and environmental stress on chaperone expression.

Finally, a productive Hsp70/transit peptide interaction might play an important role during the course of chloroplast protein import. In mitochondria, a precursor's targeting sequence has been proposed to interact with Hsp70 not only to facilitate translocation, but also to present the site of proteolytic cleavage to the matrix processing protease (Klaus et al., 1996). This interaction is supported by an earlier observation that the precursor for mitochondrial aspartate aminotransferase bound to DnaK (Schmid et al., 1992). However, unlike SStp, this interaction did not include the co-chaperones, DnaJ or GrpE, and was easily disrupted by low salt treatment. The fact that no complex was found with the mature protein suggests that DnaK recognition may be via the presequence as predicted recently (Zhang et al., 1999). However, in chloroplast protein transport, a strong Hsp70-transit peptide interaction may occur at more than one site during protein import. In fact, four different Hsp70 homologues are associated with the chloroplast: Com70 binds to the outer surface of the outer envelope (Ko et al., 1992), IAP70 resides within the intermembrane space (Marshall et al., 1990), CSS1 is the major stromal Hsp70 (Marshall et al., 1990), and a thylakoid lumen homologue was most recently discovered (Schlicher and Soll, 1996). The possible involvement of multiple Hsp70s in the chloroplast protein import pathway may constitute a significant difference between the protein translocation apparatus of the chloroplast, which contains a robust "unfoldase" activity able to overcome the folded status

of a precursor (Guera et al., 1993; America et al., 1994; Clark and Theg, 1997), and that of mitochondria, which cannot drive the import of "tightly-folded" precursors (Eilers and Schatz, 1986; Vestweber and Schatz, 1988). The placement of Com70 at the outer envelope and IAP70 in the inter-membrane space would provide two additional ATP-dependent sites for protein unfolding (Schnell et al., 1994; Kourtz and Ko, 1997). The ability of IAP70 to function as a "molecular motor" in the intermembrane space would also provide a mechanism to allow precursors to cross the chloroplast envelope one membrane at a time, as was recently reported (Scott and Theg, 1996).

Additional work in our laboratory has analyzed the transit peptides in the CHLPEP database (von Heijne et al., 1991) using the data of Rudiger and co-workers (1997) and found that most transit peptides are predicted to contain at least one predicted Hsp70 binding site (Ivey and Bruce, manuscript in preparation). Statistical analysis of the placement of these Hsp70-interacting regions suggest that primarily sequences at the N-terminus are responsible for this interaction. This observation is very intriguing since a similar analysis of mitochondrial presequences has observed a similar N-terminal placement of Hsp70-interacting domains (Zhang et al., 1999). The commonality of these two observations argues for a universal placement and involvement of Hsp70-interacting domains in the post-translational transport of proteins into both the chloroplast and mitochondria. Perhaps this observation is not surprising considering the organelles' common prokaryotic origins and evolution via endosymbiosis. It will be interesting to determine if chloroplast and mitochondrial Hsp70 homologs bind transit peptides *in vivo* and to determine where within the targeting sequence this interaction takes place.

Chapter 3-Identification of a Hsp70 recognition domain with the Rubisco small subunit transit peptide

ABSTRACT

The interaction between SStp and two Hsp70 molecular chaperones, *E. coli* DnaK and *P. sativum* CSS1, was investigated in detail. Two statistical analyses were developed and used to investigate and predict regions of SStp recognized by DnaK. Both algorithms suggested that DnaK would have high affinity for the N-terminus of SStp, moderate affinity for the central region, and low affinity for the C-terminus. Furthermore, both algorithms predicted this affinity pattern for >75% of the transit peptides analyzed in the CHLPEP database. *In vitro* association between SStp and these Hsp70s was confirmed by three independent assays: limited trypsin resistance, ATPase stimulation, and native gel shift. Finally, synthetic peptides scanning the length of SStp and C-terminal deletion mutants of SStp were used to experimentally map the region of greatest DnaK affinity to the N-terminus. CSS1 displayed a similar affinity for the N-terminus of SStp. The major stromal Hsp70's affinity for the N-terminus of SStp and other transit peptides supports a molecular motor model in which the chaperone functions as an ATP-dependent translocase, committing chloroplast precursor proteins to unidirectional movement across the envelope.

INTRODUCTION

The semi-autonomous chloroplast, which contains its own genome, acquires the vast majority of its proteins as nuclear-encoded, larger molecular weight precursors synthesized in the cytosol and transported across the envelope membranes. These precursors contain an amino-terminal extension known as a transit peptide, which is both necessary and sufficient to direct the targeting and translocation of precursors with high fidelity (reviewed in Bruce and Keegstra, 1994). Specifically, transit peptides enable the productive interaction of precursors with two distinct membrane protein complexes: the Toc components and Tic components (Schnell et al., 1997). Recent progress has been made in identifying many of the individual components associated with Tic (Kouranov et al., 1998; Lubeck et al., 1996) and Toc (Hirsch et al., 1994; Kessler et al., 1994; Seedorf et al., 1995). However, with the exception of the Hsp70 homologs, none of the components identified to date are related to proteins identified in the other membrane translocation systems, such as bacterial secretion, mitochondria, and the endoplasmic reticulum (Schatz and Dobberstein, 1996).

In contrast, much less progress has been reported on the molecular analysis of the functional properties of the transit peptide itself. Despite >250 transit peptides sequences in the CHLPEP database (von Heijne et al., 1991) and hundreds of more recently identified transit peptides, few in-depth structural or functional analyses of these sequences are in evidence (Krimm et al., 1999; Lancelin et al., 1994; Wienk et al., 1999). However, arguments have recently been made to suggest that transit peptides are modular, with discrete domains providing different functional roles. Although early

sequence analysis suggested the existence of three semi-conserved domains (Karlin Neumann and Tobin, 1986), only recent work combining both *in vitro* (Bruce, 1998; Pilon et al., 1995; Pinnaduwage and Bruce, 1996) and *in vivo* (Kindle, 1998; Rensink et al., 1998) approaches demonstrates that different regions of the transit peptide perform different functions in the import process. Although these analyses have only been performed for a few transit peptides, the emerging consensus is that transit peptides contain three functional domains. The N-terminal domain appears to perform an essential yet undefined role in the initiation and commitment of the precursor to translocation, the central region is more dispensable, functioning as a flexible hinge region between the N- and C-terminus, and finally the C-terminus may be involved both in lipid interaction and in correct processing by the stromal processing peptidase. An obvious problem with this modular organization is that transit peptides vary widely in length and share very limited sequence homology. This sequence degeneracy is particularly difficult to explain in light of the essential role that the N-terminus performs in chloroplast import (Kindle, 1998; Pilon et al., 1995). Therefore, either a common yet unknown secondary structure or the involvement of an interaction which intrinsically requires low sequence specificity would provide the best hypothesis for the mechanism of transit peptide function.

Most of the current models of protein translocation include a peripherally attached molecular motor (Schatz and Dobberstein, 1996). In the mitochondria and the ER, this motor is believed to be a Hsp70 molecular chaperone. The involvement of Hsp70 as the molecular motor assumes a direct interaction between the incoming precursor and the peptide binding domain of the molecular chaperone, and most current

models show the targeting sequence as the region of the precursor that is recognized by the chaperone (Gray and Row, 1995; Heins et al., 1998; Keegstra et al., 1995). Indeed, a recent study shows significant interaction between mitochondrial presequences and DnaK (Zhang et al., 1999). Consistent with these models, chloroplast transit peptides have been suggested to serve as substrates for Hsp70 chaperones (von Heijne and Nishikawa, 1991). Although this proposal is supported by statistical analyses indicating that transit peptides are enriched in sequences predicted to exist as random coils, to date only one report has demonstrated a direct interaction between a transit peptide and Hsp70 (Ivey and Bruce, 1999). In any event, no clear agreement exists for the involvement of Hsp70s in the chloroplast protein import process (Nielsen et al., 1997; Soll and Waegemann, 1992).

In this report we have investigated the chloroplast transit peptide sequences which enable it to function as a substrate for the Hsp70 class of molecular chaperones. Based on the results of two independent statistical algorithms which calculate an index of DnaK affinity, we predict that the transit peptide for prSSU (SStp) contains two regions which should be recognized by DnaK. When these algorithms are applied to the transit peptides in the CHLPEP database, >95% of the transit peptides analyzed contained at least one potential DnaK recognition domain. Furthermore, these sequences occurred predominantly at the N-terminus of the transit peptide. We have verified this interaction for SStp by three *in vitro* assays: a proteolysis protection assay with DnaK, substrate stimulation of ATPase activity with CSS1, and a native gel shift assay with both Hsp70s. Finally, we have confirmed the algorithms' predictions by partially mapping the transit

peptide regions responsible for DnaK/CSS1 interaction using both co-affinity precipitation of DnaK and the *in vitro* native gel shift assay. The results of these observations are discussed in the context of both transit peptide design and the potential involvement of Hsp70s as the chloroplast translocation molecular motor.

MATERIALS AND METHODS

Predictive DnaK affinity algorithms

Phage Display Based Algorithm- In work by Gragerov and co-workers (Gragerov et al., 1994), an index of each amino acid's appearance in high-affinity vs. low-affinity peptides in a RPPD library were calculated. For example, the value determined for leucine was 2, reflecting the ratio of frequency of occurrence of leucine found in selected vs. unselected phage. Using these values, we developed a simple algorithm using a sliding six amino acid window in one amino acid steps to predict DnaK's affinity to transit peptides in the CHLPEP and PTP99 (Ivey et al., manuscript in preparation) databases. For each window, we multiplied the indices of six adjacent amino acids in SStp:

$$A_n = i_{n-2} \times i_{n-1} \times i_n \times i_{n+1} \times i_{n+2} \times i_{n+3}$$

where A_n is an index of the six-amino acid window's affinity for DnaK, i_n is the third residue in the window, i_{n+1} is the fourth residue, etc. Methionine, cysteine, and glutamate were statistically underrepresented in the display library, so we assigned them values of 1 for equal probability of being in a strongly or weakly selected peptide. Based on values obtained when the algorithm was applied to several peptides described in the original

study, we designated a "cut-off" index value of 2.0. Therefore, a six amino acid window with an index value greater than 2.0 is predicted to have an affinity for bind DnaK, similar to a strongly selected peptide from the original study.

Cellulose Display Based Algorithm- A second, more recent report utilized 3725 synthetic, cellulose-bound peptides (13mers) which span the length of 37 naturally occurring proteins to develop a CBPS algorithm for DnaK affinity (Rudiger et al., 1997). In this study, each amino acid is assigned a $\Delta\Delta G^{\circ}$ value that reflects the change in free energy of the DnaK/peptide complex when that amino acid is present. Because of the apparent preferences of different amino acids to accommodate different positions relative to the center of the DnaK peptide-binding pocket, three $\Delta\Delta G^{\circ}$ values are assigned to each amino acid. As described in Rudiger et al. (1997),

$$A_n = (0.33 * L_{n-6}) + (0.66 * L_{n-5}) + (1.00 * L_{n-4}) + (1.33 * L_{n-3}) + C_{n-2} + C_{n-1} + C_n +$$

$$C_{n+1} + C_{n+2} + (1.33 * R_{n+3}) + (1.00 * R_{n+4}) + (0.66 * R_{n+5}) + (0.33 * R_{n+6})$$

where A_n is an index of the 13 amino acid window's affinity for DnaK, n describes the amino acid's position relative to the center of DnaK's binding site, and L, C, and R are experimentally derived values for each amino acid left-of-center, center, and right-of-center, respectively. The weighting values (0.33, 0.66, 1.00, and 1.33) were statistically determined by Rudiger and co-workers (1997) to maximize the accuracy of the algorithm. We applied this algorithm via a sliding 13 amino acid window in one amino acid steps to predict DnaK's affinity to transit peptides in the CHLPEP database. Based on values obtained when the algorithm was applied to two peptides described in the original study, we designated a "cut-off" index value of –4.0. Therefore, a 13 amino acid

window with a $\Delta\Delta G^{o}$ value less than –4.0 is predicted to bind DnaK similarly to a strongly selected peptide from the original study.

SStp fusion proteins

SStp fusions with GST (pGEX vector, Pharmacia) and the dual His-S Tag (pET vector, Novagen) as well as DnaK were expressed and purifed as described previously (Ivey and Bruce, 1999). SStp derived from the His-S Tag system was used for all *in vitro* analyses involving purified components.

C-terminal deletions of His-S-SStp were generated via Exonuclease III digestion using the Erase-a-Base kit (Promega). Briefly, pET30a-SStp was linearized with HindIII, and the 5' overhangs were filled in with α-phosphorylthiolates to generate blunt, exonuclease-resistant ends. This linear plasmid was then restricted with EcoRI to generate a single 5' overhang for ExoIII digestion. The exonuclease reaction was stopped at timed intervals, and the samples were treated with S1 nuclease and Klenow fragment to generate blunt, ligatable ends. The mixed plasmid species were recircularized, transformed into *E. coli* cells, and screened using direct colony PCR with the forward and reverse T7 promoter primers. Isolated DNA from appropriate transformants was sequenced using an ABI 373 automated sequencer. Three deletion mutants--His-S-SStpΔ5, His-S-SStpΔ25, and His-S-SStpΔ36--lacking 5, 25 and 36 amino acids, respectively, from the C-terminus of full length His-S-SStp were selected for use in these studies. Coincidentally, all the deletions were in frame with the optional, C-terminal His-Tag engineered into the pET30a vector.

Limited trypsin proteolysis of DnaK

DnaK was subjected to trypsin digestion (5 ng/mg Hsp70), as in (Freeman et al., 1995) in 50 µl reactions for 60 minutes at 37 °C in Buffer C (20 mM Tris-HCl, pH 6.9, 100 mM EDTA, 100 mM NaCl). Subsequent assays also contained α-lactalbumin, RCMLA, or SStp as potential DnaK substrates. Aliquots were removed during the course of the digestion and immediately boiled in SDS Sample Buffer (100 mM Tris-HCl, pH 6.8 containing 10% (v/v) glycerol, 0.04% (w/v) bromphenol blue, 0.1% (w/v) SDS). The samples were run on SDS-PAGE with protein visualization by C.B.B. staining. Quantitative scanning densitometry was performed using a Molecular Dynamics Model 3000 Series Computing Densitometer.

Purification of CSS1 from *P. sativum*

CSS1 was purified from 14 day old cotyledons applying an affinity chromatography method similar to that used to purify Hsc70 (Schlossman et al., 1984). Fractionated stroma from *P. sativum* was prepared (Bruce et al., 1994) and diluted 1:10 with Buffer M [20mM HEPES (pH 7.5), 20 mM NaCl, 2.5 mM $Mg(OAc)_2$, 1 mM DTT, and 0.1% Triton X-100]. Next, the entire sample was loaded onto an ATP-agarose column (Sigma, Catalog # A-2767) pre-equilibrated with Buffer M at 4°C. The column was washed exhaustively with Buffer M, then Buffer M containing 1 M NaCl, and finally Buffer M again. CSS1 was then eluted with 10 mM ATP in Buffer M titrated to pH 7.5. The authenticity of CSS1 was demonstrated via cross-reactivity on a Western blot probed with a polyclonal α-DnaK antiserum. Eluted fractions containing CSS1 were dialyzed

exhaustively and concentrated in Buffer M by ultra-filtration against a 30 kD MWCO membrane, aliquoted, and stored at -85 °C.

CSS1 ATPase activity

ATPase activity assays were performed with [γ-^{32}P]ATP in Buffer M as previously described (Sadis and Hightower, 1992). Each 50 µl reaction contained CSS1, unlabeled ATP, and [γ-^{32}P]ATP and was incubated at 37 °C. Peptide substrates were provided at 100-fold molar excess relative to the chaperone. Aliquots of the reaction mixture were withdrawn at regular intervals and mixed with 1 ml of 50 mM HCl / 5 mM H_3PO_4 containing 7% (w/v) activated charcoal. After microcentrifugation, 200 µl aliquots of the free ^{32}Pi-containing supernatants were removed and counted via scintillation. Monitoring spontaneous ATP hydrolysis was necessary because Hsp70 ATPase activities are extremely low.

Spreadsheet for ATPase assays of Hsp70s using [γ-^{32}P]-ATP

Calculation of Hsp70's ATPase activity from the extremely sensitive assay which uses [γ-^{32}P]-ATP was not trivial. Therefore, we developed a flexible spreadsheet (Figure 3-1) which takes user data and calculates specific activities while displaying the key factors in the calculation. The following is a step-by-step example of how the spreadsheet was used.

Figure 3-1. ATPase activity calculation spreadsheet. User data is input on the left column. The spreadsheet then adjusts the calculations to compensate for radioactive decay, Hsp70 concentration, and dilution factors before generating the specific ATPase activity in pmol ATP / min / pmol Hsp70.

^{32}P-ATPase Assays									
Assay Description:									
Name:									
Experiment Date (M/D/Y):									
Comments:									
Specific Activity:	3000	Ci/mmol		Isoptope Decay Correction Factor:			1.050		
Isotope Reference Date (M/D/Y):	2/4/98			Corrected Specific Activity:			3149	Ci/mmol	
Counting Date (M/D/Y):	2/3/98								
Specific Activity per Volume:	0.01	mCi/µl		Corrected Specific Activity per Volume:			0.010	mCi/µl	
Dilution Factor of Isotope:	1			Diluted, Corrected Spec. Act. per Volume:			0.01050	mCi/µl	
Isotope Volume per Reaction:	0.2386	µl			Isotope Concentration:		3.33E-06	M	
Cold ATP Concentration:	50	µM		Diluted Isotope Concentration:			3.33E-06	M	
Reaction Volume:	50	µl		Isotope Conc. in Reaction:			1.59E-08	M	
Hsp70 mass / Assay:	1	µg		Ci Concentration in Reaction:			5.01E-08	Ci/µl	
Hsp70 MW:	78000	Da			Ratio of Cold:Hot ATP		3143		
Time-point Volume:	8	µl				1 Ci:	2.22E+12	dpm	
HCl/Charcoal Volume:	500	µl			Ci per Time-point:		4.01E-07	Ci	
Scintillation Sample Volume:	75	µl			dpm per Time-point:		8.90E+05	dpm	
Counting Efficiency:	1.00				Isotope per Time-point:		1.27E-13	mol	
Isotope Purity Factor:	90	%		HCl/Charcoal Dilution Factor:			0.016		
				Scintillation Fraction Factor:			6.667		
					Hsp70 Molecules:		1.28E-11	mol	
	Experimental	0	5	10	15	20	Δ cpm /		pmol ATP / min
Sample	Condition	min (cpm)	min (cpm)	min (cpm)	min (cpm)	min (cpm)	min	R-squared	/ pmol Hsp70
1	ATP Only						#DIV/0!	#DIV/0!	
2	nCSS1+buffM	1895	2590	2822	4086	4257	125.3	0.9468062	2.07

Figure 3-1. ATPase activity calculation spreadsheet.

Definitions of variables

1) Specific Activity: enrichment of γ-^{32}P in ATP sample; supplied by manufacturer in Ci/mmol.

2) Isotope Reference Date: date to which specific activity is normalized.

3) Counting Date: date on which samples are counted via scintillation after ATPase assays are performed.

4) Specific Activity per Volume: specific activity of [γ-^{32}P]-ATP multiplied by the mmol of [γ-^{32}P]-ATP present, then divided by volume of the stock solution; both mmol and volume are supplied by the manufacturer.

5) Dilution Factor of Isotope: multiplicative factor by which [γ-^{32}P]-ATP is diluted before addition to reaction samples.

6) Isotope Volume per Reaction: volume of diluted isotope added to each reaction sample.

7) Cold ATP Concentration: concentration of unlabeled ATP in the reaction samples.

8) Reaction Volume: total volume of each of the reaction samples.

9) Hsp70 mass / Assay: mass of the individual Hsp70 in each of the reaction samples.

10) Hsp70 MW: molecular mass of the particular Hsp70 used in the reaction samples.

11) Time-point Volume: volume of reaction sample removed and added to the HCl/HPO_4/charcoal mixture at each time point.

12) HCl/Charcoal Volume: volume of the HCl/Charcoal mixture to which the time-point volume is added.

13) Scintillation Sample Volume: volume of the supernatant from the HCl/Charcoal mixture added to the scintillation fluid.

14) Counting Efficiency: assumed to be 100% for the high-energy β-particle emitted during ^{32}P decay; therefore, the multiplicative factor is 1.00.

15) Isotope Purity Factor: chemical purity of [γ-^{32}P]-ATP (unofficial communication with manufacturer).

16) Isotope Decay Correction Factor: using the radioactive decay law for ^{32}P, the factor is equal to the specific activity multiplied by $e^{-0.485 * (\text{Counting Date - Isotope Reference Date})}$.

17) Corrected Specific Activity: specific activity multiplied by the isotope decay correction factor.

18) Corrected Specific Activity per Volume: specific activity per volume multiplied by the isotope decay correction factor.

19) Diluted, Corrected Specific Activity per Volume: corrected specific activity per volume divided by the dilution factor of isotope.

20) Isotope Concentration: specific activity per volume divided by specific activity, then divided by 1000 mCi/Ci, then divided by 1000 mmol/mol, then divided by 10^6 µl/l.

21) Diluted Isotope Concentration: isotope concentration divided by the dilution factor of isotope.

22) Isotope Concentration in Reaction: diluted isotope concentration divided by the reaction volume, then divided by the isotope volume per reaction.

23) Ci Concentration in Reaction: diluted, corrected specific activity per volume divided by 1000 mCi/Ci, then multiplied by the isotope volume per reaction, then divided by the reaction volume.

24) Ratio of Cold:Hot ATP: molar ratio of unlabeled to radiolabeled ATP in the reaction samples; cold ATP concentration multiplied by 0.000001 μM/nM, then divided by isotope concentration in reaction.

25) 1 Ci: 2.22×10^{12} dpm; definition of a Curie.

26) Ci per Time-point: Time-point volume multiplied by Ci concentration in reaction.

27) dpm per Time-point: Ci per Time-point multiplied by 2.22×10^{12}.

28) Isotope per Time-point: isotope concentration in reaction multiplied by Time-point volume, then multiplied by 0.000001 l/μl.

29) HCl/Charcoal Dilution Factor: time-point volume divided by the sum of time-point volume and HCl/Charcoal volume.

30) Scintillation Fraction Factor: HCl/charcoal volume divided by the scintillation sample volume.

31) Hsp70 Molecules: Hsp70 mass / assay multiplied by 0.000001 μg/g, then divided by Hsp70 MW.

ATPase specific activity calculation

The raw data generated in these assays are counts of free $^{32}P_i$ per minute, presumably from hydrolyzed [γ-^{32}P]-ATP. With many time points, Δ cpm/minute can be calculated from the slope of the line of cpm vs. time. Then, Δ cpm/minute can be converted into pmol ATP hydrolyzed/minute, and ultimately the specific activity, in pmol ATP hydrolyzed / minute / pmol Hsp70, can be calculated with the following formula:

*Δ cpm/minute * Isotope per Time-point / dpm per Time-point / Hsp70 Molecules * Ratio of Cold:Hot ATP / HCl/Charcoal Dilution Factor * Scintillation Fraction Factor / Counting Efficiency / (Isotope Purity Factor * 0.01)*

An example of the spreadsheet is given in Figure 3-1 with an actual assay analysis which employs all of the calculations described here. All Hsp70 ATPase assays were performed in triplicate, realizing a standard error <10%.

Co-precipitation of DnaK with Ni-sepharose

His-S-SStp and His-S-SStp truncation mutants were expressed in *E. coli* as described previously for His-S-SStp (Ivey and Bruce, 1999). Small cell cultures (10 ml)

were grown and induced normally but lysed by sonication in native Lysis Buffer (Novagen). The crude lysates were spun at 16,000 x g; then, each of the supernatants were was added to microfuge tubes containing 100 µl of Ni-Sepharose (Pharmacia) and mixed gently for five minutes at 4 °C. After washing the Ni-Sepharose in batch three times with 1 ml of the same lysis bufferand centrifuging, SDS sample buffer was added directly to the Ni-Sepharose to elute the bound proteins. After SDS-PAGE and electroblotting onto PVDF membrane, the blot was divided laterally. The upper half was probed with α-DnaK antiserum; the lower half, with S-protein conjugated to alkaline phosphatase.

Native gel shift competition assay with ^{125}I-RCMLA

DnaK and CSS1 binding competition studies with ^{125}I-RCMLA were performed as described by Freeman and co-workers (Freeman et al., 1995). Briefly, the Hsp70 was incubated with ^{125}I-RCMLA and the competing peptide/protein for 30 minutes at 37°C in Buffer A. Native Sample Buffer (100 mM Tris-HCl, pH 6.8 containing 10% (v/v) glycerol and 0.04% (w/v) bromphenol blue) was added and the samples were resolved by electrophoresis on a 6% native acrylamide gel. The proteins were then fixed with acetic acid, the gels were dried, and autoradiograms developed. Quantitative scanning densitometry was performed with a Molecular Dynamics Model 3000 Series Computing Densitometer.

RESULTS

The N-Terminus of transit peptides are predicted to interact with DnaK

To investigate more precise region(s) within SStp responsible for chaperone association, we used previously published data in two novel algorithms, the first of which was derived from a RPPD analysis (Gragerov et al., 1994). The second algorithm was obtained from data in a CBPS analysis (Rudiger et al., 1997). The RPPD and CBPS algorithms calculate a DnaK affinity index for a sliding window of six and thirteen amino acids in length, respectively. Analysis of the entire SStp sequence by both algorithms implicated the same regions as interacting with DnaK (Figure 3-2A and 3-2D). To compare the algorithms' predictive indices against the experimentally determined DnaK binding activity to given peptide substrates, five peptides reported from the RPPD library and two from the CBPS study were analyzed with their respective algorithms (Figure 3-2A and 3-2D). In both cases, the "control" peptides defined experimental limits for DnaK affinity. Utilizing the RPPD algorithm, an index value greater than 2.0 should be strongly selected by DnaK. Using the CBPS algorithm, which describes free energy changes, high affinity regions have index values less than –4.0. Based on these criteria, DnaK is predicted to exhibit a strong association for the region of SStp centered at amino acid position 10 and may possibly interact with a second site centered at position 37. Interestingly, these two regions of SStp align well with one another when calculated from either algorithm.

Figure 3-2. Predictive DnaK Affinity Algorithms. (**A**) through (**C**) utilize data found in the RPPD study (Gragerov et al., 1994); (**D**) through (**F**) utilizes data found in the CBPS study (Rudiger et al., 1997). (**A**) and (**D**), DnaK affinity algorithms (see materials and methods for details) applied to SStp from pea. Also shown in right of (**A**) is the analysis of five peptides reported from the original study. The solid bars indicate values obtained using peptides from the original phage display study which were "Strongly Selected": A=NRLLLT, B=ARLLLT, and C=NRLLLA. The hatched bars indicate values obtained using "Weakly Selected" peptides: D=KWVHLF and E=LLTNRG. In the right of (**D**) are values from two peptides from the original study: AKTLILSHLRFVV, a strongly selected peptide, and VVHIARNYAGYG, a weakly selected peptide. (**B**) and (**E**), The algorithms applied to all angiosperm prSSU transit peptides in the CHLPEP database. The average values at each position in the sequence are plotted. (**C**) and (**F**), Distribution by thirds of predicted highest and second highest affinity regions in 115 angiosperm, stromally targeted transit peptides in the CHLPEP database. (**G**) and (**I**), RPPD analyses of nitrite reductase and fructose-1,6-bisphosphatase, respectively. (**H**) and (**J**), CBPS analyses of nitrite reductase and fructose-1,6-bisphosphatase, respectively.

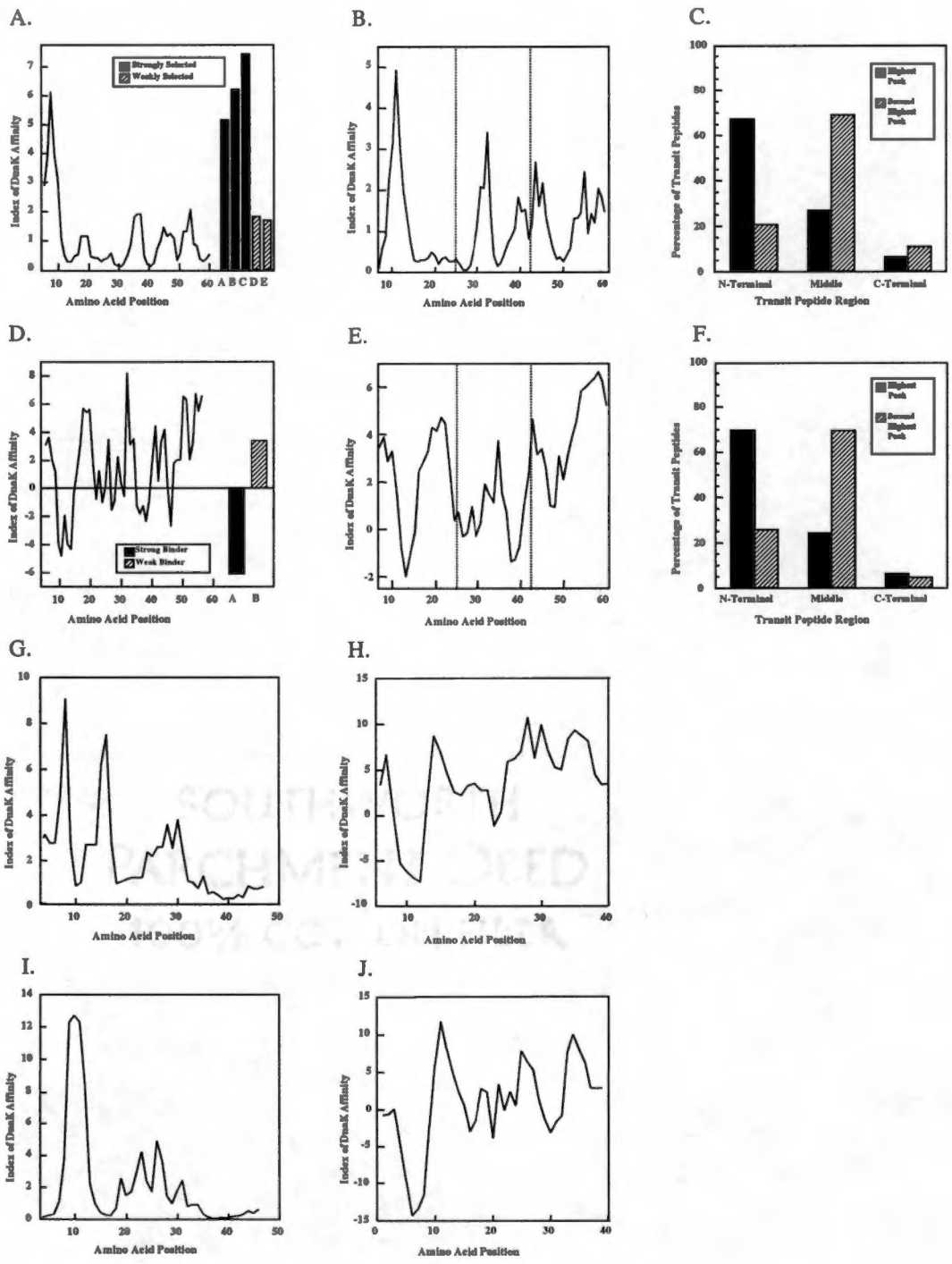

Figure 3-2. Predictive DnaK affinity algorithms.

The profile of pea SStp shown in Figure 3-2 (A and D) is typical of prSSU transit peptides from other organisms (data not shown) and the transit peptides of other stromally targeted precursors. Figure 3-2 (B and E) represents the average of all angiosperm prSSU transit peptides found in the CHLPEP database (von Heijne et al., 1991). Again, both algorithms strongly agree that these transit peptides display a major peak of predicted DnaK affinity at the N-terminus and exhibit a similar periodicity of successive peaks whose affinity for DnaK diminishes toward the C-terminal cleavage site. The apparent small peak values, especially in Figure 3-2E, reflect averaging of "misaligned" peaks.

Furthermore, when these analyses were performed for 115 transit peptides from stromally localized angiosperm precursors in the CHLPEP database, the domain with the highest predicted DnaK affinity occurred in the N-terminal region of ~70% of the transit peptides analyzed (Figure 3-2C and 3-2F). Moreover, both algorithms predicted that ~70% of the transit peptides contained a second peak of lower strength positioned in the central region. Finally, only ~5% of the peptides contained a prominent peak in the C-terminal region, indicating that this domain was largely devoid of sequences that would function as good substrates for DnaK recognition. Both algorithms predicted at least one high affinity site for >95% of transit peptides tested and were in good alignment agreement ~80% of the time (data not shown). Two unrelated transit peptides, from precursors for nitrite reductase (*Spinacia*, Figure 3-2G and 3-2H) and fructose-1,6-bisphosphatase (*Pisum*, Figure 3-1I and 3-1J), also show DnaK affinity profiles similar to that of prSSU using both algorithms.

Correlation between predictive algorithms for transit peptide homology and Hsp70 Affinity

Another way to challenge the veracity of transit peptides' N-terminal bias for Hsp70 affinity was to compare the RPPD and CPBS affinity scores for sequences which fit the loose transit peptide "consensus" very well and those for sequences which do not. Therefore, of the 636 transit peptides in the PTP99 database, we chose those with the 15 highest and 15 lowest scores on the ChloroP neural network-based transit peptide identification algorithm (Emanuelsson et al., 1999). The ChloroP analysis provides and index for the transit peptide "homology" of a putative transit peptide compared to proven sequences. Figure 3-3A shows that, indeed, the transit peptides with the highest ChloroP scores are also predicted to bind Hsp70 primarily at their N-termini, with less affinity in the middle region and little affinity at the C-terminus. In contrast, the transit peptides with the 15 lowest ChloroP scores (Figure 3-3B) are predicted to have either equal Hsp70 affinity throughout their sequences or a slight preference at their C-termini. Therefore, the more homologous a given transit peptide is to the quintessential transit peptide, the more likely that sequence is to bind Hsp70s at its N-terminus.

SStp association with DnaK provides protease protection

In order to experimentally assess the validity of the algorithms' predictions, three *in vitro* assays were performed which explored the consequences of an Hsp70/SStp interaction. Previous studies have shown that Hsp70s undergo a change in conformation upon binding to a peptide substrate such that the substrate-bound form is more resistant

Figure 3-3. RPPD and CBPS algorithms applied to the 15 highest- (**A**) and 15 lowest-ChloroP scoring (**B**) transit peptides in the PTP99 database.

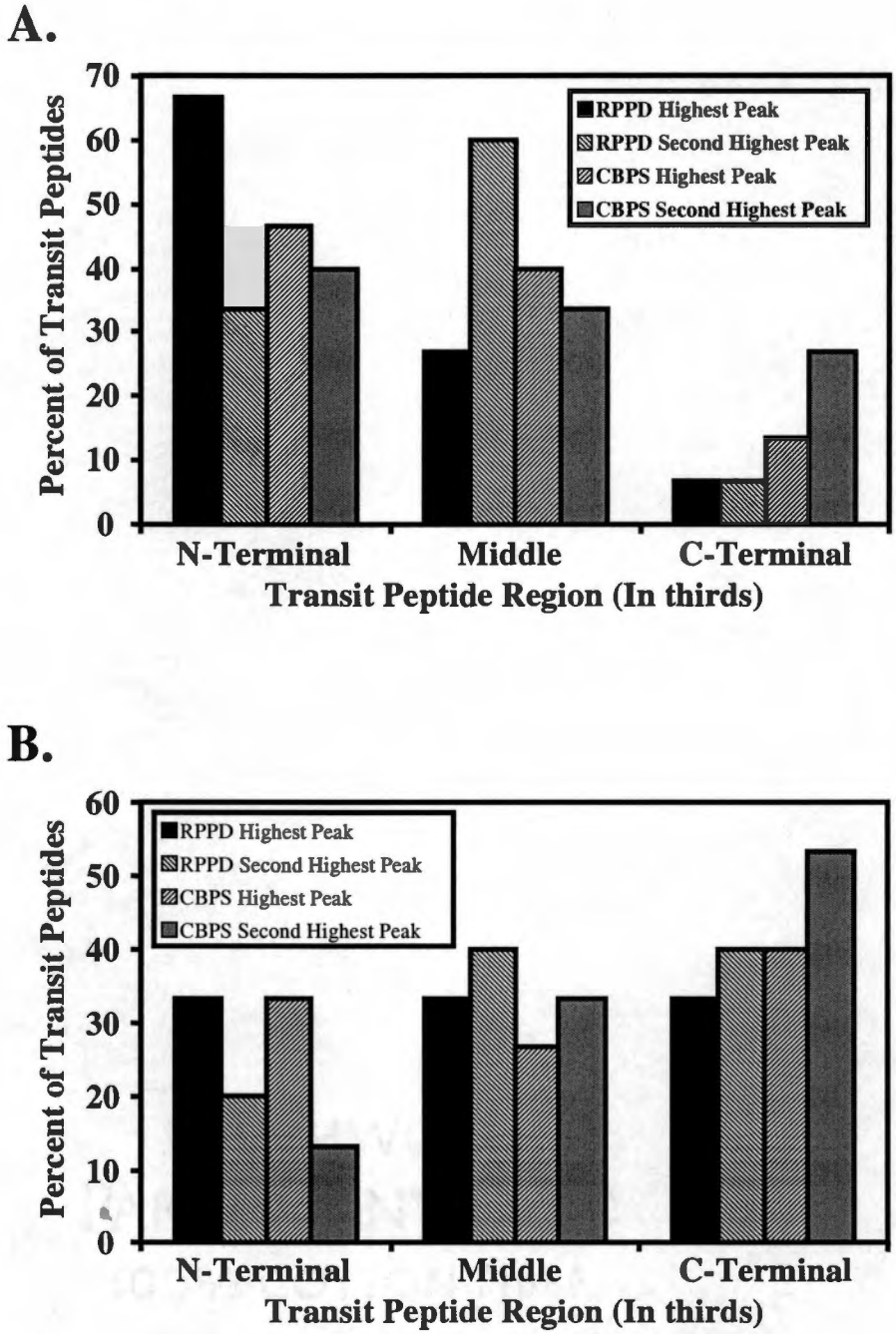

Figure 3-3. Cross-referencing RPPD, CPBS, and ChloroP analyses.

to trypsin digestion (Cyr et al., 1992; Freeman et al., 1995; Palleros et al., 1992). Using the components purified above, we investigated whether a similar interaction could be demonstrated *in vitro* by employing the limited trypsin proteolysis technique. RCMLA, a permanently unfolded protein and model Hsp70 substrate, and SStp were also utilized to protect DnaK from trypsin degradation. When incubated with trypsin alone, DnaK was readily digested, yielding a 43 kD fragment (Figure 3-4A, top panel). This fragment probably corresponded to the N-terminal ATPase domain of DnaK. However, in the presence of 10-fold molar excesses of RCMLA (Figure 3-4A, middle panel) or SStp (Figure 3-4, bottom panel), DnaK was protected substantially from proteolysis. This protection is not simply the result of unfolded substrates competing for the protease because the control substrate, native α-lactalbumin, failed to protect DnaK from trypsin digestion (data not shown). The amount of intact DnaK remaining at each time point was quantitated via scanning densitometry and plotted in Figure 3-4B. Whereas ~40-60% of the DnaK remained intact after one hour of trypsin digestion in the presence of RCMLA or SStp, DnaK alone was almost completely digested (<5% remaining) by trypsin in the same time frame. These results support previous observations that *in vitro* binding of a substrate, either RCMLA or SStp, induces a significant, substrate-dependent conformational change, rendering the DnaK much more resistant to trypsin digestion. These results confirm that SStp contains at least one sequence which serves as a good substrate for Hsp70 binding as was predicted from earlier secondary structural analyses (von Heijne and Nishikawa, 1991).

Figure 3-4. Substrate Protection of DnaK from Trypsin Degradation. A, 0.7 μM DnaK was treated with trypsin after a five minute incubation in the presence of no unfolded protein substrate (upper panel), 7 μM RCMLA (middle panel), and 7 μM SStp (lower panel). Aliquots were removed at the given times and immediately boiled in SDS sample buffer. All samples were examined by SDS-PAGE and C.B.B. stained. B, Quantitation of the amount of intact DnaK remaining at each time point in A for each treatment.

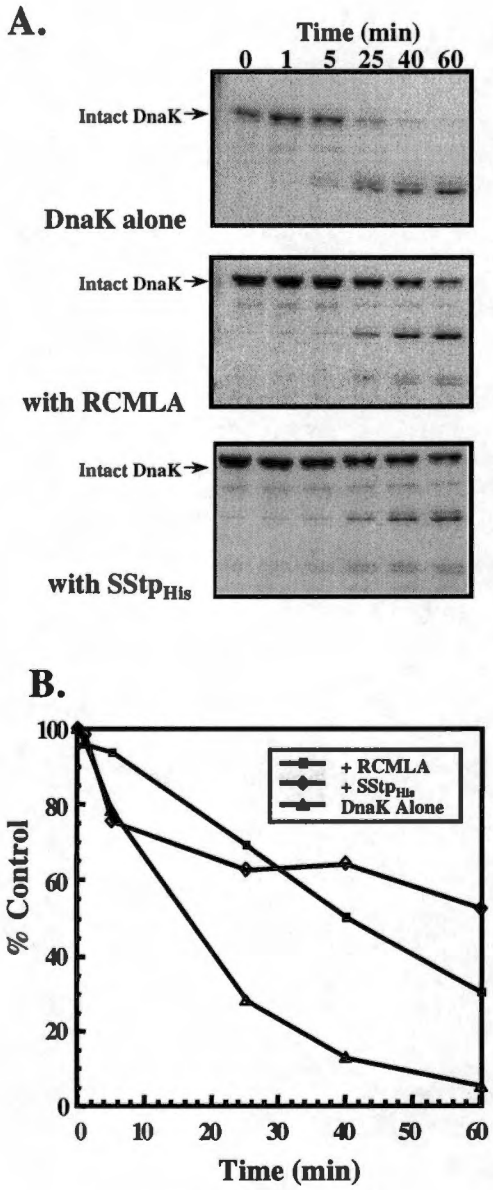

Figure 3-4. Substrate protection of DnaK from trypsin degradation.

SStp stimulates the ATPase activity of CSS1

A second indicator of a protein or peptide's interaction with Hsp70/DnaK as a substrate is the stimulation of the intrinsic ATPase activity of the chaperone (Sadis and Hightower, 1992; Ziegelhoffer et al., 1995). We have used this assay to evaluate the ability of both RCMLA and full-length SStp to stimulate the intrinsic ATPase activity of purified CSS1. First, CSS1 was purified from intact *P. sativum* chloroplasts via ATP affinity chromatography. Figure 3-5A shows the ATP elution profile from the ATP-Sepharose affinity column. Western blotting indicated that the major band at 73 kD was CSS1 (Figure 3-5B). Subsequent CSS1 ATPase assay results, as shown in Figure 3-6, showed a basal activity of ~2.6 pmole ATP/min/pmole enzyme. This rate was stimulated to ~5.1 pmole ATP/min/pmole enzyme when a 100-fold molar excess of either RCMLA or SStp was added to the reaction. This effect was dependent on the specific interaction of the chaperone with a substrate since an equal addition of native α-lactalbumin did not result in ATPase stimulation. Both the substrate levels required and the level of stimulation observed were quite similar to those observed for DnaK's stimulation by RDMLA (Liberek et al., 1991).

Mapping of the SStp regions recognized by in *E.coli*

The *in vivo* association of SStp and DnaK, described by Ivey and Bruce (1999), was used to experimentally map the region of SStp responsible for DnaK binding and provide support for the algorithms' predictions. First, C-terminal deletion mutants of SStp fused to the dual His-S Tag (Figure 3-7A) were expressed in *E. coli*. Then, co-

Figure 3-5. Biochemical Purification of CSS1 from Pea. A, C.B.B. stained SDS gel of the elution profile from an ATP-agarose column after incubation with 10 mM ATP. B, Western blot of the fractions in A probed with α-DnaK.

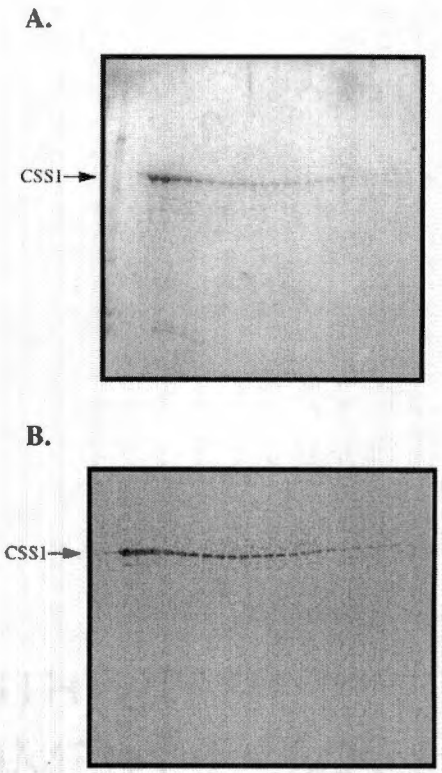

Figure 3-5. Biochemical purification of CSS1 from *P. sativum*.

Figure 3-6. SStp Stimulation of CSS1 ATPase Activity. 0.7 μM CSS1 was incubated with 50 μM cold ATP and [γ-^{32}P]ATP (3000 Ci/mmol; molar ratio of unlabeled:^{32}P-labeled, 5250:1) in the absence and presence of 70 μM native α--lactalbumin, RCMLA, or SStp. Spontaneous hydrolysis indicates liberated ^{32}Pi in the absence of chaperone.

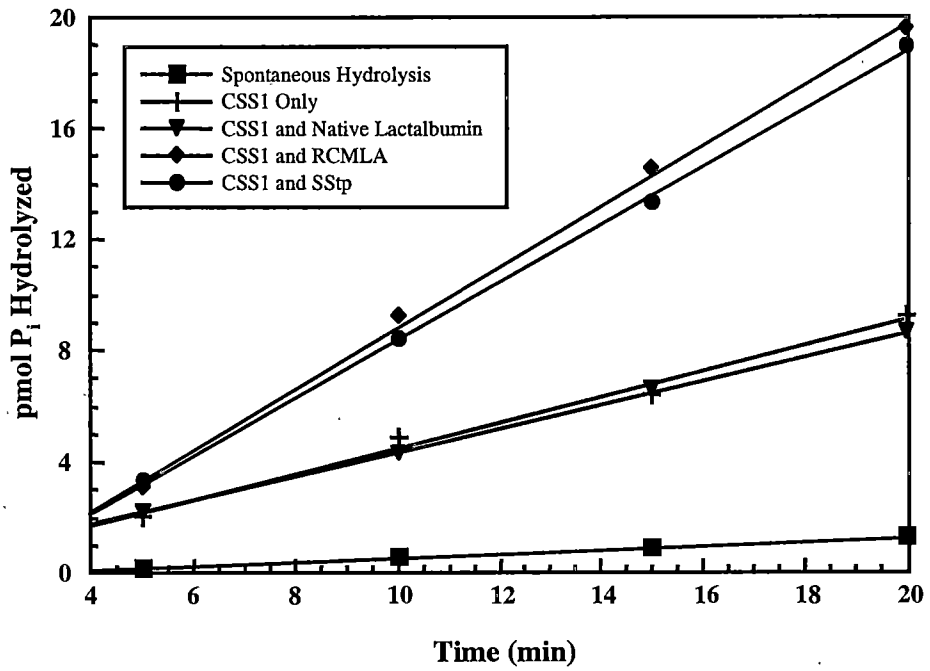

Figure 3-6. Stimulation of CSS1 ATPase activity.

Figure 3-7. Affinity Precipitation of DnaK with C-terminal Deletions of SStp. A, Amino acid sequences of His-S-SStp and C-terminal deletions. Residues in bold correspond to SStp. Black boxes indicate the N- and C-terminal His-Tags, while grey boxes indicate N-terminal S-Tags. B, upper panel, Far-western of His-S-SStp deletions and the His-S Tag alone using the S-Protein conjugated to alkaline phosphatase; lower panel, western blot of the samples in the upper panel using α-DnaK antiserum.

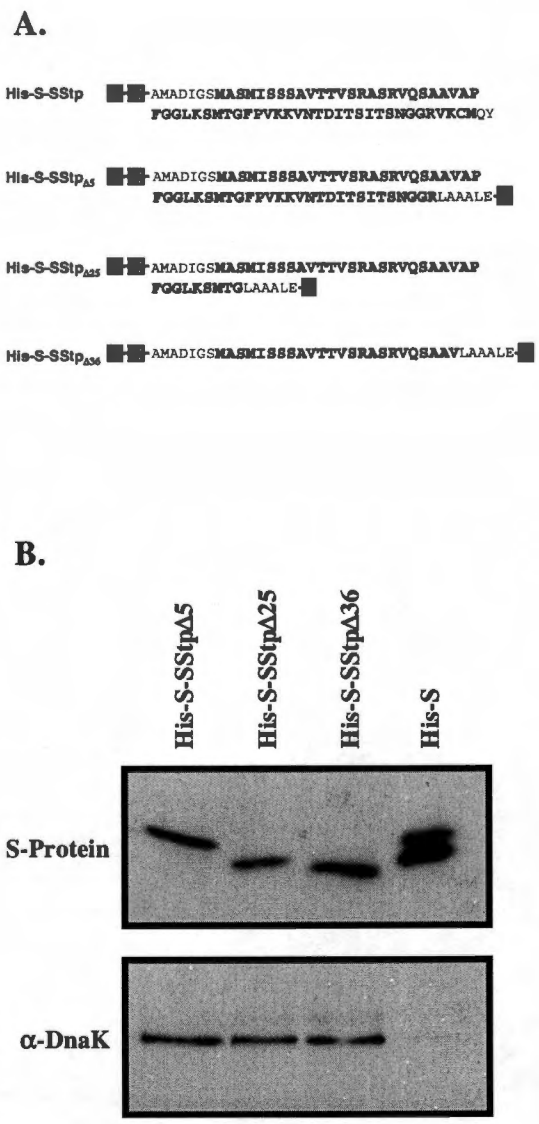

Figure 3-7. Affinity precipitation of DnaK with C-terminal deletions of SStp.

affinity precipitations of DnaK using Ni-Sepharose were performed for each deletion and the His-S Tag alone. Figure 3-7B, upper panel, shows equal loadings of the three deletions and the His-S Tag visualized by Far-Western blotting. The lower panel is a Western blot of the same samples showing DnaK binding to every deletion containing at least part of the SStp sequence. However, DnaK did not bind to the His-S Tag itself, which serves as a negative control. Therefore, sequences in the first 24 residues of SStp must contain a DnaK recognition motif allowing this interaction *in vivo*. Because the experiment did not include N-terminal SStp deletions, these data do not exclude the possibility of other DnaK binding sites C-terminal to amino acid position 24.

In vitro interaction of DnaK and CSS1 with the N-terminus of SStp

To further test the algorithms' predictions for SStp, a competitive native gel shift assay was used. Incubation of ^{125}I-RCMLA with purified DnaK results in the formation of at least two stable complexes whose electrophoretic mobilities on native polyacrylamide gels are retarded relative to ^{125}I-RCMLA alone (Figure 3-8A, lanes 1-3). The two discrete complexes may represent ^{125}I-RCMLA associated with a monomeric and a dimeric form of DnaK, since several Hsp70s exist in an equilibrium between a monomeric and dimeric species (Azem et al., 1997; Palleros et al., 1991). To determine the relative affinity of DnaK for different peptide substrates, synthetic, unlabeled peptides were added to the ^{125}I-RCMLA-DnaK incubation as competitors for binding to DnaK. Competitive association between the unlabeled peptide and DnaK displaces ^{125}I-RCMLA, thus reducing the amount of ^{125}I-RCMLA-DnaK

Figure 3-8. Mapping the High Affinity DnaK Binding Site(s) Within SStp. A, Autoradiogram demonstrating ^{125}I-RCMLA/DnaK complex stability and subsequent competition by unlabeled competitors in a native gel system. DnaK was added to a final concentration of 0.7 μM, while the concentrations of ^{125}I-RCMLA and SStp were 7 μM and 70 μM, respectively. B, Autoradiograms of ^{125}I-RCMLA /DnaK complexes in the presence of the N-terminal (upper panel), middle (middle panel), and C-terminal (lower panel) thirds of SStp from pea. Again, the DnaK concentration was 0.7 μM and ^{125}I-RCMLA concentration was 7 μM. Molar ratios of the unlabeled competitor to ^{125}I-RCMLA are shown in lanes 5 through 8.

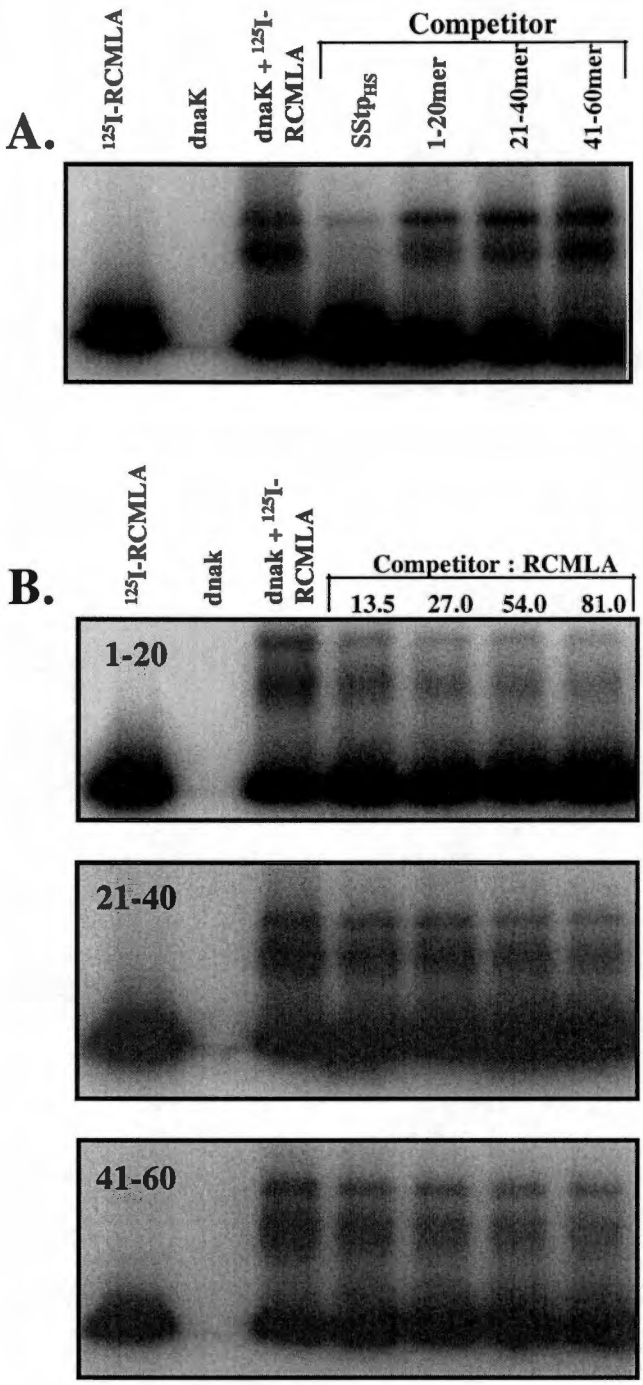

Figure 3-8. Mapping the high affinity DnaK binding site(s) within SStp.

complexes. Figure 3-8A shows an autoradiogram of a competitive gel shift assay in which ^{125}I-RCMLA-DnaK complexes formed in the presence of 10-fold molar excess of SStp or synthetic 20 amino acid peptides spanning the SStp sequence. SStp effectively competed with ^{125}I-RCMLA for DnaK binding as previously shown (Ivey and Bruce, 1999). Synthetic peptides (20-mers) corresponding to the N-terminal (1-20), middle (21-40), and C-terminal (41-60) thirds of SStp clearly competed with an activity very similar to their predicted values of DnaK affinity (Figure 3-2A and 3-2D). This difference in activity was confirmed when the unlabeled SStp 20-mers were titrated relative to ^{125}I-RCMLA (Figure 3-8B). The N-terminal sequences (peptide 1-20) competed best with ^{125}I-RCMLA for DnaK, whereas the central region (peptide 21-40) was considerably less effective and the C-terminal region (peptide 41-60) displaced ^{125}I-RCMLA even less than the central region (Figure 3-8B).

In previous work, three peptides of similar length which are not predicted by either algorithm to bind DnaK and are thus clear negative controls, were tested and failed to disrupt the ^{125}I-RCMLA-DnaK complex (Ivey and Bruce, 2000). Thus, SStp bound DnaK with higher affinity than any of the 20-mers, but the greatest local affinity for DnaK was detected in the N-terminal 20 amino acids, and progressively less affinity was found toward the middle and C-terminal thirds of SStp.

Thus far, we have shown that SStp functions *in vivo* and *in vitro* as an effective substrate for DnaK. The major chloroplast Hsp70 homologue, CSS1, is most similar to prokaryotic homologs of DnaK, with 55% amino acid sequence identity and 74% similarity (Marshall and Keegstra, 1992). Therefore, one would predict similar peptide

binding properties for both chaperones. Using purified CSS1 instead of DnaK, competitive gel shift assays were performed as described above. The results for both DnaK and CSS1 are represented graphically in Figure 3-9. The trend observed for DnaK binding to SStp was almost identical to that observed for CSS1, suggesting that both chaperones preferred sequences found at the N-terminal region of SStp.

DISCUSSION

Although several recent studies have attempted to identify the linear peptide sequences recognized by Hsp70s (Blond-Elguindi et al., 1993; Gragerov et al., 1994; Rudiger et al., 1997), only one has directly analyzed targeting sequences (Zhang et al., 1999). Zhang and coworkers also used the same CBPS algorithm used in this study to predict interactions between mitochondrial presequences and DnaK. The current study, however, demonstrates for the first time a direct interaction between an organellar molecular chaperone and a physiologically relevant precursor targeting sequence. Specifically, our data confirm that the transit peptide of prSSU contains one or more sequences that are recognized by two Hsp70 chaperones, DnaK and CSS1.

Transit peptide design

Both the X-ray crystal structure of the DnaK peptide-binding domain and peptide binding studies of a eukaryotic Hsp70 indicate a preference for binding substrates 6-8 amino acids in length (Flynn et al., 1991; Zhu et al., 1996). Therefore, the full-length SStp may contain up to seven contiguous DnaK/CSS1 binding sites. To identify the

Figure 3-9. Comparison of SStp Binding by DnaK and CSS1. Native gel shift competition assays were used to compare the binding of SStp by DnaK and CSS1 and to map the highest affinity site for both Hsp70's. The solid bars were quantified from the autoradiogram in Figure 6A. Using the same ^{125}I-RCMLA, chaperone, and competitor concentrations as before, the hatched bars were obtained similarly using CSS1 instead of DnaK.

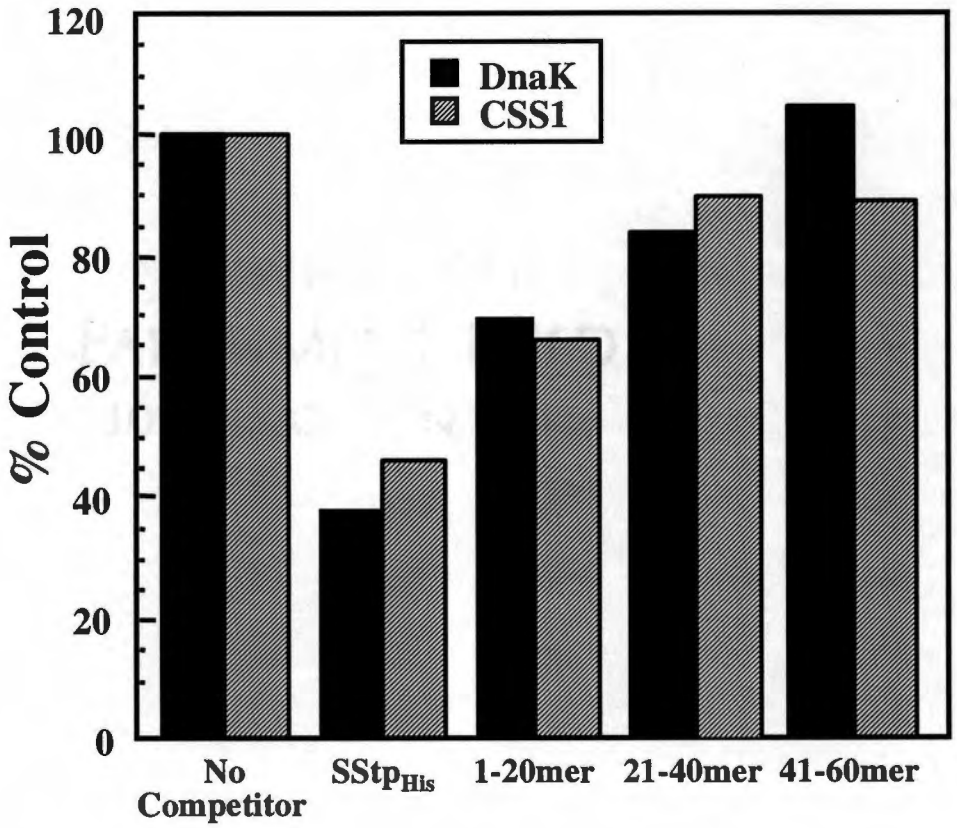

Figure 3-9. Comparison of SStp binding by DnaK and CSS1.

number and position of potential DnaK binding sites in SStp, we utilized data from two extensive studies (Gragerov et al., 1994; Rudiger et al., 1997) which provide statistical data on the probability of individual amino acids to occur in DnaK selected peptides. Both algorithms predict potential DnaK binding sites in SStp. Moreover, both algorithms predicted that the strongest peptide-DnaK interactions were restricted primarily to the N-terminus. When these analyses were applied to all prSSU transit peptides from angiosperms in the CHLPEP database (von Heijne et al., 1991), N-terminal bias was observed by both algorithms. This suggests that the Hsp70 binding site(s) at the N-terminus of prSSU is a conserved trait, independent of phylogeny.

Although many stromal proteins, such as the precursors to fructose-1,6-bisphosphatase (*Pisum*) and nitrite reductase (*Spinacia*), show very similar patterns to SStp, analyses of 115 angiosperm transit peptides for stromally localized precursors indicate that the placement of high-affinity binding sites is not absolutely conserved. However, both algorithms indicate that >95% of these transit peptides contain at least one potential Hsp70 recognition domain and that ~70% of these transit peptides contain sequences at their N-terminus predicted to most favorably interact with Hsp70s. In addition, both analyses indicate additional site(s) with lower affinity found within the central third of the transit peptide and that, for most transit peptides, the C-terminal third is largely devoid of Hsp70 binding sites. Additionally, transit peptides which best fit the criteria for identification as transit peptides are predicted to bind Hsp70s in the same manner. Because import data does not exist for the PLP99 transit peptides tested, we cannot correlate predicted Hsp70 affinity to import efficiency.

However, the predictions discussed above were confirmed experimentally for SStp, which scores relatively high in the ChloroP analysis. The trypsin resistance and the ATPase stimulation data reported here support previous observations that *in vitro* binding of a substrate, either RCMLA or SStp, induces a significant, substrate-dependent conformational change. Binding of the peptide substrate renders DnaK more resistant to trypsin digestion and more active as a ATPase. These results confirm that SStp contains at least one sequence which serves as a good substrate for Hsp70s, as was predicted from earlier secondary structural analyses (von Heijne and Nishikawa, 1991).

Together these results suggest that chloroplast transit peptides have one or more regions which may function as a high-affinity substrate for Hsp70s. A shared peptide sequence preference among chaperones is expected since a recent study with three Hsp70 homologs (Hsc70, BiP, and DnaK) shows several common peptide binding tendencies (Fourie et al., 1994). Interestingly, the full length transit peptide appeared to display greater interaction than any of the 20-mers. These data argue strongly that CSS1-peptide substrate interactions are generally governed by the same rules as those for DnaK.

Our observation that CSS1 exhibits high affinity for the N-terminus of transit peptides and diminishing affinity toward the C-terminus has several important implications. First, if translocation proceeds with the N-terminus first, as most models depict, the suggested design would enable the emerging transit peptide to encounter the chaperone at the earliest possible point in the translocation process. This initial interaction may represent the first committed step of protein translocation. Second, most transit peptides may contain additional secondary Hsp70-binding sites which would

enable multiple chaperone molecules to concurrently bind the precursor and drive translocation. The observation that full-length SStp was a better substrate than any of the 20-mers suggests that multiple potential binding sites may promote some level of cooperativity, possibly by interaction with both substrate binding domains of the DnaK dimer. This multiplicity of binding sites could be the basis for why certain precursors are translocated more efficiently. Third, these observations may confirm the hypothesis of a modular organization of transit peptides.

Chloroplast Hsp70s as molecular motors and "unfoldases"

The most widely accepted generic protein import model describes an active, energy-dependent "molecular motor" which is bound to the membrane and directly utilizes a conformational change in the chaperone to unidirectionally drive translocation (Gisler et al., 1998; Glick, 1995). Our data directly support the hypothesis that an individual transit peptide contains one or more Hsp70 recognition domains, enabling a precursor to simultaneously engage more than one chaperone molecule concurrently during translocation. Analyses of prSSU transit peptides in CHLPEP indicate at least two such sites. Interestingly, the two sites are separated by ~26 amino acids, which would be sufficient to span a bilayer. Therefore, this spacing could allow one transit peptide to simultaneously engage two chaperones on either side of a membrane. If both high affinity sites are active in recruiting Hsp70s, the ability of SStp to interact concurrently with two Hsp70 molecules may synergistically promote a much stronger "unfoldase" activity than might be expected from the sum of their individual contributions, assuming

a steady supply of ATP to promote release of the transit peptides. Differences in amino acid sequences of transit peptides from different precursors could then affect their translocation efficacies, which would constitute a novel form of post-transcriptional/post-translational regulation of gene expression.

Although most investigators agree that isolated translocation complexes contain one or more Hsp70s (Schnell et al., 1994; Waegemann and Soll, 1991), recent reports also describe a second potential molecular chaperone, ClpC, associated with the translocation complex (Akita et al., 1997; Nielsen et al., 1997). However, no evidence of transit peptide or precursor binding has been presented, and the presence of ClpC in a translocation complex is independent of the presence of a precursor protein (Nielsen et al., 1997). Furthermore, organellar Clp homologs have been implicated in the degradation of misfolded precursor proteins post-import (Halperin and Adam, 1996; Schmitt et al., 1995)

Concluding remarks

Our study utilizes the first statistical analyses which predict a common biochemical activity associated with chloroplast transit peptides. This general profile defines a novel property intrinsic to the design of stromally targeted transit peptides whose primary sequences are otherwise unrelated. It will be interesting to extend these analyses to transit peptides of precursors destined to other chloroplast compartments and other organelles to determine the universality of this observation.

Interestingly, recent work has shown that when a small N-terminal region is deleted from the ferredoxin or plastocyanin transit peptide, transport into chloroplasts is reduced to an undetectable level both *in vitro* and *in vivo* (Kindle, 1998; Pilon et al., 1995). Although these reports conclude that the N-terminal region of the transit peptide is required for efficient protein translocation, neither provide an explanation for this effect. Analyses of these two transit peptides by the above algorithms indicate that the characterized deletions remove potentially critical Hsp70 binding sites.

Chapter 4-Expression, purification, and characterization of a recombinant form of the major stromal Hsp70, CSS1

ABSTRACT

We have expressed the mature form of the nuclear-encoded pea chloroplast Hsp70, CSS1, in *E. coli*. Using the pET30a expression vector (Novagen), we have replaced the transit peptide at the N-terminus of prCSS1 with the dual epitope tag His-S. The His_6-Tag allows for affinity purification with Ni-Sepharose while the S-Tag provides an antigenic marker. Purification of large quantities of soluble, active His-S-CSS1 were not feasible under mild buffer conditions, so we developed a novel purification method which employs initial denaturation of the crude cellular extract with urea. Renatured CSS1 functioned similarly to the chaperone purified from *P. sativum* with respect to basal and peptide-stimulated ATPase activities. Finally, protein expression conditions in *E. coli* were optimized. This recombinant form of the major stromal chloroplast Hsp70 provides a valuable tool further characterization of CSS1 and the chloroplast protein import system.

INTRODUCTION

Involvement of the Hsp70 class of molecular chaperones in protein trafficking is well documented in bacterial, ER, and mitochondrial systems (Schatz and Dobberstein, 1996). In most models, the hsp70 homolog is attached peripherally to the *trans* side of the translocating membrane and functions either passively as a ratchet (Matlack et al., 1999) or actively as a motor (Voisine et al., 1999) to drive protein translocation in an ATP dependent manner.

Although no direct evidence exists, each model assumes that chaperone interaction is directed by the N-terminal targeting sequences of the precursor proteins. In fact, most of the evidence for chaperone involvement in protein trafficking stems from genetic and crosslinking studies (reviewed in Schatz and Dobberstein, 1996). Our laboratory has approached the question of Hsp70 involvement in chloroplast protein import from a different perspective. We initially established a novel and physiologically relevant property of the targeting sequence, or transit peptide, for the precursor of the small subunit of rubisco (SStp) involving explicit interactions with the the Hsp70 class of molecular chaperones, specifically with bacterial Hsp70, DnaK (Ivey and Bruce, 2000). Next, we showed that SStp interacts with the major stromal Hsp70 from pea, CSS1, in a similar manner, and that this interaction can be mapped to the N-terminal portion of most stromally targeted transit peptides (Ivey et al., 2000).

Since CSS1 may serve as the molecular motor driving translocation from the *trans* side of the chloroplast inner envelope, we decided to characterize the protein purified from *P. sativum* (Ivey and Bruce, manuscript in preparation). However, in order to fully manipulate CSS1's behavior *in vitro* and to study its roles *in vivo*, a recombinant form of the protein is needed. To this end, we have generated a recombinant form of the protein from a gene construct of the nuclear-encoded precursor and expressed the His-S-CSS1 fusion protein in *E. coli*.

Since Hsp70's are abundantly expressed throughout biology, most are not engineered into an expression system, but instead are purified from the source organism via standard biochemical techniques. For example, DnaK from *E. coli* was originally purified using

ammonium sulfate precipitation with a combination of ion exchange, affinity, and hydrophobic interaction chromatographic techniques followed by differential sedimentation centrifugation (Zylicz and Georgopoulos, 1984). Even organellar homologs, such as that from *N. pseudonarcissus* chromoplasts, have been purified by similar, conventional means (Bonk et al., 1996). When recombinant forms are available, most are still expressed homologously, as in the case of yeast mitochondrial Hsp70, or SSC1 (Kubo et al., 1999). His-tagged SSC1 can be purified from mitochondria either by nickel affinity chromatography or a combination of ATP affinity and ion exchange chromatography. In fact, the only heterologously expressed Hsp70, other than CSS1, of which we are aware is human cytosolic Hsp70 expressed in *E. coli* (Macejak et al., 1990). Macejak and co-workers observed poor expression, low solubility, and only partial purification of their protein after applying ion exchange and ATP affinity chromography to a crude lysate containing their overexpressed protein. Overall, the protein yield was calculated to be 1-3 μg per liter of *E. coli* culture.

Therefore, we opted for the high-yield, T7 Polymerase-based pET expression system from Novagen. Initially, we expressed His-S-CSS1 and attempted to purify it by standard nickel-affinity chromatography protocols. When we could not obtain pure protein, we utilized a novel technique which uses denaturing cell lysis conditions and, although developed entirely independently, is similar in certain aspects to a protocol used to resolubilize the non-catalytic surfactant protein b (Holzinger et al., 1996). By then performing nickel affinity chromatography, stepwise dialysis, and ion exchange chromatography, we obtained pure His-S-CSS1 in high quantity. Finally, we demonstrate that recombinant CSS1 has basal and peptide-stimulated ATPase activities similar to CSS1

purified from *P. sativum* stroma.

MATERIALS AND METHODS

His-S-CSS1 subcloning

The gene for the nuclear-encoded precursor of the major stromal Hsp70, CSS1, was kindly provided by Dr. K. Keegstra in the cloning vector pSP65. The gene was amplified out of the cloning vector via PCR using the pfu editing DNA polymerase (Stratagene). The 5' sense oligonucleotide hybridized to the coding region for the N-terminus of the mature domain of the protein and contained an NcoI restriction site. The 3' antisense oligonucleotide hybridized to the coding region for the C-terminus of CSS1 and contained an EcoRI site. After the PCR product was digested, the gene was ligated into the expression vector pET30a as shown in Figure 4-1, which engineered a dual N-terminal tag, His-S, as explained before for His-S-SStp. The inserted CSS1 gene was sequenced in its entirety to confirm that no mutations were present due to PCR amplification (Figure 4-2).

Attempts at His-S-CSS1 purification using native lysis conditions

The pET30a-CSS1 construct was transformed into *E. coli* BL21(DE3) cells and grown at 37°C to an $O.D._{600}$ of 0.6 and induced with 1 mM IPTG for three hours. The cells were lysed with a French Pressure Cell at 1500 p.s.i. in 20 mM Tris-HCl, pH 7.9, 500 mM NaCl, 5 mM imidazole, 1 mM DTT to maintain protein structure. After centrifugation at 50,000 x g for one hour at 4°C, the crude supernatant was subjected to affinity chromatography by application to a nickel-charged chelating sepharose resin (Pharmacia)

Figure 4-1. Vector design of His-S-CSS1. The region of the prCSS1 gene encoding the N-terminal transit peptide was excluded during PCR amplification. Upon ligation into the pET30a vector, an N-terminal dual epitope tag, His-S, is engineered to generate the fusion protein.

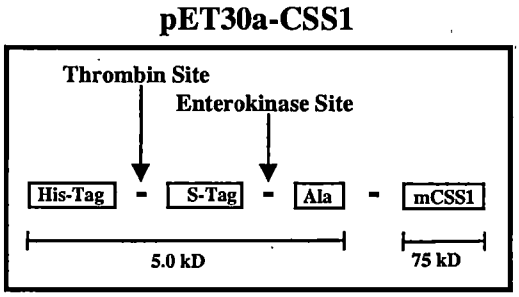

Figure 4-1. Vector Design of His-S-CSS1

Figure 4-2. Sequencing the CSS1 gene. Primer sequences: T7 Promoter, TTAATACG-ACTCACTATAGGG ; 171-193 Primer, GCGGCAGGCGGTTGTGAATCCCG; 567-596 Primer, AACTATTTTGGTATTTGACCTTGGAGGTGG; 986-1016 Primer, AGG-ATATTGATGAGGTGATTCTTGTTGGTGG ; 1361-1385 Primer, TCCGTTTAGACG-GTATCCCTCCCGC ; and T7 Terminator Primer, GCTAGTTATTGCTCAGCGG.

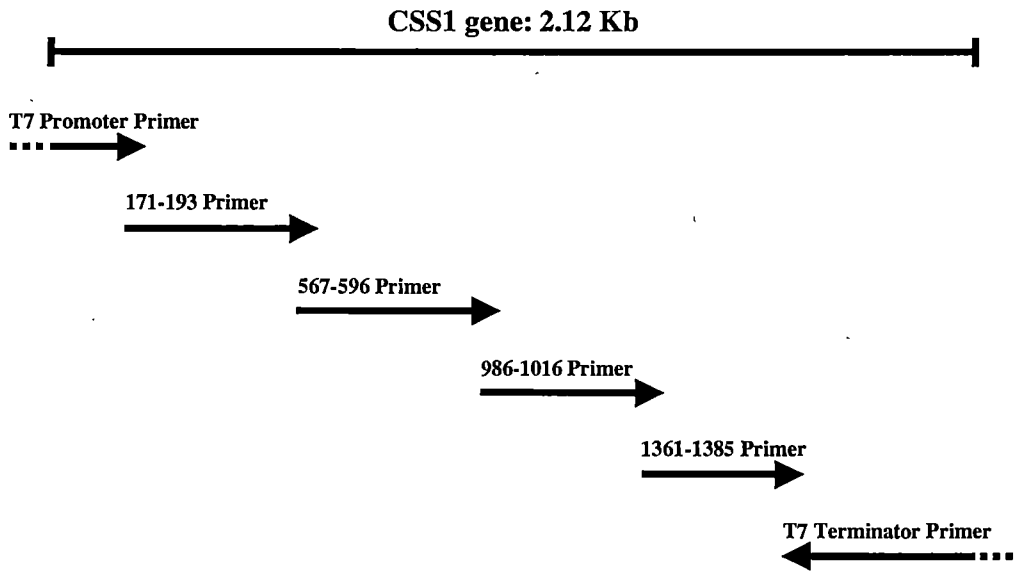

Figure 4-2. Sequencing the CSS1 gene.

equilibrated in Binding Buffer according to a Novagen protocol. The resin was washed exhaustively, and His-tagged CSS1 was eluted into 1 ml fractions with 1 M imidazole.

Fractions from the affinity chromatography containing the fusion protein were pooled and dialyzed against Buffer M. The protein sample then was concentrated via ultrafiltration using a 30 kD MWCO membrane and subjected to an anionic exchange resin, Q-Sepharose (Pharmacia), equilibrated in Buffer M. After exhaustive washing with Buffer M, the protein was eluted into 5 ml fractions using a continuous NaCl gradient from 0.1 M to 0.5 M.

Fractions from the ion exchange chromatography were pooled and dialyzed against Buffer M. The protein sample then was concentrated via ultrafiltration using a 30 kD MWCO membrane and subjected to native acrylamide gel electrophoretic elution on a Bio-Rad 491 Prep Cell. The native gel consisted of 90 ml of 7% acrylamide in the running gel and 20 ml of 5% acrylamide in the stacking gel. Gel and buffer components for native electrophoresis are described in more detail in Chapter 3. After loading 10 ml of the protein sample, the gel was run with buffer recirculation at 35 mA for 15 hours. With the flow rate of the collection buffer at 0.25 ml/min, fraction collection (5 ml each) was started after 8 hours. Samples from every fifth fraction were boiled in SDS and subjected to PAGE.

His-S-CSS1 purification using denaturing lysis buffer conditions

E. coli BL21(DE3) cells were transformed with pET30a-CSS1, grown, and induced as before. After induction, the cells were lysed in Buffer M containing 6 M urea using a French Pressure cell. After centrifugation at 50,000 x g for one hour at 4 °C, the crude supernatant was subjected to affinity chromatography by application to a nickel-charged

chelating sepharose resin (Pharmacia) equilibrated in denaturing Binding Buffer according to a Novagen protocol. After the resin was washed exhaustively with Binding Buffer containing 6 M urea, the buffer was changed to native Binding Buffer through a linear gradient over 10 column volumes and two hours at 4°C. Refolded His-S-CSS1 was then eluted from the resin with 1 M imidazole.

Fractions from the affinity chromatography containing the fusion protein were pooled and dialyzed against Buffer M_1, which is Buffer M lacking $Mg(OAc)_2$ and containing 5 mM DTT and 2% glycerol. After dialysis, $Mg(OAc)_2$ was added to 2.5 mM. The protein sample was concentrated via ultrafiltration using a 30 kD MWCO membrane and subjected to an anionic exchange resin, Q-Sepharose, equilibrated to Buffer M_2 (Buffer M containing 5 mM DTT and 2% glycerol). After exhaustive washing with Buffer M_2, the protein was eluted into 5 ml fractions using a continuous NaCl gradient from 0.1 M to 0.5 M. After dialysis into Buffer M_2, the protein was concentrated, aliquotted, and stored at –85°C.

ATPase assays

Hsp70 ATPase activity was measured as described in Chapter 3. Briefly, each 50 µl reaction contained His-S-CSS1, unlabeled ATP, and [γ-^{32}P]ATP and was incubated at 37 °C. Peptide substrates were provided at 100-fold molar excess relative to the chaperone. Aliquots of the reaction mixture were withdrawn at regular intervals and mixed with 1 ml of 50 mM HCl / 5 mM H_3PO_4 containing 7% (w/v) activated charcoal. After microcentrifugation, 200 µl aliquots of the free $^{32}P_i$-containing supernatants were removed and counted via scintillation. Observation of spontaneous ATP hydrolysis was necessary because Hsp70

ATPase activities are extremely low.

RESULTS

Novel purification methodologies for recombinant CSS1

Figure 4-3 displays the alternative schemes used for His-S-CSS1 purification. Initially, we attempted to purify His_6-tagged CSS1 by conventional means in buffer conditions designed to maintain the chaperone's native three dimensional structure. A crude extract from cells expressing His-S-CSS1 was applied to a column containing a nickel-charged chelating resin. Unfortunately, an estimated majority of the protein, eluted from the column after washing with an intermediate concentration of imidazole, appeared to be endogenous *E. coli* proteins and/or N-terminal CSS1 degradation products (Figure 4-4).

CSS1 contains a signature trypsin cleavage site which is common to most Hsp70's (Chappell et al., 1987) and yields the intact N-terminal ATPase (domain confirmed by western blot; data not shown). Coincidentally, *E. coli* contains many proteases which have specificities similar to that of trypsin.. Therefore, the broad spectrum of fragment sizes in our gel must have contained many other proteins as well and thus required further explanation.

Before further purifications attempts were made, the protein sample was dialyzed in Buffer M_2 (see Materials and Methods). Many, combinations of buffers, pH's, salts, divalent cations, reducing agents, detergents, and even dialysis techniques were tried unsuccessfully in attempts to maintain protein solubility while removing the imidazole from the protein sample (data not shown). Finally, rapid dialysis using a buffer containing glycerol and the detergent Triton X-100 but without any divalent cation (Buffer M_1), followed by addition of

Figure 4-3. Alternate purification schemes for His-S-CSS1. *Left*, initial attempts to purify the fusion protein without denaturation. The ATPase fragment, which contained the His-tag, bound to the affinity column and associated with the intact chaperone throughout the process. *Right*, purification of His-S-CSS1 via denaturation and refolding. Denaturation removed most of the contaminant proteins and also prevented the His-tagged ATPase domain from associating with the intact chaperone.

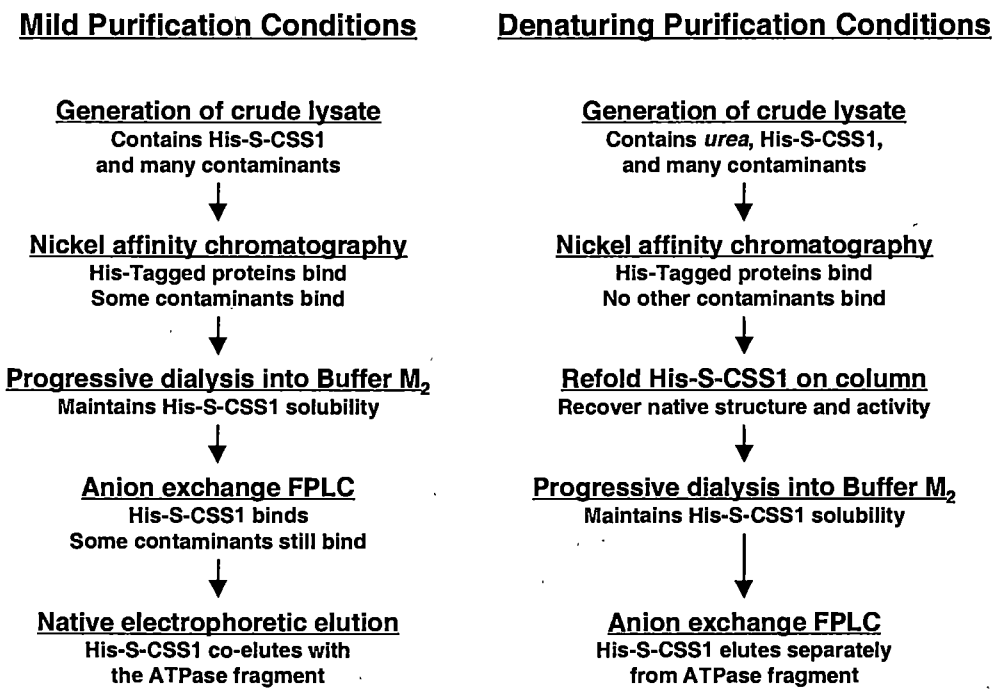

Figure 4-3. Alternate purification schemes for His-S-CSS1.

Figure 4-4. Affinity chromatography using native lysis conditions. Coomassie stained SDS-PAGE gel showing the imidazole elution profile of His-S-CSS1 from a Ni^{2+}-Seapharose resin.

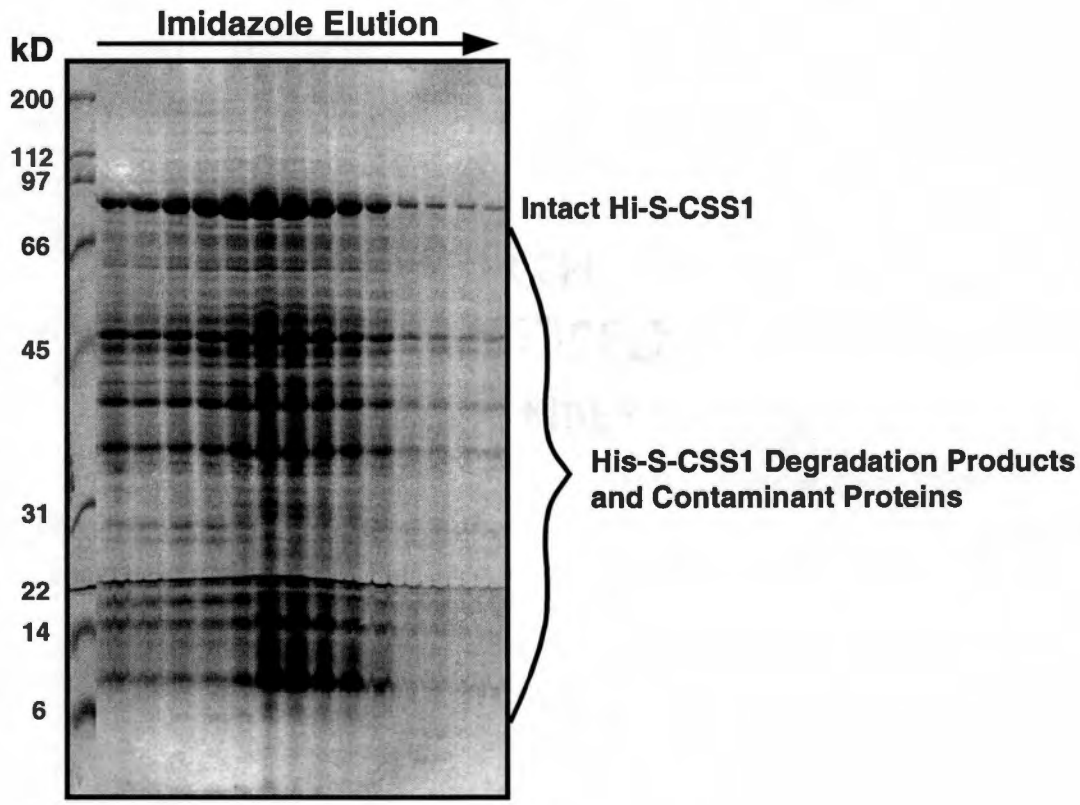

Figure 4-4. Affinity chromatography using native lysis conditions.

$Mg(OAc)_2$, proved successful. Apparently, millimolar concentrations of divalent cation, when present with 1 M imidazole and a highly concentrated His-Tagged protein, cause aggregation

of that protein. Even when using Buffer M_1, a significant portion of the contaminant proteins preferentially precipitated during dialysis, possibly because they were not correctly folded during urea removal in the affinity chromatography step (data not shown).

To further purify the recombinant CSS1, we applied fractions which contained the protein from the previous step to ion exchange FPLC (Figure 4-5). However, the technique failed to significantly enrich the concentration of the recombinant protein (based on western blotting; data not shown). Again, degradation/contamination appeared to be the source of the majority of the eluted protein. Thus far, the proteins eluting with His-S-CSS1 demonstrated high affinity for nickel as well as a similar affinity for the ion exchange resin and possibly affinity for His-S-CSS1 itself.

Next, we applied the ion exchange fractions which contained His-S-CSS1 to native acrylamide gel electrophoretic elution (Figure 4-6). We observed the first significant enrichment of the chaperone with respect to the contaminants since the affinity chromatography--the smallest contaminants eluted first. However, many proteins, including the major contaminant at 47 kD which appeared CSS1's ATPase fragment fused to the His-S dual eptitope tag since it cross reacted with an α-DnaK polyclonal antiblody, co-eluted with intact His-S-CSS1.

Having failed to purify the recombinant chaperone using affinity chromatography based on His_6-Tag technology, ion exchange chromatography based on protein charge, and

Figure 4-5. Ion exchange chromatography using native lysis conditions. Coomassie stained SDS-PAGE gel showing the NaCl gradient elution of His-S-CSS1 from a Q-Sepharose resion.

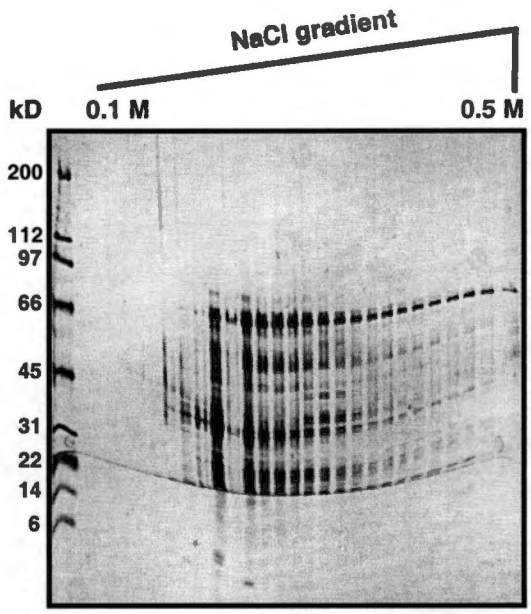

Figure 4-5. Ion exchange chromatography using native lysis conditons.

Figure 4-6. Native polyacryamide gel electroelution. Coomassie stained SDS-PAGE gel showing the elution profile over time from a native preparative acrylamide gel.

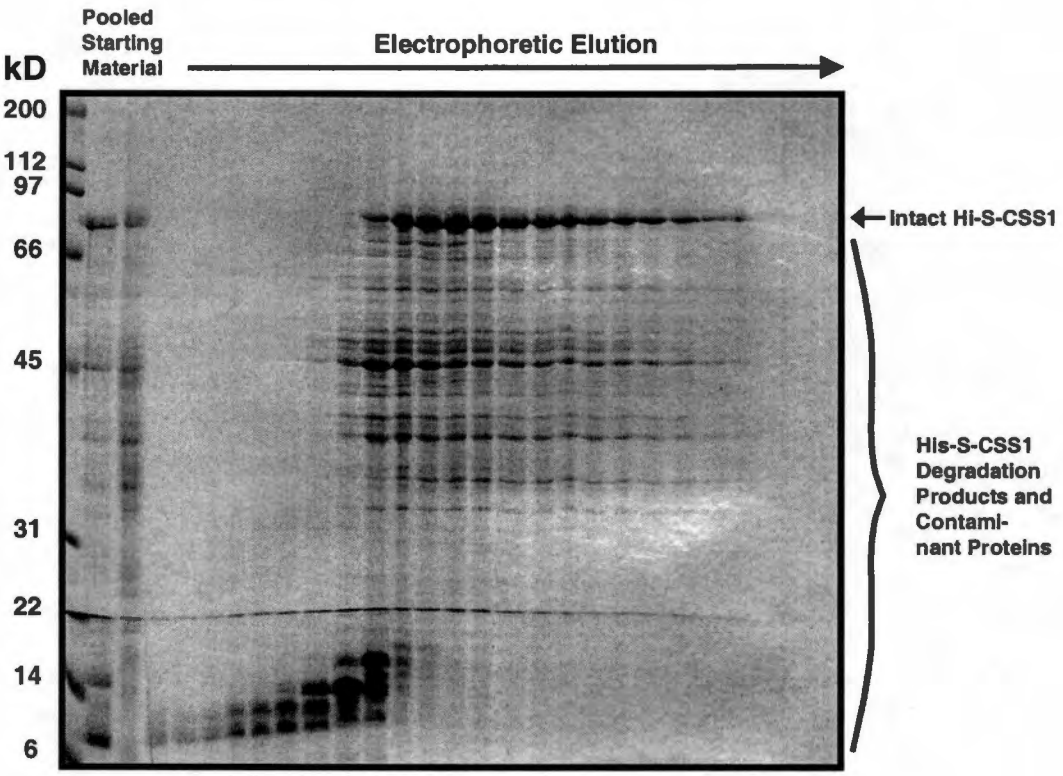

Figure 4-6. Native polyacrylamide gel electroelution.

native electrophoretic elution based on protein size, we concluded that native bufferconditions were not suitable for this purification. Given that the His_6-Tag/Ni^{2+} interaction, unlike other protein/Ni^{2+} interactions, can withstand denaturing buffer conditions (Novagen protocol) and that DnaK is at least partially refoldable in vitro (Palleros et al., 1992), we decided to use 6 M urea in the initial cell lysis buffer. Under these conditions, when the crude extract was subjected to affinity chromatography, the imidazole-eluted fractions contained only intact His-S-CSS1 and its N-terminal degradation products (Figure 4-7). Note the apparent loss of Ni^{2+} affinity of many of the contaminant bands (compare to Figure 4-4) due to the chaotropic action of urea.

It was important to clarify that the affinity chromatography did not yield proteins which had no chance of proper folding. After the crude sample was loaded onto the column and washed exhaustively in urea-containing buffer, the urea was removed in a linear gradient until the the column was equilibrated with the original, native buffer. This process allowed for slow refolding of the proteins on the column. After dialyzing the protein sample in Buffer M_2, the sample was subjected to ion exchange chromatography as before, when the protein sample had never been denatured. This time, however, an acceptable separation between the contaminant bands and the intact fusion protein was achieved with the linear NaCl gradient (Figure 4-8). Therefore, initial denaturation of all the proteins in the crude cellular extract with urea enabled the combination of affinity and ion exchange chromatographies to purify His-S-CSS1.

Finally, yield of the recombinant protein was optimized by varying the growth and induction temperatures and the IPTG levels. The optimum conditions were growth and

Figure 4-7. Affinity chromatography using denaturing lysis conditions. Coomassie stained SDS-PAGE gel showing the imidazole elution profile of His-S-CSS1 from a Ni^{2+}-Seapharose resin.

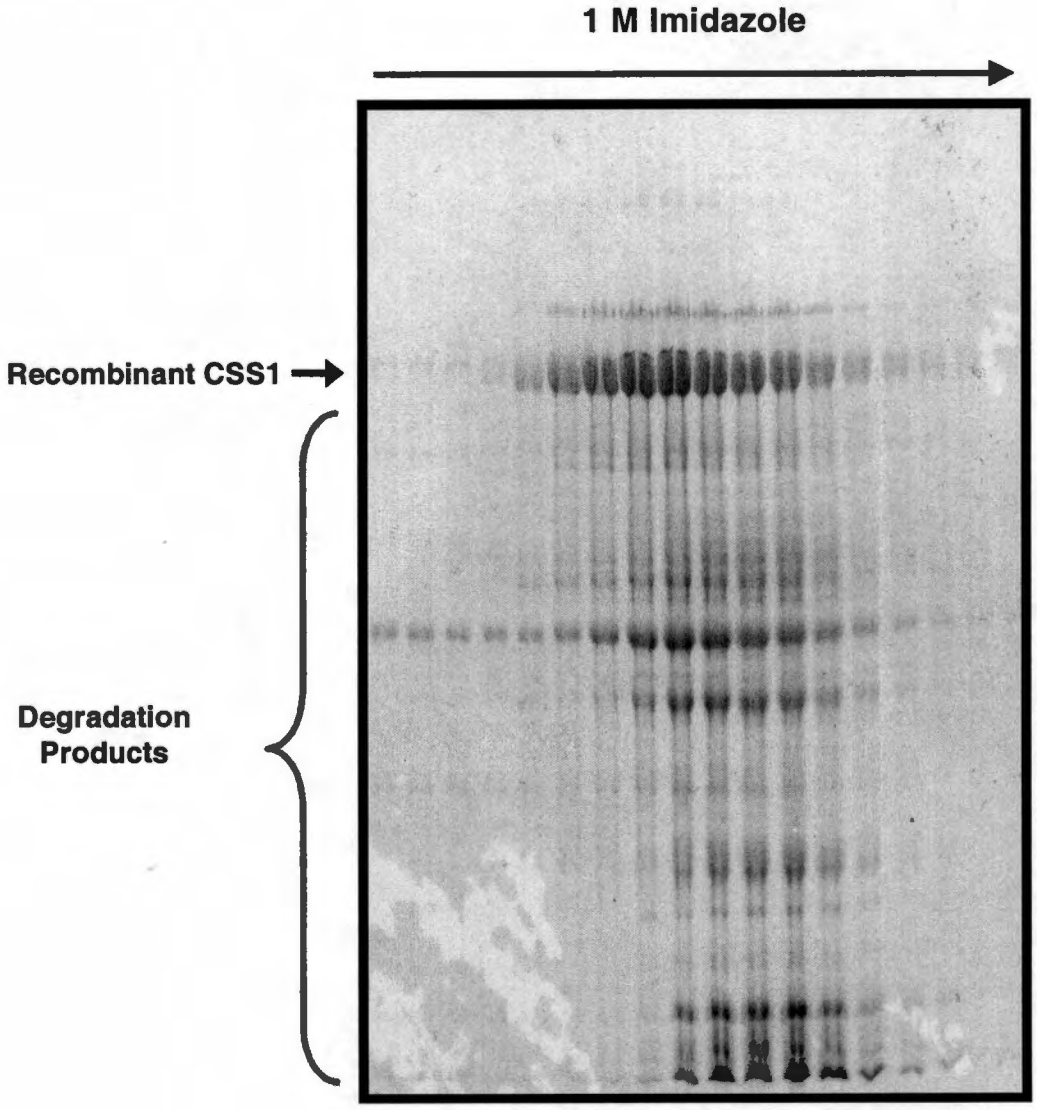

Figure 4-7. Affinity chromatography using denaturing lysis conditions.

Figure 4-8. Ion exchange chromatography using denaturing lysis conditions. Coomassie stained SDS-PAGE gel showing the NaCl gradient elution of His-S-CSS1 from a Q-Sepharose resion.

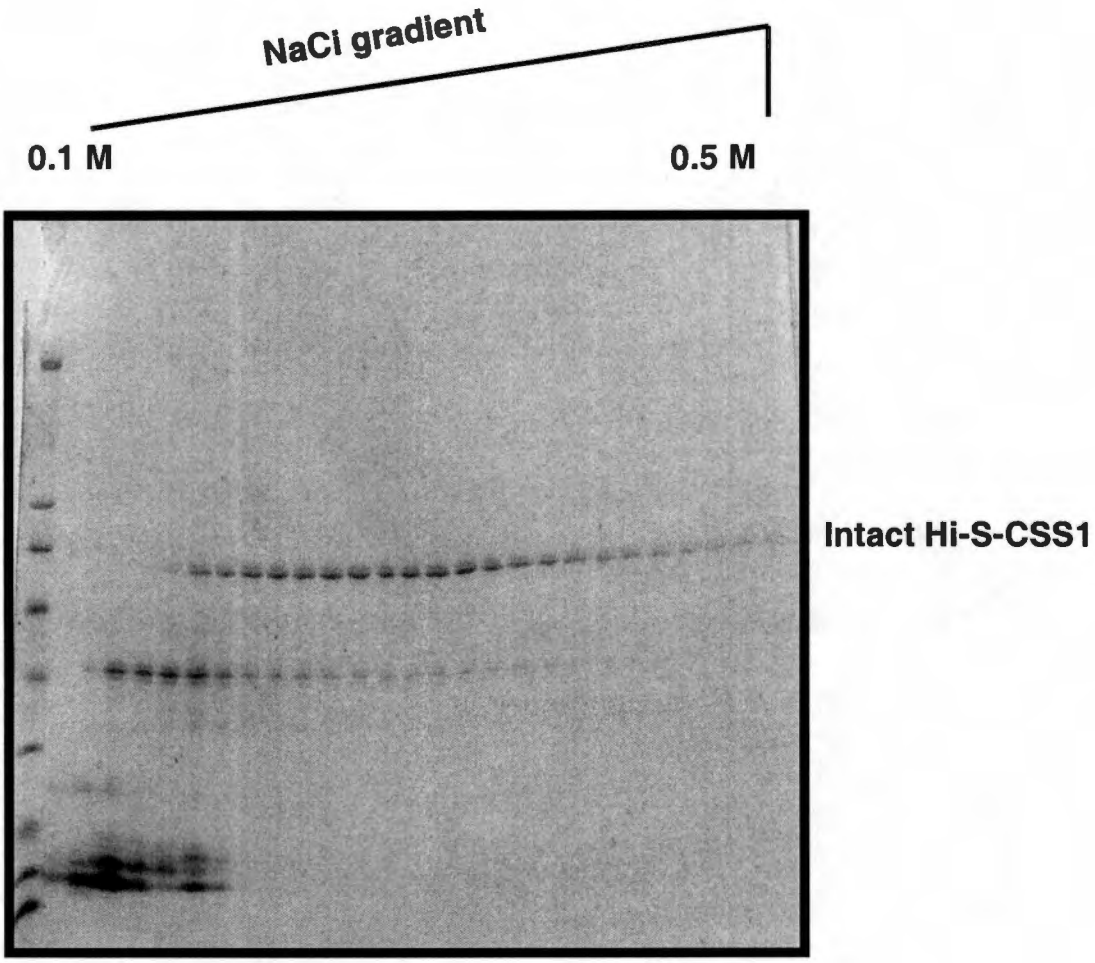

Figure 4-8. Ion exchange chromatography using denaturing lysis conditions.

induction at 27°C and induction with IPTG at 2 mM. The improvement in the recombinant protein expression level when compared to the initial expression conditions (growth and induction at 37°C, 1 mM IPTG) was quite remarkable. For the gel shown in Figure 4-4, the bacterial culture was grown and induced normally. Each lane of the gel was loaded with 20 µl from 1 ml fractions, and the initial cell culture volume was 8 liters. For the gel shown in Figure 4-8, the lower temperatures and higher IPTG concentration were used. However, each lane of this gel was loaded with only 2 µl from 1 ml fractions, and the initial cell culture volume was only 1 liter. Given that the peak band intensities in both gels are similar, the amount of induction and/or protein stability is greatly enhanced under the optimized expression conditions.

ATPase activity of recombinant CSS1

To demonstrate that His-S-CSS1 was properly refolded during its purification, we performed a functional assay to determine whether the chaperone exhibited ATPase activity, and if so, whether that activity could be stimulated by an unfolded peptide substrate. Figure 4-9 shows a basal ATPase activity of ~2.8 pmole ATP/min/pmole enzyme. This rate was stimulated to ~4.3 pmole ATP/min/pmole enzyme when a 100-fold molar excess of RCMLA was added to the reaction. This effect was dependent on the specific interaction of the chaperone with a substrate since an equal addition of native α-lactalbumin did not result in ATPase stimulation (data not shown). As in the case of native CSS1 purified from pea stroma (Ivey et al., 2000), both the substrate levels required and the levels of basal and stimulated ATPase activity observed were similar to those for DnaK (Liberek et al., 1991).

Figure 4-9. ATPase activity of renatured His-S-CSS1. The recombinant Hsp70 displays basal and peptide-stimulated ATPase activities. Spontaneous ATP hydrolysis must be monitored because Hsp70's are very weak ATPases.

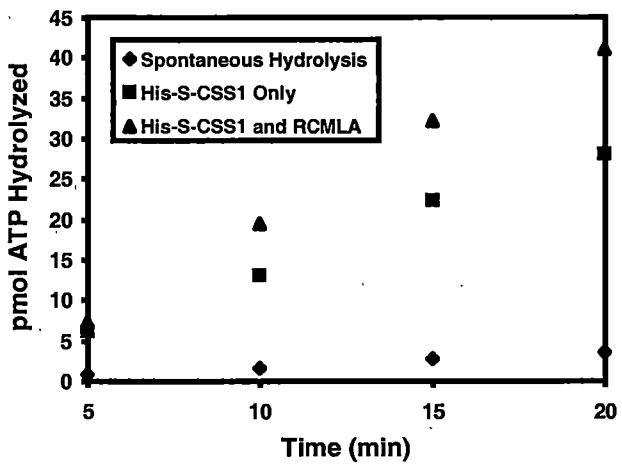

Figure 4-9. ATPase activity of renatured His-S-CSS1.

DISCUSSION

Lessons learned in His-S-CSS1 purification

Several factors contributed to the difficulty of purifying intact recombinant CSS1. First, the affinity column likely did not bind the His-tagged protein exclusively and, therefore, additional purification steps would have been required in any event. Second, the signature trypsin cleavage site in Hsp70's between the ATPase and peptide binding domains, which has been exploited by others in structural studies (DeLuca-Flaherty et al., 1988), worked to our disadvantageThis is evidenced in Figures 4-5, 4-6, 4-7, 4-8, and 4-9, where the ATPase domain remains after obvious proteolytic cleavage in vivo. Third, when not subjected to denaturing conditions, the ATPase domain, and possibly other proteins as well, formed complexes with His-S-CSS1 stable enough to withstand ion exchange chromatography and native electrophoretic elution. Fourth, the observation that a His-tagged protein, imidazole, and a divalent cation were not simultaneously soluble in aqueous buffer was not intuitive, but required extensive trial and error to discover. Finally, the divalent cation Mg^{2+} was required for protein stability as discussed for pea CSS1 in Chapter 3. Therefore, we were initially reluctant to proceed with a purification protocol containing even brief steps which lacked Mg^{2+}.

Fortunately, the protein solubility difficulties were solved and purification proceeded. However, we were unable to obtain the purified recombinant protein until we employed urea in the initial lysis buffer. The purpose of urea was three-fold. First, the urea prevented any molecular interaction weaker than that of the His-tag/Ni^{2+} interaction from occurring during sample loading and washing, thereby preventing any non-His-tagged protein from binding

to the affinity resin. Second, the urea prevented protein-protein interactions which might have lead to co-purification of some unfolded protein with high affinity for Hsp70's. Third, the circumstances under which the urea was removed from the affinity column allowed each molecule of the His-tagged proteins to refold independently from one another. Having the proteins bound to a single Ni^{2+} ion effectively isolated each protein molecule and prevented intermolecular interactions which might have lead to aggregation. Thus, refolding was carried out in a virtual "infinite dilution" of the protein.

Fortunately, the ATPase fragment did not dimerize with the intact chaperone after refolding. Whether dimerization must occur in vivo, or the stucture of the refolded ATPase fragment and/or intact His-S-CSS1 did not allow for dimerization in vitro, or some other factor present only under mild buffer conditions promoted dimerization is not clear. In fact, there is little agreement on whether the ATPase domain is involved in dimerization at all (Palleros et al., 1993; Richarme and Kohiyama, 1993; Benaroudj et al., 1995; Schonfeld et al., 1995).

Alternative Purification Methods

In the future, more facile recombinant CSS1 purification methodologies, which have been used to purify other Hsp70's, may be developed. For example, a monoclonal antibody generated against the relatively unique C-terminal peptide binding domain of CSS1 could be employed in an antibody column to purify the protein in a single step, as in the case of bovine cytosolic Hsp70 (Peake et al., 1991). We had no oppurtunity to use such a technique since we did not have an antibody generated specifically against CSS1.

Another option may be to employ a denatured peptide covalently bound on a column. A mixture of yeast Hsp70's from a crude extract were purified using immobilized, denatured alcohol oxidase (Evers et al., 1993). In our laboratory, we have a column to which SStp is bound at its C-terminus. However, we decided not to use it to purify His-S-CSS1 from a crude lysate for several reasons. First, SStp is extremely susceptible to proteases in crude *E. coli* extracts (Ivey and Bruce, 2000), probably because of its unfolded nature in aqueous solution (Bruce, 1998). Second, we suspected that CSS1 would bind not only His-S-CSS1, but also DnaK, GroEL (Hsp60), and a host of other molecular chaperone contaminants. Third, we have only a few milliliters of the column prepared, which is difficult to produce and was originally intended for use with purified protein components.

Finally, perhaps the most interesting CSS1 purification system to employ would be an affinity tagged form of CSS1 expressed in the plant itself, similar to His-tagged SSC1 in yeast mitochondria (Kubo et al., 1999). One-step purification from the organelle would be relatively simple and possibly rewarding. First, the protein expressed homologously would most likely remain intact. Without His-tagged fragments, purification would much less complicated. Second, other proteins of interest in protein folding and protein import may co-purify with CSS1 due to pre-existing complexes formed in vivo. This technique could be used to purify and clone chloroplast homologs of the co-chaperones DnaJ and GrpE. More importantly, this method, coupled with controlled membrane solubilization, could show whether Tic40 is the CSS1 membrane anchor, which could ultimately demonstrate that CSS1 is the translocation motor of chlorplast protein import.

Chapter 5-Phylogenetic and Biochemical Characterization of the Major Stromal Hsp70, CSS1

ABSTRACT

Although Hsp70s have been isolated in complexes containing chloroplast precursor proteins and the major stromal Hsp70, CSS1, binds transit peptides specifically, the role of Hsp70 involvement in chloroplast protein import remains unclear. Also, little characterization of the chloroplast chaperone itself is in evidence. The Hsp70 class of molecular chaperones is conserved throughout biology, and we have performed phylogenetic analyses with many recently available sequences of Hsp70s from cyanobacteria, algae, and higher plants–from several cellular compartments–to support the theories of prokaryotic chloroplast origin and evolutionary divergence in eukaryotic Hsp70s. We have also purified CSS1 from pea and tested it for several known Hsp70 functions including ATPase and autophosphorylation activities, cation and pH dependencies, co-chaperone interaction, and protein folding. These results are discussed in the contexts of Hsp70 evolutionary conservation and the chloroplast protein import system.

INTRODUCTION

The vast majority of organelle-bound precursor proteins synthesized in the cytosol contain necessary and sufficient targeting information within their amino acid sequences (reviewed in Schatz and Dobberstein, 1996). Targeting sequences of the same precursor from different organisms lack, in addition to any significant secondary

structure (von Heijne et al., 1991; von Heijne and Nishikawa, 1991), high sequence similarity. Furthermore, unrelated precursors share almost very low sequence similarity, even though they might be targeted for the same organelle and share a common import pathway. Because of this lack of similarity among targeting sequences, most models of organellar protein import include a homolog of the Hsp70 class of molecular chaperones attached peripherally as a molecular motor (Craig et al., 1989; Ostermann et al., 1990; Scherer et al., 1990; Brodsky et al., 1995; Schatz and Dobberstein, 1996). Hsp70s are well known for their degenerate peptide substrate specificities and their ability to bind a diverse set of unfolded proteins (Fourie et al., 1994; Rudiger et al., 1997).

The major chloroplast Hsp70 homolog, CSS1 (Chloroplast Stress Seventy 1) forms a stable complex *in vivo* and *in vitro* with the chloroplast targeting sequence, or transit peptide, of the precursor for the small subunit of Rubisco (ribulose-1,5-bisphosphate carboxylase/oxygenase) (Ivey and Bruce, 2000). Likewise, significant interaction between mitochondrial presequences and DnaK, a prokaryotic Hsp70 homolog, has been reported (Zhang et al., 1999). Unlike the mitochondrial system, no clear agreement that the Hsp70 class of molecular chaperones is involved in protein import to the chloroplast exists (Soll and Waegemann, 1992; Nielsen et al., 1997). However, recently reported statistical arguments for Hsp70 affinity for transit peptides are quite compelling (Ivey et al., 2000). Not only are virtually all transit peptides predicted to bind Hsp70s, but a significant majority are expected to share high affinity at the N-terminus of the targeting sequence, moderate affinity in the middle, and little if any affinity at the C-terminus. This region-specific affinity, while not direct evidence of CSS1's role as an ATP-driven molecular motor in chloroplast protein import, provides

the only rationale for the almost complete lack of primary sequence similarity among transit peptides and for the uni-directional movement of precursor proteins across the chloroplast envelope.

In this study, we relate CSS1 to the Hsp70 class of molecular chaperones at-large. Many algal and higher plant Hsp70s have been cloned recently which provided the basis for in-depth phylogenetic comparisons and other analyses. Therefore, we first report the evolutionary conservation and divergence of Hsp70s with emphasis on the origins of chloroplastic homologs. We also outline a novel purification strategy using denaturation and on-the-column refolding techniques to achieve an active, soluble, and monomeric enzyme species. Finally, we show that CSS1 behaves similarly to other Hsp70s *in vitro* with respect to ATPase and autophosphorylation activities. These results provide insight into the commonalities of Hsp70 function and therefore lend credence to the argument for CSS1 involvement in chloroplast protein import.

MATERIALS AND METHODS

Sequence similarity analyses

Hsp70 protein sequences were acquired from the GenBank protein sequence database between 10/28/98 and 11/2/98. Accession numbers are as follows: *Synechococcus* DnaK 2, 1706478; *Synechocystis* DnaK 2, 118730; *Cyanella* (chloroplast-encoded, ct.), 1016208; ct. *Cryptomonas*, 99343; ct. *Porphyra*, 2147178; ct. *Pavlova*, 232002 ; ct. Cucumber, 1143427 ; ct. Watermelon, 092815; ct. Spinach, 2654208; ct. Pea, 399942; ct. *Chlamydomonas*, 1225970; *Synechosystis* DnaK 3, 3122023; *Anabaena*, 2073390; *Synechococcus* DnaK 3, 1706479; *Synechocystis* DnaK 1, 2495354;

Synechococcus DnaK 1, 1706477; *Arabidopsis* (cytosolic, cy.), 3043415; cy. Rice, 763160; cy. Spinach, 2642648; cy. Maize, 123593; cy. Tomato, 2119719, cy. Wheat, 2827002; cy. Pea, 1771479; cy. Soybean, 123601; cy. *Chlamydomonas*, 81239; Tomato (endoplasmic reticulum, er.), 1346172; er. Soybean, 2642238; er. Tobacco, 729620; er. Maize, 1571520; er. Rice, 024182; er. *Arabidopsis*, 1303695; er. Spinach, 388065; Pea (mitochondrial, mt.), 20835; mt. Kidney Bean, 22636; mt. Potato, 300264; mt. Spinach, 049045; ct. Daffodil, 1839631; ct. Squash, 421811; ct. Maize, 6478933.

The amino acid sequence of each Hsp70 was divided according to the consensus pentapeptide sequence, DIVLL, between the N-terminal ATPase and C-terminal peptide-binding domains (approximately residue 383) prior to analysis via the Clustal Method (Higgins and Sharp, 1988; Thompson et al., 1994; Higgins et al., 1996). For Hsp70s with cleavable N-terminal targeting sequences, the consensus pentapeptide sequence, VGDIL, was chosen to signify the N-terminus of the ATPase domain.

Purification of Hsp70s, co-chaperones, and SStp

Native CSS1 from *P. sativum* was purified as described previously (Ivey et al., 2000). Briefly, CSS1 was purified from 14 day old cotyledons using an affinity chromatography method similar to that used to isolate bovine clathrin uncoating ATPase, or Hsc70 (Schlossman et al., 1984). Fractionated stroma was prepared (Bruce et al., 1994) and diluted 1:10 with Buffer M [20mM HEPES (pH 7.5), 20 mM NaCl, 2.5 mM $Mg(OAc)_2$, 1 mM DTT, and 0.1% Triton X-100]. The sample was loaded onto an ATP-agarose column (Sigma, Catalog #A-2767) which had been pre-equilibrated with Buffer M at 4°C. The column was washed with Buffer M, then with Buffer M containing 1 M

NaCl, and finally with Buffer M again. Finally, CSS1 was eluted with 10 mM ATP in Buffer M titrated to pH 7.5. Eluted fractions containing CSS1 were dialyzed and concentrated into Buffer M by ultra-filtration against a 30 kD MWCO membrane, aliquoted, and stored at -85 Oc.

DnaK was purified as described previously (Ivey and Bruce, 2000). Briefly, *E. coli* BL21 cells transformed with pGEX-2T-SStp were grown to a cell density corresponding to an OD_{600} of 0.6, induced with 100 μM IPTG for one hour, pelleted, resuspended, and lysed by sonication on ice in PBS, pH 8.0 containing 1% (v/v) Triton X-100, 1 mM DTT, 5 mM EDTA, 2 μM leupeptin, 2 μM pepstatin, 1 mM PMSF, 5 mM 1,10-phenanthroline, and 3 mM ADP. The lysate was centrifuged at 25,000 x g for 30 min at 4 °C. The resulting supernatant was then loaded at 4 °C onto a column of glutathione-Sepharose (Pharmacia). The column was first washed with PBS containing 1% Triton, then equilibrated with DnaK elution buffer (PBS, pH 8.0 containing 2 mM $MgCl_2$ and 50 mM KCl). DnaK was eluted with 3 mM ATP in the same buffer. After the column was equilibrated with thrombin buffer (PBS, pH 8.0 containing 2.5 mM $CaCl_2$), thrombin was then added onto the column in the same buffer and allowed to digest the fusion protein for 4-6 hours. SStp was then eluted with thrombin buffer. Eluted fractions containing DnaK or SStp were dialyzed and concentrated into Buffer M by ultra-filtration, aliquoted, and stored at -85 °C.

Hsc70 from wheat germ was purified as described previously (Miernyk et al., 1992). Briefly, pulverized wheat germ was steeped in an appropriate buffer and centrifuged to remove particulate matter. The supernatant was applied to an ATP affinity

matrix (Sigma). After washing, Hsc70 was eluted with 10 mM ATP. After dialysis into Buffer M, the protein was concentrated, aliquotted and stored at –85°C.

His-tagged forms of AtE1 from *A. thaliana* (Accession #1498064) and MgE1 from *S. cerevisiae* (Accession #585221) were purified using techniques described in Chapter 4 (Ivey and Bruce, manuscript in preparation). Briefly, *E. coli* BL21(DE3) cells were transformed with either pET30a-CSS1, pETXXXX-AtE1, or pETXXXX-MgE1. Each of the cultures of 4l was grown to a cell density corresponding to an OD_{600} of 0.6 at 37°C, and induced for three hours with 1 mM IPTG. After induction, the cells were lysed in Buffer M containing 6 M urea using a French Pressure cell. Each lysate was clarified via centrifugation at 50,000 x G for one hour at 4°C. The crude supernatant was then applied to a nickel-charged, chelating affinity matrix (Pharmacia) equilibrated in denaturing Binding Buffer according to a Novagen protocol. After the resin was washed with Binding Buffer containing 6 M urea, the buffer was changed to native Binding Buffer through a linear gradient over 10 column volumes and two hours at 4°C. Then, either refolded AtE1 or MgE1 was eluted from the resin with 1 M imidazole. AtE1 and MgE1 eluted as pure, intact proteins. Fractions from the affinity chromatography containing each of the fusion proteins were pooled and dialyzed against Buffer M_1. After dialysis, $Mg(OAc)_2$ was added to 2.5 mM. The protein samples were concentrated via ultrafiltration using a 10 kD MWCO membrane, aliquotted, and stored at –85°C.

Purified forms of *E. coli* DnaJ (Accession #1786197) and GrpE (Accession #462364) were purchased from StressGen Biotechnologies Corporation (Victoria, BC). RCMLA and native α-lactalbumin were purchased from Sigma. The N-terminus of the

mature form of CSS1 from *P. sativum* was determined by automated peptide sequencing using the Edman method (reviewed in Walsh et al., 1981) at St. Jude Children's Research Hospital.

ATPase assays

Hsp70 ATPase activity was measured as described in Chapter 3. Briefly, each 50 µl reaction contained His-S-CSS1, unlabeled ATP, and [γ-^{32}P]ATP and was incubated at 37 °C. Peptide substrates were provided at 100-fold molar excess relative to the chaperone. Aliquots of the reaction mixture were withdrawn at regular intervals and mixed with 1 ml of 50 mM HCl / 5 mM H_3PO_4 containing 7% (w/v) activated charcoal. After microcentrifugation, 200 µl aliquots of the free $^{32}P_i$-containing supernatants were removed and counted via scintillation. Observation of spontaneous ATP hydrolysis was necessary because Hsp70 ATPase activities are extremely low.

Autophosphorylation of CSS1

His-S-CSS1's autophosphorylation activity was tested essentially as described previously for DnaK (Zylicz et al., 1983). Briefly, 50 µl reactions containing purified CSS1 in Buffer M_2 were incubated for 30 minutes in the presence of 50 µM total ATP (unlabeled and [γ-^{32}P]ATP) and varying concentrations of either $MgCl_2$, $MnCl_2$, or $CaCl_2$. The protein was precipitated with TCA to remove unincorporated [^{32}P], washed with acetone, and counted via a scintillation counter. In the cation dependence studies, the buffer was set to pH 7.5.

Luciferase refolding assays

Luciferease was renatured using molecular chaperone systems essentially as previously described (Schumacher et al., 1996). Briefly, 100 nM Firefly Luciferase (Promega) in Stability Buffer (25 mM Tricine-HCl, pH 7.8, 8 mM $Mg(OAc)_2$, 0.1 mM EDTA, 10 mg/ml BSA, 10% glycerol, and 0.25% Triton X-100) was denatured to less that 1% of its original catalytic activity by incubation at 42°C for 15 minutes and subsequent incubation on ice for 10 minutes (data not shown). Refolding samples of 100 µl containing 5 nM luciferase, 1 µM each of chaperone and co-chaperones, and 50 µM competitor were prepared in Refolding Buffer (10 mM Tris-HCl, pH 7.5, 3 mM $Mg(OAc)_2$, 50 mM KCl, 2 mM DTT, and 4mM ATP) and incubated at 22°C for two hours. At 30 minute intervals, 5 µl of each reaction was added to 120 µl of Assay Buffer (25 mM Tricine-HCl, pH 7.8, 8 mM $Mg(OAc)_2$, 0.1 mM EDTA, 8 mM DTT, 100 µM D-luciferin, 240 µM coenzyme A, and 0.5 mM ATP). Microtiter plates were blocked for 1 hour at 37°C with Buffer M containing 1% gelatin prior to sample addition. Light production was measured immediately on a luminometer. In all experiments, recovered luciferase activities were compared to samples which had not been denatured at 42°C.

Molecular modeling

The peptide-binding domain of CSS1 (residues 450-608) was modeled after the X-ray crystal structure (Zhu et al., 1996) of the peptide-binding domain of the prototypical Hsp70, DnaK (residues 389-597). First, the DnaK/peptide structural coordinates were downloaded from the Protein Data Bank (Brookhaven). Then, using the

software Insight II (1995 version), the amino acid compositions were changed to those of CSS1/SStp. All subsequent calculations were carried out using the AMBER force field (Weiner et al., 1986) interfaced with the molecular mechanics package DISCOVER (BIOSYM/Molecular Simulations) operating on a Silicon Graphics Indigo-2 workstation. After restrained conjugate gradient minimizations (500 iterations), random structures were generated by subjecting the model to unrestrained dynamics at 600 K for 10 ps. Then, "folding" was simulated through a series of restrained (X-ray coordinates for DnaK imposed) molecular dynamics (1 ps) at 400, 350, and finally 300 K, with a final restrained conjugate gradient minimization until the r.m.s. derivative was less than 0.01 kcal/Å. Molecular modeling calculations were carried out with a 2-atom-thick water shell with a dielectric constant of 80.

RESULTS

Evolutionary conservation among chloroplastic Hsp70s

Although cyanobacteria contain three distinct classes of prototypical Hsp70s, higher plants and algae express only one as the major stromal form, CSS1. Figure 5-1 illustrates this point with phenograms for both the highly conserved N-terminal ATPase domain as well as the C-terminal peptide binding domain. Not surprisingly, cyanobacteria *Synechococcus* and *Synechocystis* share at least some similarity among all three CSS classes. Interestingly, all chloroplast-encoded algal and nuclear-encoded higher plant CSS1's are most homologous to Class 2 cyanobacterial Hsp70, clearly demonstrating that Class 2 is the progenitor of the evolutionarily conserved, major

Figure 5-1. Phenograms of the three classes of Hsp70 present in cyanobacteria, algal chloroplasts, and higher plant chloroplasts. The N-terminal ATPase and C-terminal peptide-binding domains are analyzed separately. Chloroplasts from both algae and higher plants show the highest sequence similarity with Class 2 cyanobacterial DnaK.

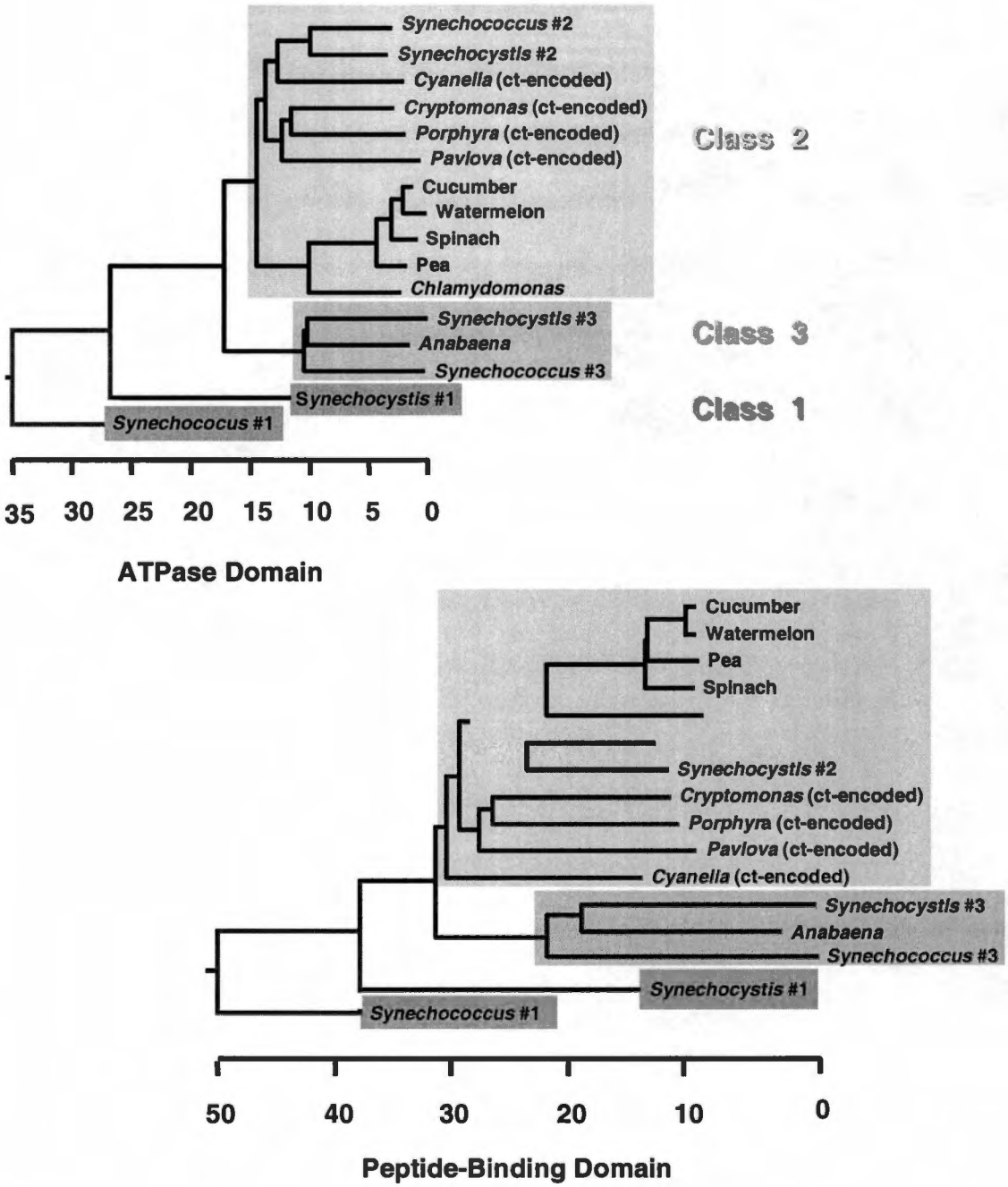

Figure 5-1. Phenograms of Hsp70s

stromal Hsp70 for both algae and higher plants. Further analysis shows the expected patterns of higher similarity between the displayed members of cyanobacteria, algae, and plants, respectively. The lone exception is Class 1, showing little similarity even among cyanobacteria.

Higher plant Hsp70 similarity

As in mammalian systems, Hsp70 similarity in higher plants and the alga, *Chlamydomonas*, is based primarily on compartmentalization. Although an earlier work suggested this concept with much fewer examples (Miernyk, 1997), the phenograms in Figure 5-2 strongly supports this and several other points as well. First, the more recently evolved eukaryotic Hsp70 homologs reside in the cytosol and ER. For all higher plant and *Chlamydomonas* examples shown, the cytosolic and ER Hsp70s show less variance between each other than any other possible comparison. This argument holds for both the N-terminal ATPase domain as well as the C-terminal peptide binding domain. Second, plastidic and mitochondrial forms share less similarity between each other or to either the cyotosolic or ER forms. These data suggest three distinct evolutionary origins for the Hsp70s shown here: eukaryotic, plastidic, and mitochondrial.Third, while *Chlamydomonas* cytosolic Hsp70 (CcHsp70) is most distantly related within the cytosolic Hsp70s, it is even more distantly related to any other sequence shown. Therefore, CcHsp70 suggests an evolutionary link between higher plants and algae.

Figure 5-2. Phenograms of cytosolic, ER, plastidic, and mitochondrial CSS1 from higher plants. The N-terminal ATPase and C-terminal peptide-binding domains are analyzed separately. Similarity relationships are based on subcellular compartmentalization.

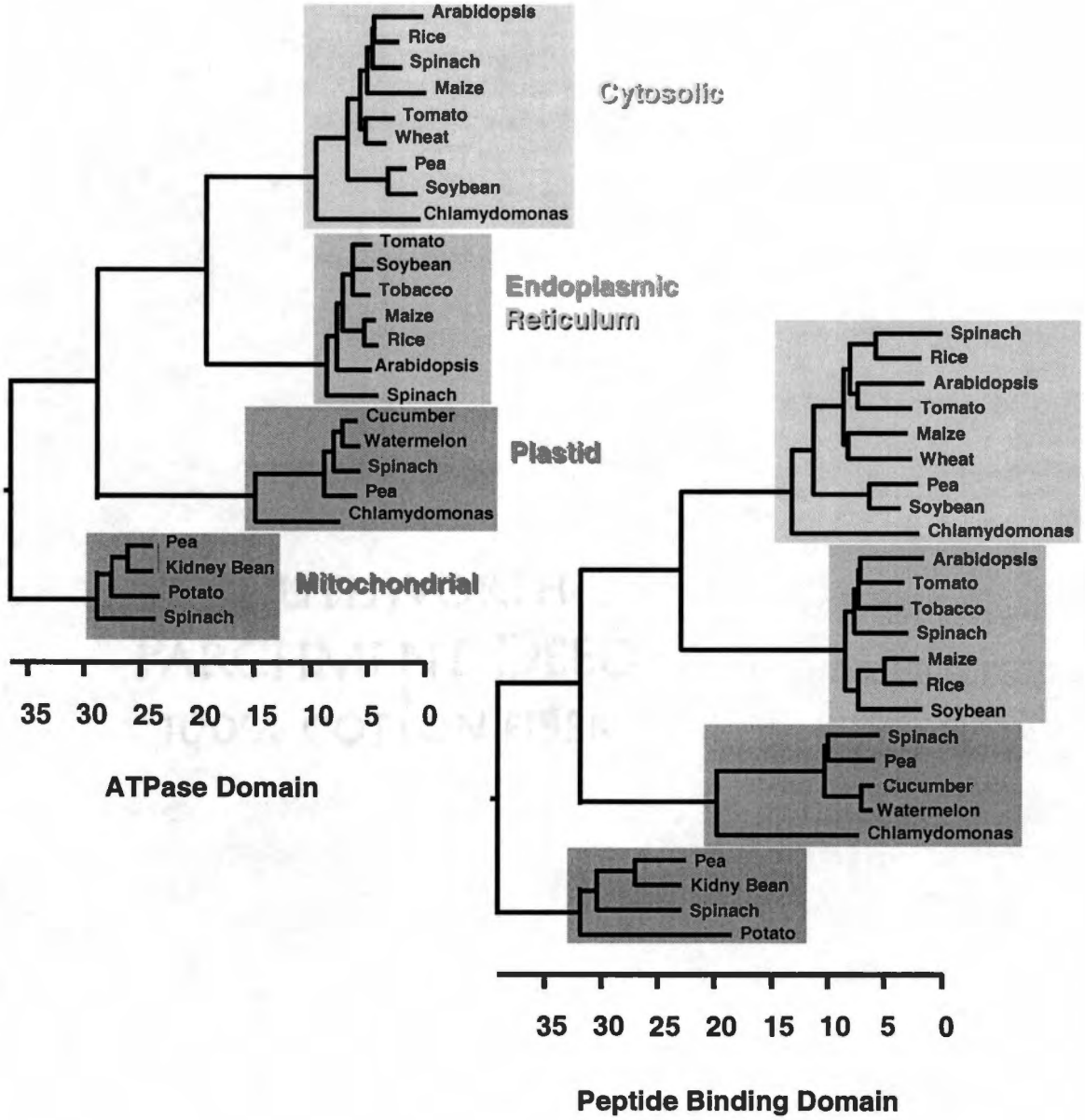

Figure 5-2. Higher plant Hsp70 phenograms.

The true N-terminus of CSS1

After confirming the unblocked N-terminus of CSS1 purified from pea, we compared the transit peptides and SPP cleavage sites from higher plant CSS1 sequences (Figure 5-3). The transit peptides for cucumber, watermelon, spinach, and pea CSS1 share a moderate level of similarity (54%). In contrast, their predicted SPP cleavage sites and mature N-termini are identical from position –3 to +7. These observations agree with documented levels of similarity between transit peptides and Hsp70s, respectively (Gavel and von Heijne, 1990; Boorstein et al., 1994).

Interestingly, pea CSS1's true SPP cleavage site is IVS▼EKV, which is shifted N-terminally by three amino acids relative to it's predicted cleavage site (Emanuelsson et al., 1999). Although not in agreement with the neural network consensus sequence for transit peptides or the older consensus, R-(X)3-I/V-R-A/C▼C (Gavel and von Heijne, 1990), of CSS1. Our data are corroborated by previously sequenced N-termini of daffodil, squash, and maize CSS1.

Chaperone and co-chaperone purification

Figure 5-4 is a demonstration of of the purification of chaperones and co-chaperones not seen previously. The 68 kD native form of wheat germ Hsc70 is shown in

Figure 5-3. The predicted vs. the experimentally confirmed N-terminus of CSS1 in higher plants. The stromal processing protease does not cleave CSS1 at the predicted site, but three residues toward the N-terminus.

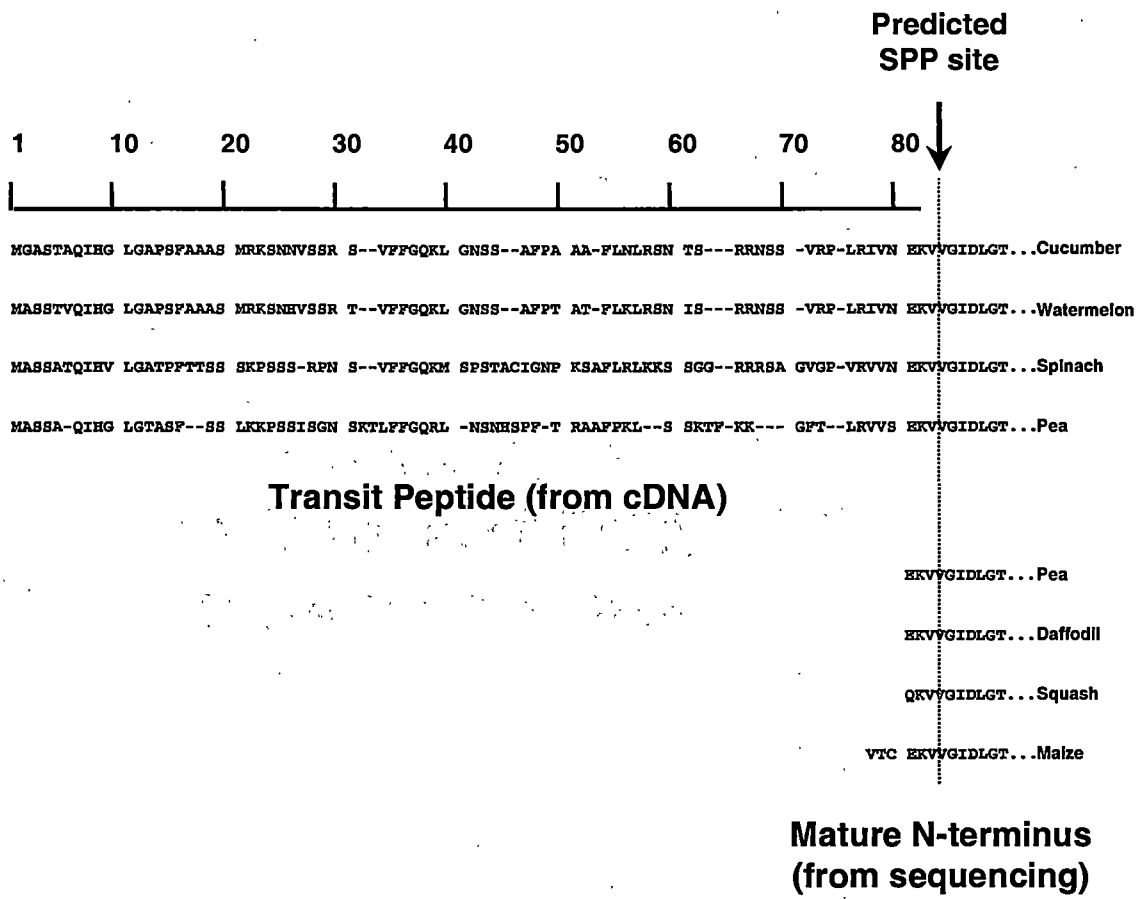

Figure 5-3. The true N-terminus of CSS1.

Figure 5-4. Purification of chaperones and co-chaperones. Coomassie stained SDS gel demonstrating protein purity: 1) MW Standards; 2) Hsc70 from wheat germ; 3) AtE1 from *A. thaliana*; 4) GrpE from *E. coli*; 5) MgE1 from *S. cerevisiae*; and 6) DnaJ from *E. coli*.

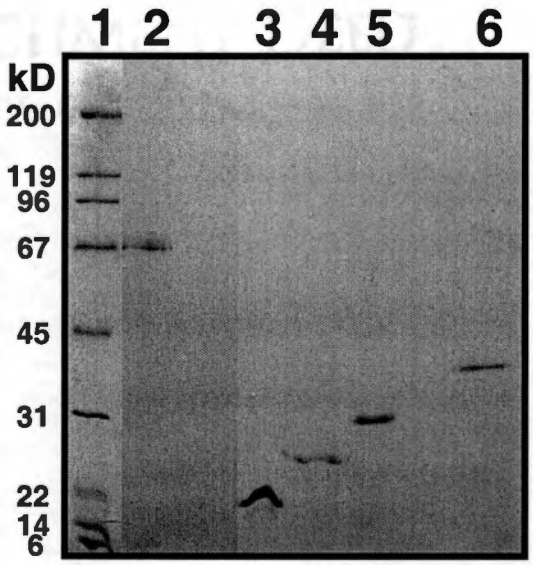

Figure 5-4. Purification of chaperones and co-chaperones.

lane 2. Lanes 3 and 5 show His-tagged forms of AtE1 and MgE1, respectively. Both proteins were refolded on the nickel-chelating affinity column. Finally, native forms of GrpE and DnaJ, purchased from StressGen Biotechnologies Corp. are shown in lanes 4 and 6, respectively.

Comparative Hsp70 ATPase activities

As a primary indicator of CSS1 function, we performed a functional assay to determine whether the chaperone exhibited ATPase activity, and if so, whether that activity could be stimulated by an unfolded peptide substrate. Figure 5-5 (middle panel) shows a basal activity of ~1.9 pmole ATP/min/pmole enzyme. This rate was stimulated to ~3.3 pmole ATP/min/pmole enzyme when a 100-fold molar excess of RCMLA was added to the reaction. This effect was dependent on the specific interaction of the chaperone with a substrate since an equal addition of native α-lactalbumin did not result in ATPase stimulation (data not shown). As in the case of native CSS1 purified from *P. sativum* stroma, both the substrate levels required and the level of stimulation observed were similar to those observed for DnaK (Liberek et al., 1991). For comparison, identical ATPase assays were performed with *E. coli* DnaK (Figure 5-5, top panel) and wheat germ Hsc70 (Figure 5-5, bottom panel). The basal and stimulated ATPase activities for DnaK were 1.2 and 4.6 ATP/min/pmole enzyme, respectively; for Hsc70, 0.6 and 2.5 ATP/min/pmole enzyme, respectively.

Figure 5-5. ATPase activities of Hsp70s. The basal (solid squares) and substrate stimulated (solid circles) ATPase activities of E. coli DnaK (**A**), His-S-CSS1 (**B**), and wheat germ Hsc70 (**C**) are shown.

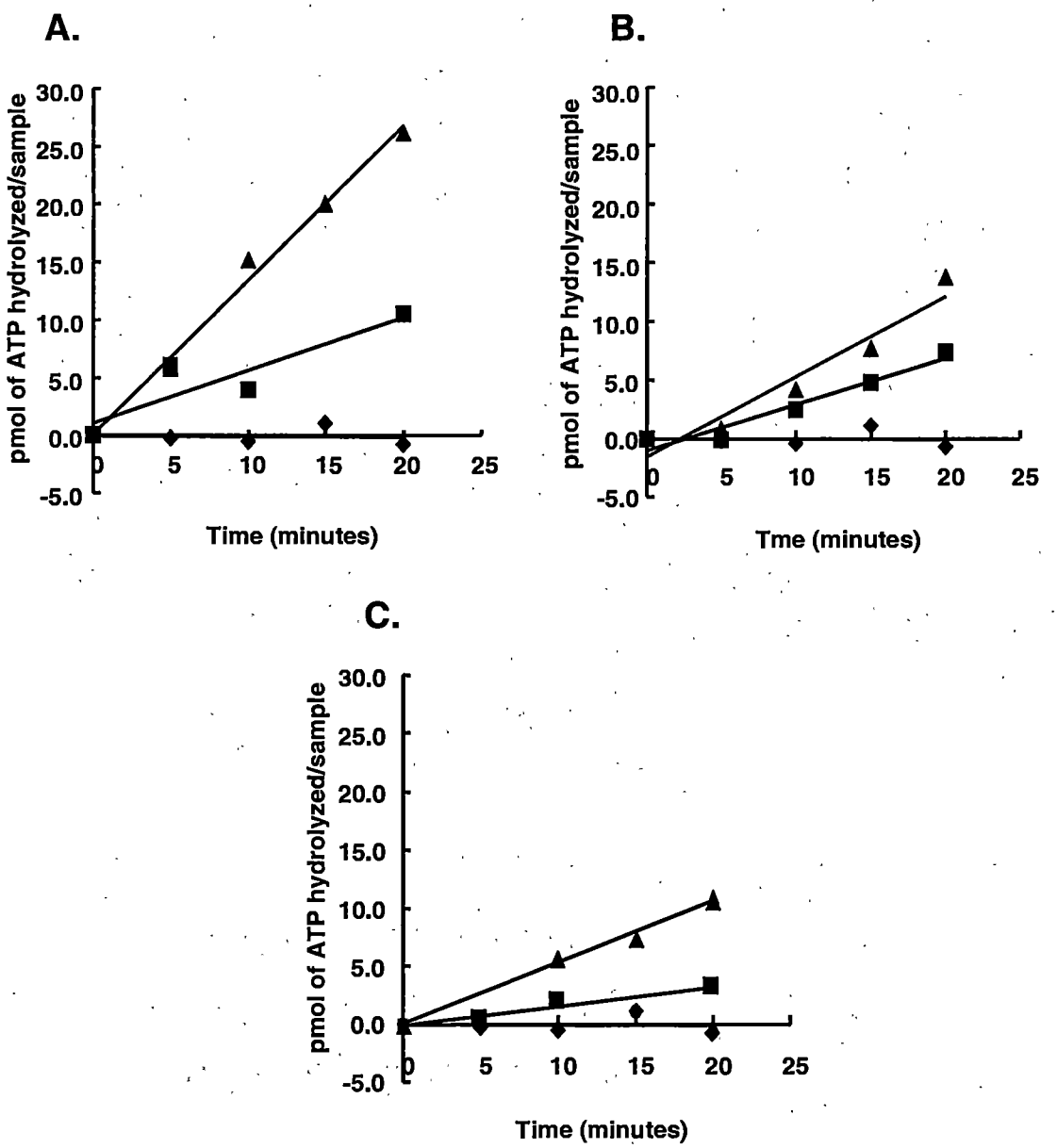

Figure 5-5. ATPase activities of Hsp70s.

Cation effects and pH optima for CSS1 Activities

CSS1's enzymatic activities were further characterized by determining the pH optima for the chaperone's ATPase as well as its autophosphorylation activities. Figure 5-6 shows pH profiles for both. As in the case for DnaK (Zylicz et al., 1983), CSS1 showed a marked difference in pH optima for these two activities. The ATPase optimum was ~7.5, while the autophosphorylation optimum was ~6.2. Therefore, at physiological pH, the ATPase activity, which is the normal catalytic activity during non-stress conditions, would be predominant, whereas the autophosphorylation activity would appear to be triggered by stress.

In addition to stimulation at low pH, autophosphorylation of CSS1 was stimulated specifically by Ca^{2+}. Figure 5-7 shows autophosphorylation as a function of increasing concentration of magnesium, calcium, or manganeseions. Only high concentrations of Ca^{2+}, much higher than those required by protein kinases involved in signal cascades, such as Ca^{2+}/Calmodulin kinase II (Nairn and Greengard, 1987), stimulated activity. While the calcium requirement *in vivo* may be much lower than seen here, our results agree with other data concerning stimulation of DnaK's autophosphorylation activity (Cegielska and Georgopoulos, 1989; Dalie et al., 1990).

ATPase stimulation of native CSS1 by co-chaperones

These results show that CSS1 by itself exhibits basal and peptide-stimulated ATPase activities (Ivey et al., 2000). However, in every prokaryotic and organellar system thoroughly studied to date, Hsp70s can function with at least two co-chaperones

Figure 5-6. pH optima for ATPase and autophosphorylation activities of CSS1. The pH optimum for ATPase activity is ~6.2, which is well below physiological pH; for ATPase activity, ~7.5, which is within the physiological pH range.

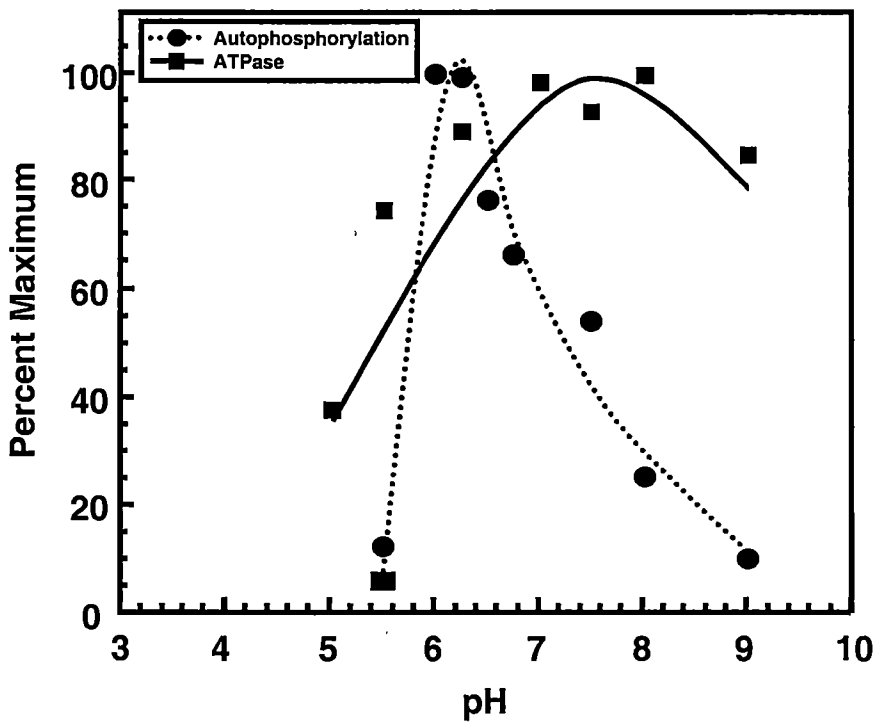

Figure 5-6. pH optima for ATPase and autophosphorylation activities of CSS1.

Figure 5-7. Calcium stimulation of CSS1's autophosphorylation activity. Unlike calcium, neither magnesium nor manganese stimulates CSS1 autophosphorylation. The calcium requirement for peak stimulation is 10 mM, which is well above the physiological range.

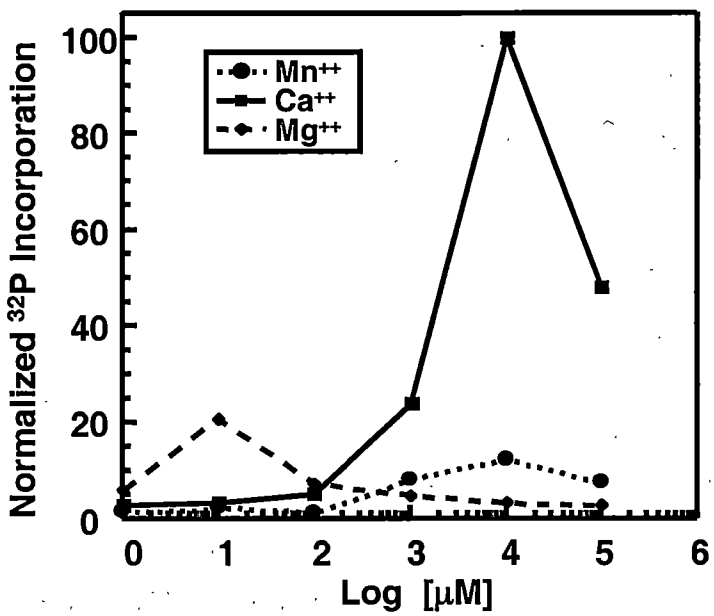

Figure 5-7. Ca^{++} stimulation of CSS1's autophosphorylation activity.

which are homologs of bacterial DnaJ and GrpE, which stimulate ATP hydrolysis and nucleotide exchange, respectively (reviewed in Brodsky, 1996). Since no chloroplast co-chaperone homologs were available for analysis, we chose one DnaJ (from *E. coli*) and three GrpE homologs (from *E. coli*, *A. thaliana* cytosol, and *S. cerevisiae* mitochondria) to examine possible co-chaperone stimulation of the ATPase cycle of CSS1.

Table 5-1 summarizes the results of native CSS1's basal and co-chaperone stimulated ATPase activities. The basal activity of 1.7 pmol ATP/min/pmol CSS1 is only two-thirds the activity previously reported (Ivey et al., 2000), However, batch-to-batch variation is not uncommon in such enzyme preparations. All of the results shown are averages from triplicate experiments using the same batch of CSS1.

Surprisingly, DnaJ alone did not significantly stimulate CSS1's ATPase activity. Of the three GrpE homologs, only the bacterial form stimulated activity beyond standard deviation limits. Since GrpE had a greater stimulatory effect on activity than DnaJ, nucleotide exchange may be a more limiting factor than ATP hydrolysis in the overall ATPase cycle.

When heterologous versions of the entire DnaK/DnaJ/GrpE molecular chaperone machine were reconstituted, only those versions containing "prokaryotic" components (i.e., evolutionarily conserved from prokaryotic origins) exhibited ATPase activity significantly higher than the basal. MgE1 as well as GrpE, in combination with DnaJ, stimulated CSS1 ATPase activity, whereas AtE1 was not significant as a nucleotide exchange factor by DnaJ.

Table 5-1. Co-chaperone stimulation of CSS1 ATPase activity. All assays were conducted in triplicate. Activities are shown with standard deviations.

Table 5-1. Co-chaperone stimulation of CSS1 ATPase activity.

Hsp70	DnaJ	GrpE	pmol ATP/min/ pmol CSS1	Fold Stimulation
(1 molar eq.)	(2 molar eq.)	(2 molar eq.)		
CSS1	-	-	1.7 ± 0.3	1x
CSS1	*E. coli*	-	1.8 ± 0.4	1.1x
CSS1	-	MgE1	2.1 ± 0.3	1.3x
CSS1	-	AtE1)	2.2 ± 0.4	1.3x
CSS1	-	*E. coli*	3.9 ± 0.2	2.3x
CSS1	*E. coli*	MgE1	2.7 ± 0.4	1.5x
CSS1	*E. coli*	AtE1)	2.1 ± 0.2	1.2x
CSS1	*E. coli*	*E. coli*	5.3 ± 0.2	3.2x

Interestingly, CSS1 was stimulated most (~3-fold) by the *E. coli* co-chaperones. Whether the co-chaperones functioned better with each other and/or CSS1 to produce this effect is unknown. However, given that CSS1 is more closely related to DnaK than mitochondrial or cytosolic Hsp70s (Ivey and Bruce, manuscript in preparation), it is appealing to think that CSS1 would function better with bacterial co-chaperones than with mitochondrial or cytosolic ones.

CSS1-mediated recovery of luciferase activity and SStp competition

DnaK and CSS1 have been shown to bind SStp (Ivey and Bruce, 2000; Ivey et al., 2000), and CSS1's ATPase activity is stimulated by SStp and bacterial co-chaperones (Ivey et al., 2000). However, the ultimate test of any chaperone is to repeatedly bind proteins trapped in non-native states in order to allow for recovery of protein function. Renaturation of luciferase, denatured by heat and trapped in an unfolded conformation, by the Hsp70 molecular chaperone machine has long been established (Hendrick et al., 1993; Schroder et al., 1993; Schumacher et al., 1994; Szabo et al., 1994). To further characterize CSS1 as a legitimate chaperone, we performed luciferase refolding assays, substituting CSS1 for DnaK.

Though CSS1's ATPase activity was only stimulated 3-fold by DnaJ and GrpE, refolding of luciferase was entirely dependent on addition of the co-chaperones (data not shown), which is consistent with earlier studies (Schumacher et al., 1994; Szabo et al., 1994). Therefore, all experiments were performed using CSS1 and DnaJ, with GrpE as the reaction initiator.

Figures 5-8A and 5-8B show luciferase activity recovery mediated by DnaK and CSS1, respectively. Initially, no recovery of luciferase activity could be observed. After many attempts, it was concluded that the microtiter plates, which awere dvertised as having a low affinity for non-specific protein interactions, required additional blocking by gelatin.

Both data sets were normalized to 100% of the recovered activity of any sample within each set of experiments. Overall, DnaK was able to facilitate recovery of approximately 11% of the original luciferase activity prior to denaturation, whereas CSS1 only helped recover approximately 2% activity within 2 hours. However, recovery seemed to approach a plateau with DnaK, whereas recovery proceeded at a linear rate in the experiments with CSS1. Therefore, the data suggest that, given enough time, CSS1 may renature as much luciferase as DnaK. The apparent discrepancy may be due to differences in cooperation between the homologous and heterologous chaperone machines.

As in the cases of Hsp70 binding and ATPase activity stimulation (Ivey and Bruce, 2000; Ivey et al., 2000), RCMLA and SStp competed effectively in this *in vitro* assay to affect Hsp70 activity. At 10,000-fold molar excess, both unfolded competitors reduced luciferase recovery to background levels (negative control not shown). In contrast, native α-lactalbumin appeared to slightly stimulate luciferase recovery in both cases, possibly by blocking the microtiter plates from non-specifically binding denatured luciferase. Overall, the data demonstrate that CSS1 is able to productively

Figure 5-8. Luciferase renaturation by Hsp70s. Recovery of luciferase activity is based as a percentage of the total activity recovered in 2 hours for DnaK (**A**) or CSS1 (**B**) in individual experiments.

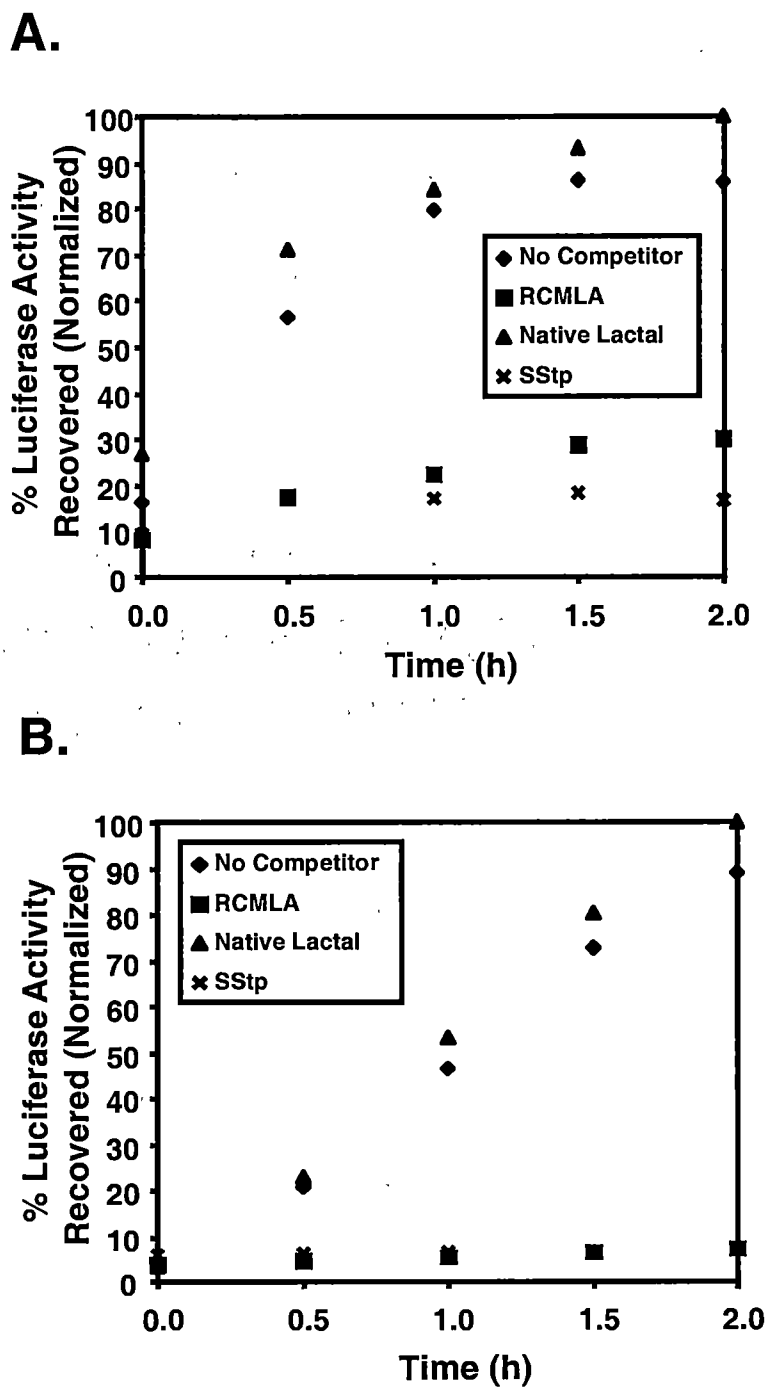

Figure 5-8. Luciferase renaturation by Hsp70s.

function in a chaperone machine to recover the enzymatic activity of luciferase and that unfolded physiological substrates can compete with luciferase for chaperone binding.

CSS1 and DnaK bind unfolded peptides "virtually" identically

Other questions of CSS1 functionality remain. For example, how does CSS1 REALLY bind peptide substrates? Since no structural data for CSS1 is available, our laboratory simulated CSS1-peptide binding using DnaK as a model. Figure 5-9 shows the imposition of two peptide-binding domain structures: (1) DnaK (red) binding the sequence NRLLLT (yellow), and (2) simulated CSS1 (blue) binding a sequence from the N-terminus of SStp, ASMISSS (white). The virtual CSS1/SStp structure was generated by modeling after a known DnaK/peptide structure (Zhu et al., 1997) and then simulating denaturation and refolding. Even after complete structural randomization, CSS1's peptide-binding domain was predicted to refold into a tertiary structure which strongly resembles that of DnaK. The β-sheet peptide-binding "pocket" just underneath the peptide substrate is very similar to that of DnaK, as is the α-helix "lid" situated above the β-turns. Not suprisingly, the SStp fragment occupies the binding site in an extended conformation.

DISCUSSION

Evolutionary conservation of CSS1

Algae and higher plants appear to have universally conserved a homolog from Class 2 of the cyanobacterial Hsp70s as the major stromal isoform of the chaperone. The

Figure 5-9. Molecular Modeling of CSS1. Peptide-binding domains of DnaK (red) and CSS1 (blue) binding the unfolded peptide substrates NRLLLT (yellow) and ASMISSS (white), respectively.

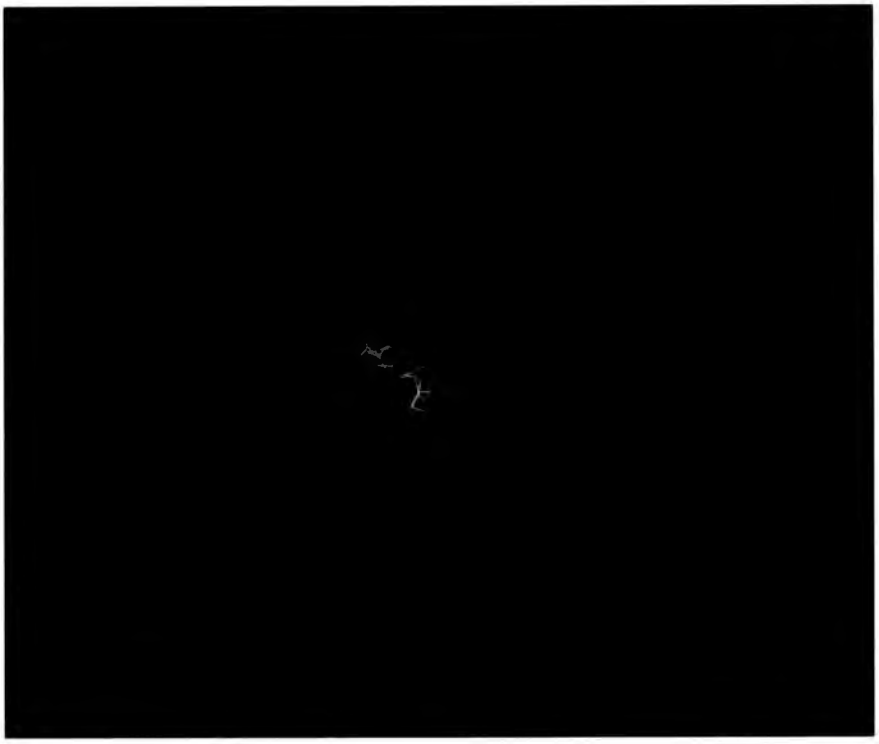

Figure 5-9. Molecular modeling of CSS1

highly conserved gene is higly expressed in cyanobacteria, chloroplast-encoded in algae, and nuclear-encoded higher plants. This genetic trail strongly suggests a direct evolutionary line from cyanobacteria to algae chloroplasts to plant chloroplasts. Strikingly, similarity is conserved even in the more variable peptide binding domains of the chaperone, further suggesting long-term retention of substrate specificity.

Another feature common to chloroplasts and cyanobacteria is the number of Hsp70 homologs present in each. Three homologs have been detected in pea chloroplasts (Marshall et al., 1990), although only CSS1 has been cloned (Marshall and Keegstra, 1992). CSS2 and CSS3 are expressed at much lower levels than CSS1 and, upon cloning, their mature domains may exhibit high sequence similarity with Class 1 and/or Class 3 cyanobacterial DnaK's. Alternatively, mitochondrial and/or the "eukaryotic Hsp70s" may have evolved from Class 1 and/or Class 3 DnaK, since the phenograms in Figure 5-2 suggest three predecessors for the major groups of higher plant Hsp70s: eukaryotic, mitochondrial, and plastidic. The latter two organellar systems, while believed to have evolved through endocytotic events, share higher similarity through CSS1 conservation than either do with more recently evolved higher plants which also encode, in the nucleus, cytosolic and ER homologs (Boston et al., 1996; Miernyk, 1997).

Transit peptide evolution and conservation are much less obvious. Cyanobacterial Hsp70s do not require organellar targeting and therefore contain no targeting information in their amino acid sequences. The algal CSS1's shown are chloroplast- encoded and are synthesized in the same cellular compartment in which they function, thereby bypassing the need for a transit peptide. Higher plant CSS1 transit peptides, unlike mature precursor domains, share little similarity, even between precursors of the same protein from

different organisms (von Heijne et al., 1991). Even the most recently developed *a priori* primary sequence-based prediction methods cannot accurately forecast either transit peptide identification (~80% accuracy) or cleavage site (~60% accuracy) given a chloroplast precursor sequence (Emanuelsson et al., 1999). Therefore, the most likely basis for the common functions of transit peptides—targeting, interaction with the translocation machinery, and presentation of the precursor to the stromal processing protease—is probably founded in secondary structural properties (or lack thereof) and/or interaction with a protein(s), such as CSS1, which has the capacity to accommodate such diverse sequences.

Functional characterization of CSS1

CSS1 displayed wild-type characteristics for ATPase activity, both basal and peptide-stimulated. These activities are similar to those of other Hsp70s, of both prokaryotic and eukaryotic origin. In all cases, the Hsp70s exhibited a marked stimulation by addition of the permanently unfolded protein, RCMLA, a model substrate, presumably by stimulating nucleotide exchange (Sadis and Hightower, 1992).

CSS1 also behaved similarly to *E. coli* DnaK in terms of pH optima for ATPase and autophosphorylation activites. The reason for the difference in the pH optima for these two activities is significant. Under healthy growth conditions, the ATPase activity is favored. Therefore, Hsp70 functions normally in the cell. In fact, normal cycling with co-chaperones and peptide substrates along with nucleotide exchange actually inhibits Hsp70s autophosphorylation activity (Panagiotidis et al., 1994). Stress conditions on the other hand, such as high temperature (Sherman and Goldberg, 1993) or low pH (Zylicz et

al., 1983), stimulate both the ATPase and autophosphorylation activities of Hsp70s, providing the chaperone with an enhanced ability to bind fragile proteins and prevent misfolding and aggregation (McCarty and Walker, 1991). Apparently, phosphorylated Hsp70s are handicapped in other roles, such as assisting in the translocation of secretory precursors (Miernyk et al., 1992).

CSS1 can function *in vitro* with co-chaperones as well. In this study, CSS1's ATPase activity was stimulated over 5-fold by the nearest evolutionary homologs of DnaJ and GrpE tested. As suggested by Figure1 5-1 and 5-2, CSS1 and its homologous chaperone machine should be more closely related to that in the bacterial system than to those either in the "eukaryotic" or mitochondrial systems. Therefore, it is not suprising that CSS1 functioned best with *E. coli* co-chaperones. It will be interesting to see whether CSS1's ATPase activity is stimulated to a higher degree by chloroplast DnaJ and GrpE homologs. However, explict involvement of co-chaperones in chloroplast protein import is not known, although there is evidence of GrpE participation in the mitochondrial import apparatus (Kronidou et al., 1994; Laloraya et al., 1994; Voos et al., 1994; Laloraya S, 1995; Westermann et al., 1995).

GrpE is essential in other Hsp70 functions, such as luciferase refolding (Schroder et al., 1993). Upon addition of GrpE to a mixture of DnaK or CSS1, DnaJ, and denatured luciferase, the chaperone proceeded to refold luciferase such that its native activity was recovered. Without the nucleotide exchange factor, both chaperones were unable to proceed through their ATPase cycles at rates sufficient to refold luciferase in the observed time frame. It is significant to note the difference is the rates of luciferase recovery between DnaK and CSS1. Because chloroplast co-chaperone homologs were

unavailable, all conclusions concerning the data must be qualified. Most likely, DnaK refolded luciferase faster because its ATPase activity was stimulated up to 50-fold by DnaJ and GrpE (reviewed in Bukau and Horwich, 1998), whereas CSS1's ATPase activity was only stimulated 5-fold by E. coli's co-chaperones.

Finally, the most direct proof to date that SStp binds CSS1 via the peptide binding site in its C-terminal domain is provided by the competition studies with RCMLA, SStp, and native α-lactalbumin. As seen in simple binding (Ivey and Bruce, 2000) competitions and in ATPase stimulation studies (Ivey et al., 2000), native proteins do not affect Hsp70 function, whereas RCMLA and SStp, both unfolded proteins in aqueous solution, compete effectively for DnaK and CSS1 binding against each other and other unfolded proteins. Here, a molar excess of SStp actually prevents CSS1 from refolding denatured luciferase, as evidenced from the lack of luciferase activity even after two hours. Thus, we have strong evidence that SStp can bind CSS1 in a physiologically relevant manner. However, definitive proof of CSS1 involvement in chloroplast protein import will require detailed transgenic studies including anti-sense suppression and dominant-negative mutant phenotype generation.

Modeling CSS1 after DnaK

One of the ultimate goals of our work is to fully characterize CSS1 as a molecular chaperone. To do this, we must not only establish catalytic and chaperone activities, but also describe the mechanisms of these activities in detailed structural terms. Our preliminary attempt to do so involved an exercise in molecular simulations based on the

DnaK model whose structure is known. Interestingly, we found that CSS1 adopts a structure very similar to that of DnaK when bound to an unfolded peptide substrate, even after complete structural randomization. Given the high degree of similarity between the peptide-binding domains of CSS1 and DnaK (~75 %), it stands to reason that their overall structures, binding sites, and ultimately their substrate specificities, would be similar.

Chapter 6 - Final remarks

PROJECT SUMMARY

Ultimately, this project accomplished four important objectives all of which suggest that CSS1 (and/or possibly IAP70) functions as molecular motor which drives ATP-dependent protein import into chloroplasts. First, we described a bona fide interaction between the transit peptide, SStp, and CSS1. To our knowledge, this is still the only direct evidence for an organellar Hsp70 interaction with a physiologically revelant peptide substrate. In all other studies to date, interaction of the transit peptide with *any* protein involved in import has been assumed because of indirect observations such as isolated protein complexes and crosslinking studies using whole precursor proteins. We have demonstrated the validity of Hsp70-SStp interaction by many *in vivo* and *in vitro* criteria: 1) co-purification with DnaK; 2) deliberate dissociation from DnaK using ATP; 3) biophysical analyses to look at DnaK conformational changes upon transit peptide binding; 4) peptide binding competition studies with DnaK and CSS1; 5) ATPase stimulation of DnaK and CSS1; 6) substrate protection from proteolysis studies with DnaK; and 7) protein folding competition studies with DnaK and CSS1.

Second, we have experimentally mapped the Hsp70-SStp interaction to the N-terminal third of SStp. This was accomplished *in vivo* using truncated C-terminal deletion mutants of SStp, Using a His-S fusion which contained the N-terminal portion of SStp we co-purified DnaK. Synthetic peptides corresponding to the N-terminal, middle, and C-terminal thirds were used to prove the N-terminal bias for Hsp70 affinity *in vitro*. We then used statistical analyses to generalize this affinity pattern as an intrinsic property of

transit peptides and the first common biochemical characteristic attributable to these unrelated sequences.

Third, we have biochemically characterized the native form of the first cloned chloroplast Hsp70 homolog, CSS1. All of the known Hsp70 functions, including ATPase catalytic activity (basal, peptide-stimulated, and co-chaperone stimulated), autophosphorylation (basal and cation-stimulated), pH dependence, peptide binding, and protein folding, indicate that CSS1 functions similarly to other Hsp70's and is functionally related most closely to its prokaryotic progenetors.

Finally, we have developed the means to conduct all the experiments described in this study and many more with a recombinant form of CSS1. The relative ease of generating large quantities of highly pure CSS1 will allow for many more experimental permutations and repetitions, which will increase confidence in all future studies. Also, the novel denaturation-renaturation protocol we developed may have applications in other cases in which proteins are expressed as aggregates or where purification is especially difficult.

SELF-CRITICISM AND FUTURE STUDIES

Perhaps the single greatest criticism of our work is that we failed to conclusively show that chloroplast protein import requires a molecular motor and that CSS1 (or IAP70) is that motor. We concede the pointr, but we argue that the work presented in this study constitutes the necessary groundwork to ensure that ongoing studies are conducted with as much forethought and foresight as possible. Because we have dissected the CSS1-

SStp interaction primarily *in vitro*, future investigations will benefit from a detailed understanding of the phenomenon and *in vivo* will therefore yield more meaningful results. For example, one could attempt to reconstitute protein import into liposomes comprised of chloroplast envelopes, which form right-side-out vesicles (Waegemann et al., 1992). Waegemann and co-workers did not observe protein import; however, they sonicated their envelopes in a simple buffer during liposome preparation. We would like to prepare liposomes in the presence of concentrated stroma, which contains CSS1. We believe that measurable protein import will proceed in such a system.

Import in this thylakoidless "chloroplast" system would provide many advantages over conventional organellar import. First, experiments could be performed more often because plants would not have to be grown for every experiment. More importantly, the investigator would gain virtually unlimited freedom in what components could be added or removed from the envelopes and stroma prior to liposome preparation. CSS1 could be immunodepleted or added in excess to show a potential concentration dependence on import rate. CSS1 could even be used alone with and without ATP, leaving out the rest of the stromal components. Since we now have recombinant CSS1, extensive mutational analyses could be performed to determine the critical residues for transit peptide binding, ATPase activity, and envelope anchoring.

These experiments could progress relatively quickly because a wealth of mutational analysis is already available for Hsp70's and transit peptides. For example, one could make an I4A mutation in SStp, which should lower the peptide's affinity for Hsp70's, and perform the same kinds of import experiments. Alternatively, one could use

the DnaK mutant E171A, which exhibits no protein folding activity yet retains its ATP hydrolysis activity. Since the highly conserved residue E171 is in the ATPase domain, this amino acid most likely helps couple ATP hydrolysis to peptide binding. This structure-function relationship could be explored in the CSS1 system as well.

The real proof of CSS1 involvement in the import process, must ultimately come from *in vivo* work with transgenic plants. With the advent of plant knockout technologies (Gaymard et al., 1998; Miao and Lam, 1995), these studies may become routine in the near future. Observing altered phenotypes and subsequent organellar import characteristics may result from several transgenic techniques: 1) overexpressing wild-type CSS1, 2) suppressing CSS1 expression with anti-sense constructs, and 3) introducing mutant forms of CSS1 and precursor proteins (we only characterized one wild-type transit peptide thus far). These types of systematic analyses in model systems such as *A. thaliana* will ultimately prove or disprove one of the central hypotheses of our work.

Another limitation of this study was the exclusion of other chloroplast Hsp70 and co-chaperone homologs. These proteins were simply not available to us within the time frame of this study. In the future, characterization of the homologous chaperone machine should be performed to simply verify the conclusions presented in this study. Then, if recombinant forms are available, all of the *in vitro* and transgenic work described above may be attempted with these proteins also.

Finally, the functional homology between CSS1 and its prokaryotic homologs may be further explored. Novel studies may include *in vivo* complementation with pre-

existing *E. coli* strains carrying the temperature sensitive, conditionally lethal dnaK$^-$ mutation. CSS1 could be engineered into an expression construct under the control of a bacterial heat shock promoter and transformed into the mutant host. At the non-permissive temperature, the endogenous DnaK would become inactive while CSS1 expression would be induced. Bacterial survival would then indicate successful complementation. The same set of CSS1 mutational analysis could be done in parallel with the work described above.

One of the most promising directions for this project has already been started: the PTP99 database of transit peptides. This newer version of the CHLPEP database has more than twice as many sequences, complete information on each sequence, multiple accession number cross-referencing, ChloroP transit peptide homology predictions, stromal processing peptidase cleavage site prediction, and many other improved logistical features. More importantly, we have incorporated many novel statistical analyses into the database as well. For example, we have examined the distribution of a number of amino acids with transit peptides, such as serine and threonines as well as the helix-break residues, proline and glycine. We have also been developing a unique software package which will apply the RPPD and CBPS algorithms to all transit peptides. These predictive tools will accelerate our understanding of the modular design of transit peptides and will help target future efforts toward productive mutational analyses to determine the functional arrangement of individual amino acids.

Unfortunately, not all of these and other original project goals of this study were realized. Perhaps, some of the plans described above were overly ambitious for a single

Ph.D. dissertation. In any event, the time has come for this author to move on. However, many unique experimental tools are now available, and this project is poised to continue along many paths.

BIBLIOGRAPHY

BIBLIOGRAPHY

Aitken, A., Collinge, D. B., van Heusden, B. P., Isobe, T., Roseboom, P. H., Rosenfeld, G., and Soll, J. (1992). 14-3-3 proteins: a highly conserved, widespread family of eukaryotic proteins. Trends Biochem. Sci. *17*, 498-501.

Akita, M., Nielsen, E., and Keegstra, K. (1997). Identification of protein transport complexes in the chloroplastic envelope membranes via chemical cross-linking. J. Cell. Biol. *136*, 983-994.

Alberts, B., Bray, D., Lewis, J., Raff, M., Roberts, K., and Watson, J. D. (1994). Molecular Biology of the Cell, Third Edition (New York: Garland Publishing, Inc.).

Alberts, B., Bray, D., Lewis, J., Raff, M., Roberts, K., and Watson, J. D. (1994). Molecular Biology of the Cell, Third Edition (New York: Garland Publishing, Inc.).

Alconada, A., Kubrich, M., Moczko, M., Honlinger, A., and Pfanner, N. (1995). The mitochondrial receptor complex: the small subunit Mom8b/Isp6 supports association of receptors with the general insertion pore and transfer of preproteins. Mol. Cell Biol. *15*, 6196-6205.

America, T., Hageman, J., Guera, A., Rook, F., Archer, K., Keegstra, K., and Weisbeek, P. (1994). Methotrexate does not block import of a DHFR fusion protein into chloroplasts. Plant Mol. Biol. *24*, 283-294.

Anfinsen, C. B. (1973). Principles that govern the folding of protein chains. Science *181*, 223-30.

Azem, A., Oppliger, W., Lustig, A., Jeno, P., Feifel, B., Schatz, G., and Horst, M. (1997). The mitochondrial Hsp70 chaperone system. Effect of adenine nucleotides, peptide substrate, and mGrpE on the oligomeric state of mHsp70. J. Biol. Chem. *272*, 20901-20906.

Ballinger, C. A., Connell, P., Wu, Y., Hu, Z., Thompson, L. J., Yin, L. Y., and Patterson, C. (1999). Identification of CHIP, a novel tetratricopeptide repeat-containing protein that interacts with heat shock proteins and negatively regulates chaperone functions. Mol. Cell Biol. *19*, 4535-4545.

Benaroudj, N., Batelier, G., Triniolles, F., and Ladjimi, M. (1995). Self-Association Of the Molecular Chaperone Hsc70. Biochemistry *34*, 15282-15290.

Berthold, J., Bauer, M. F., Schneider, H. C., Klaus, C., Dietmeier, K., Neupert, W., and Brunner, M. (1995). The MIM complex mediates preprotein translocation across the mitochondrial inner membrane and couples it to the mt-Hsp70/ATP driving system. Cell *81*, 1085-1093.

Blond-Elguindi, S., Cwirla, S. E., Dower, W. J., Lipshutz, R. J., Sprang, S. R., Sambrook, J. F., and Gething, M. J. (1993). Affinity panning of a library of peptides displayed on bacteriophages reveals the binding specificity of BiP. Cell *75*, 717-728.

Bolter, B., May, T., and Soll, J. (1998). A protein import receptor in pea chloroplasts, Toc86, is only a proteolytic fragment of a larger polypeptide. FEBS Lett. *441*, 59-62.

Bomer, U., Maarse, A. C., Honlinger, A., Dekker, P. J. T., Pfanner, N., and Rassow, J. (1997). Multiple interactions of components mediating preprotein translocation across the inner mitochondrial membrane. EMBO J., 2205-2216.

Bonk, M., Tadros, M., Vandekerckhove, J., Al-Babili, S., and Beyer, P. (1996). Purification and characterization of chaperonin 60 and heat-shock protein 70 from chromoplasts of Narcissus pseudonarcissus. Plant Physiol. *111*, 931-939.

Boorstein, W. R., Ziegelhoffer, T., and Craig, E. A. (1994). Molecular evolution of the HSP70 multigene family. J. Mol. Evol. *38*, 1-17.

Boston, R. S., Viitanen, P. V., and Vierling, E. (1996). Molecular chaperones and protein folding in plants. Plant Mol. Biol. *32*, 191-222.

Brodsky, J. L. (1996). Post-translational protein translocation: not all hsc70s are created equal. Trends Biochem. Sci. *21*, 122-126.

Brodsky, J. L., Goeckeler, J., and Schekman, R. (1995). BiP and Sec63p are required for both co- and posttranslational protein translocation into the yeast endoplasmic reticulum. Proc. Natl. Acad. Sci. USA *92*, 9643-9646.

Bruce, B. D. (1998). The role of lipids in plastid protein transport. Plant Mol Biol *38*, 223-46.

Bruce, B. D., and Keegstra, K. (1994). Translocation of proteins across chloroplast membranes. In Advances in Molecular and Cell Biology: Molecular Processes of Photosynthesis., J. Barber, ed. (Greenwich, CT: Jai Press Inc.), pp. 389-430.

Bruce, B. D., Perry, S., Froehlich, J., and Keegstra, K. (1994). *In vitro* import of proteins into chloroplasts. In Plant Molecular Biology Manual (Belgium: Kluwer Academic Publishers), pp. 1-15.

Buchberger, A., Theyssen, H., Schroder, H., McCarty, J. S., Virgallita, G., Milkereit, P., Reinstein, J., and Bukau, B. (1995). Nucleotide-induced conformational changes

in the ATPase and substrate binding domains of the DnaK chaperone provide evidence for interdomain communication. J. Biol. Chem. *270*, 16903-16910.

Bukau, B., and Horwich, A. L. (1998). The Hsp70 and Hsp60 chaperone machines. Cell *92*, 351-366.

Caliebe, A., Grimm, R., Kaiser, G., Lubeck, J., Soll, J., and Heins, L. (1997). The chloroplastic protein import machinery contains a Rieske-type iron- sulfur cluster and a mononuclear iron-binding protein. Embo J. *16*, 7342-7350.

Caliebe, A., Grimm, R., Kaiser, G., Lubeck, J., Soll, J., and Heins, L. (1997). The chloroplastic protein import machinery contains a Rieske-type iron-sulfur cluster and a mononuclear iron-binding protein. EMBO J. *16*, 7342-7350.

Cegielska, A., and Georgopoulos, C. (1989). Biochemical properties of the *E. coli* DnaK heat shock protein and its mutant derivatives. Biochimie *71*, 1071-1077.

Chappell, T. G., Konforti, B. B., Schmid, S. L., and Rothman, J. E. (1987). The ATPase core of a clathrin uncoating protein. J. Biol. Chem. *262*, 746-751.

Chua, N. H., and Schmidt, G. W. (1978). Post-translational transport into intact chloroplasts of a precursor to the small subunit of ribulose-1,5-bisphosphate carboxylase. Proc. Natl. Acad. Sci. USA *75*, 6110-6114.

Clark, S. A., and Theg, S. M. (1997). A folded protein can be transported across the chloroplast envelope and thylakoid membranes. Mol. Biol. Cell *8*, 923-934.

Cline, K., and Henry, R. (1996). Import and routing of nucleus-encoded chloroplast proteins. Ann. Rev. Cell Dev. Biol. *12*, 1-26.

Cline, K., Werner-Washburne, M., Lubben, T. H., and Keegstra, K. (1985). Precursors to two nuclear-encoded chloroplast proteins bind to the outer envelope membrane before being imported into chloroplasts. J. Biol. Chem. *260*, 3691-3696.

Craig, E. A. (1989). Essential roles of 70kDa heat inducible proteins. Bioessays *11*, 48-52.

Craig, E. A. (1985). The heat shock response. CRC Crit Rev Biochem *18*, 239-280.

Craig, E. A., Kramer, J., Shilling, J., Werner-Washburne, M., Holmes, S., Kosic-Smithers, J., and Nicolet, C. M. (1989). SSC1, an essential member of the yeast HSP70 multigene family, encodes a mitochondrial protein. Mol. Cell Biol. *9*, 3000-3008.

Cyr, D. M., Lu, X., and Douglas, M. G. (1992). Regulation of Hsp70 function by a eukaryotic DnaJ homolog. J. Biol. Chem. *267*, 20927-20931.

Dabney-Smith, C., van Den Wijngaard, P. W., Treece, Y., Vredenberg, W. J., and Bruce, B. D. (1999). The C terminus of a chloroplast precursor modulates its interaction with the translocation apparatus and PIRAC. J Biol Chem *274*, 32351-32359.

Dalie, B. L., Skaleris, D. A., Kohle, K., Weissbach, H., and Brot, N. (1990). Interaction of DnaK with ATP: Binding, hydrolysis and Ca+2 -stimulated autophosphorylation. Biochem. Biophys. Res. Commun. *166*, 1284-1292.

Dekker, P. J., and Pfanner, N. (1997). Role of mitochondrial GrpE and phosphate in the ATPase cycle of matrix Hsp70. J. Mol. Biol. *270*, 321-327.

DeLuca-Flaherty, C., Flaherty, K. M., McIntosh, L. J., Bahrami, B., and McKay, D. B. (1988). Crystals of an ATPase fragment of bovine clathrin uncoating ATPase. J. Mol. Biol. *200*, 749-750.

Dubois, T., Howell, S., Amess, B., Kerai, P., Learmonth, M., Madrazo, J., Chaudhri, M., Rittinger, K., Scarabel, M., Soneji, Y., and Aitken, A. (1997). Structure and sites of phosphorylation of 14-3-3 protein: role in coordinating signal transduction pathways. J. Protein Chem. *16*, 513-522.

Eilers, M., and Schatz, G. (1986). Binding of a specific ligand inhibits import of a purified precursor protein into mitochondria. Nature *322*, 228-232.

Emanuelsson, O., Nielsen, H., and von Heijne, G. (1999). ChloroP, a neural network-based method for predicting chloroplast transit peptides and their cleavage sites. Protein Sci. *8*, 978-984.

Evers, M. E., Huhse, B., Titorenko, V. I., Kunau, W. H., Hartl, F. U., Harder, W., and Veenhuis, M. (1993). Affinity purification of molecular chaperones of the yeast Hansenula polymorpha using immobilized denatured alcohol oxidase. FEBS Lett. *321*, 32-36.

Fanning, A. S., and Anderson, J. M. (1996). Protein-protein interactions: PDZ domain networks. Curr. Biol. *6*, 1385-1388.

Fayet, O., Ziegelhoffer, T., and Georgopoulos, C. (1989). The groES and groEL heat shock gene products of *E. coli* are essential for bacterial growth at all temperatures. J. Bacteriol. *171*, 1379-1385.

Fluegge, U. I., and Hinz, G. (1986). Energy dependence of protein translocation into chloroplasts. Eur. J. Biochem. *160*, 563-570.

Flynn, G. C., Chappell, T. G., and Rothman, J. E. (1989). Peptide binding and release by proteins implicated as catalysts of protein assembly. Science *245*, 385-390.

Flynn, G. C., Pohl, J., Flocco, M. T., and Rothman, J. E. (1991). Peptide-binding specificity of the molecular chaperone BiP. Nature *353*, 726-730.

Fourie, A. M., Sambrook, J. F., and Gething, M. J. (1994). Common and divergent peptide binding specificities of Hsp70 molecular chaperones. J. Biol. Chem. *269*, 30470-30478.

Freeman, B. C., Myers, M. P., Schumacher, R., and Morimoto, R. I. (1995). Identification of a regulatory motif in Hsp70 that affects ATPase activity, substrate binding and interaction with HDJ-1. EMBO J. *14*, 2281-2292.

Frydman, J., and Hohfeld, J. (1997). Chaperones get in touch: the Hip-Hop connection. Trends Biochem. Sci. *22*, 87-92.

Gamer, J., Multhaup, G., Tomoyasu, T., McCarty, J. S., Rudiger, S., Schonfeld, H. J., Schirra, C., Bujard, H., and Bukau, B. (1996). A cycle of binding and release of the DnaK, DnaJ and GrpE chaperones regulates activity of the *E. coli* heat shock transcription factor sigma32. EMBO J. *15*, 607-617.

Gao, B., Greene, L., and Eisenberg, E. (1994). Characterization of nucleotide-free uncoating ATPase and its binding to ATP, ADP, and ATP analogues. Biochemistry *33*, 2048-2054.

Gavel, Y., and von Heijne, G. (1990). A conserved cleavage site motif in chloroplast transit peptides. FEBS Lett. *261*, 455-458.

Gaymard, F., Pilot, G., Lacombe, B., Bouchez, D., Bruneau, D., Boucherez, J., Michaux-Ferriere, N., Thibaud, J. B., and Sentenac, H. (1998). Identification and disruption of a plant shaker-like outward channel involved in K+ release into the xylem sap. Cell *94*, 647-655.

Gething, M. J., and Sambrook, J. (1992). Protein folding in the cell. Nature *355*, 33-45.

Gisler, S. M., Pierpaoli, E. V., and Christen, P. (1998). Catapult mechanism renders the chaperone action of Hsp70 unidirectional. J. Mol. Biol. *279*, 833-840.

Glick, B. S. (1995). Can Hsp70 proteins act as force-generating motors? Cell *80*, 11-14.

Gragerov, A., Zeng, L., Zhao, X., Burkholder, W., and Gottesman, M. E. (1994). Specificity of DnaK-peptide binding. J. Mol. Biol. *235*, 848-854.

Gray, J., and Row, P. (1995). Protein Translocation Across Chloroplast Envelope Membranes. Trends In Cell Biology *5*, 243-247.

Guera, A., America, T., van Waas, M., and Weisbeek, P. J. (1993). A strong protein unfolding activity is associated with the binding of precursor chloroplast proteins to chloroplast envelopes. Plant Mol. Biol. *23*, 309-324.

Ha, J. H., and McKay, D. B. (1995). Kinetics of nucleotide-induced changes in the tryptophan fluorescence of the molecular chaperone Hsc70 and its subfragments suggest the ATP- induced conformational change follows initial ATP binding. Biochemistry *34*, 11635-11644.

Hachiya, N., Alam, R., Sakasegawa, Y., Sakaguchi, M., Mihara, K., and Omura, T. (1993). A mitochondrial import factor purified from rat liver cytosol is an ATP-

dependent conformational modulator for precursor proteins. EMBO J. *12*, 1579-1586.

Hachiya, N., Komiya, T., Alam, R., Iwahashi, J., Sakaguchi, M., Omura, T., and Mihara, K. (1994). MSF, a novel cytoplasmic chaperone which functions in precursor targeting to mitochondria. EMBO J. *13*, 5146-5154.

Halperin, T., and Adam, Z. (1996). Degradation of mistargeted OEE33 in the chloroplast stroma. Plant Mol. Biol. *30*, 925-933.

Hamman, B. D., Hendershot, L. M., and Johnson, A. E. (1998). BiP maintains the permeability barrier of the ER membrane by sealing the lumenal end of the translocon pore before and early in translocation. Cell *92*, 747-758.

Harrison, C. J., Hayer Hartl, M., Di Liberto, M., Hartl, F., and Kuriyan, J. (1997). Crystal structure of the nucleotide exchange factor GrpE bound to the ATPase domain of the molecular chaperone DnaK. Science *276*, 431-435.

Haucke, V., Horst, M., Schatz, G., and Lithgow, T. (1995). The Mas20p and Mas70p subunits of the protein import receptor of yeast mitochondria interact via the tetratricopeptide repeat motif in Mas20p: Evidence for a single hetero-oligomeric receptor. EMBO J. *15*, 1231-1237.

Haucke, V., Horst, M., Schatz, G., and Lithgow, T. (1996). The Mas20p and Mas70p subunits of the protein import receptor of yeast mitochondria interact via the tetratricopeptide repeat motif in Mas20p: evidence for a single hetero-oligomeric receptor. EMBO J. *15*, 1231-1237.

Heins, L., Collinson, I., and Soll, J. (1998). The protein translocation apparatus of chloroplast envelopes. Trends Plant Sci *3*, 56-61.

Hemmingsen, S. M., Woolford, C., van der Vies, S. M., Tilly, K., Dennis, D. T., Georgopoulos, C. P., Hendrix, R. W., and Ellis, R. J. (1988). Homologous plant and bacterial proteins chaperone oligomeric protein assembly. Nature *333*, 330-334.

Hendrick, J. P., and Hartl, F. U. (1993). Molecular chaperone functions of heat-shock proteins. Ann. Rev. Biochem. *62*, 349-384.

Hendrick, J. P., Langer, T., Davis, T. A., Hartl, F. U., and Wiedmann, M. (1993). Control of folding and membrane translocation by binding of the chaperone DnaJ to nascent polypeptides. Proc. Natl. Acad. Sci. USA *90*, 10216-10220.

Higgins, D. G., and Sharp, P. M. (1988). CLUSTAL: a package for performing multiple sequence alignment on a microcomputer. Gene *73*, 237-244.

Higgins, D. G., Thompson, J. D., and Gibson, T. J. (1996). Using CLUSTAL for multiple sequence alignments. Methods Enzymol. *266*, 383-402.

Highfield, P. E., and Ellis, R. J. (1978). Synthesis and transport of the small of ribulose bisphosphate carboxylase. Nature *271*, 420-424.

Hinnah, S. C., Hill, K., Wagner, R., Schlicher, T., and Soll, J. (1997). Reconstitution of a chloroplast protein import channel. EMBO J. *16*, 7351-7360.

Hirsch, S., Muckel, E., Heemeyer, F., von Heijne, G., and Soll, J. (1994). A receptor component of the chloroplast protein translocation machinery. Science *266*, 1989-1992.

Hohfeld, J., and Jentsch, S. (1997). GrpE-like regulation of the hsc70 chaperone by the anti-apoptotic protein BAG-1 [published erratum appears in EMBO J. 1998 Feb 2;17(3):847]. EMBO J. *16*, 6209-6216.

Hohfeld, J., Minami, Y., and Hartl, F. U. (1995). Hip, a novel cochaperone involved in the eukaryotic Hsc70/Hsp40 reaction cycle. Cell *83*, 589-598.

Holzinger, A., Phillips, K. S., and Weaver, T. E. (1996). Single-step purification/solubilization of recombinant proteins: application to surfactant protein B. Biotechniques *20*, 804-806, 808.

Irmer, H., and Hohfeld, J. (1997). Characterization of functional domains of the eukaryotic co-chaperone Hip. J. Biol. Chem. *272*, 2230-2235.

Ivey, R. A., and Bruce, B. D. (2000). In vivo and in vitro interaction of DnaK and a chloroplast transit peptide. Cell Stress & Chaperones *5*, 62-71.

Ivey, R. A., Subramanian, C., and Bruce, B. D. (2000). Identification of a Hsp70 Recognition Domain Within the Rubisco Small Subunit Transit Peptide. Plant Physiol. *122*, 1289-1310.

Jackson, D. T., Froehlich, J. E., and Keegstra, K. (1998). The hydrophilic domain of Tic110, an inner envelope membrane component of the chloroplastic protein translocation apparatus, faces the stromal compartment. J. Biol. Chem. *273*, 16583-16588.

Kang, P. J., Ostermann, J., Shilling, J., Neupert, W., Craig, E. A., and Pfanner, N. (1990). Requirement for Hsp70 in the mitochondrial matrix for translocation and folding of precursor proteins. Nature *348*, 137-143.

Karlin Neumann, G. A., and Tobin, E. M. (1986). Transit peptides of nuclear-encoded chloroplast proteins share a common amino acid framework. EMBO J. *5*, 9-13.

Karzai, A. W., and McMacken, R. (1996). A bipartite signaling mechanism involved in DnaJ-mediated activation of the *E. coli* DnaK protein. J. Biol. Chem. *271*, 11236-11246.

Keegstra, K., Bruce, B. D., Hurley, M., Li, H.-m., and Perry, S. (1995). Targeting of proteins into chloroplasts. Physiol. Plant. *93*, 157-162.

Keegstra, K., and Cline, K. (1999). Protein import and routing systems of chloroplasts. Plant Cell *11*, 557-570.

Keegstra, K., and Froehlich, J. E. (1999). Protein import into chloroplasts. Curr Opin Plant Biol *2*, 471-6.

Keiler, K. C., Waller, P. R., and Sauer, R. T. (1996). Role of a peptide tagging system in degradation of proteins synthesized from damaged messenger RNA [see comments]. Science *271*, 990-993.

Kessler, F., and Blobel, G. (1996). Interaction of the protein import and folding machineries of the chloroplast. Proc. Natl. Acad. Sci. USA *93*, 7684-7689.

Kessler, F., Blobel, G., Patel, H. A., and Schnell, D. J. (1994). Identification of two GTP-binding proteins in the chloroplast protein import machinery. Science *266*, 1035-1039.

Kim, J. S., and Raines, R. T. (1993). Ribonuclease S-peptide as a carrier in fusion proteins. Protein Sci. *2*, 348-356.

Kindle, K. L. (1998). Amino-terminal and hydrophobic regions of the Chlamydomonas reinhardtii plastocyanin transit peptide are required for efficient protein accumulation in vivo. Plant Mol. Biol. *38*, 365-377.

King, C., Eisenberg, E., and Greene, L. (1995). Polymerization of 70-kDa heat shock protein by yeast DnaJ in ATP. J. Biol. Chem. *270*, 22535-22540.

Klaus, C., Guiard, B., Neupert, W., and Brunner, M. (1996). Determinants in the presequence of cytochrome b2 for import into mitochondria and for proteolytic processing. Eur. J. Biochem. *236*, 856-861.

Ko, K., Bornemisza, O., Kourtz, L., Ko, Z. W., Plaxton, W. C., and Cashmore, A. R. (1992). Isolation and characterization of a cDNA clone encoding a cognate 70-kDa heat shock protein of the chloroplast envelope. J. Biol. Chem. *267*, 2986-2993.

Ko, K., Budd, D., Wu, C., Seibert, F., Kourtz, L., and Ko, Z. W. (1995). Isolation and characterization of a cDNA clone encoding a member of the Com44/Cim44 envelope components of the chloroplast protein import apparatus. J. Biol. Chem. *270*, 28601-28608.

Kouranov, A., Chen, X., Fuks, B., and Schnell, D. J. (1998). Tic20 and Tic22 are new components of the protein import apparatus at the chloroplast inner envelope membrane. J. Cell Biol. *143*, 991-1002.

Kouranov, A., and Schnell, D. J. (1997). Analysis of the interactions of preproteins with the import machinery over the course of protein import into chloroplasts. J Cell Biol *139*, 1677-1685.

Kourtz, L., and Ko, K. (1997). The early stage of chloroplast protein import involves Com70. J. Biol. Chem. *272*, 2808-2813.

Krimm, I., Gans, P., Hernandez, J. F., Arlaud, G. J., and Lancelin, J. M. (1999). A coil-helix instead of a helix-coil motif can be induced in a chloroplast transit peptide from chlamydomonas reinhardtii. Eur. J. Biochem. *265*, 171-180.

Kronidou, N. G., Oppliger, W., Bolliger, L., Hannavy, K., Glick, B. S., Schatz, G., and Horst, M. (1994). Dynamic interaction between Isp45 and mitochondrial Hsp70 in the protein import system of the yeast mitochondrial inner membrane. Proc. Natl. Acad. Sci. USA *91*, 12818-12822.

Kubo, Y., Tsunehiro, T., Nishikawa, S., Nakai, M., Ikeda, E., Toh-e, A., Morishima, N., Shibata, T., and Endo, T. (1999). Two distinct mechanisms operate in the reactivation of heat-denatured proteins by the mitochondrial Hsp70/Mdj1p/Yge1p chaperone system. J. Mol. Biol. *286*, 447-464.

Kwok, F., and Churchich, J. E. (1994). The binding of substrates and inhibitors to the metal center of myoinositol monophosphatase. FEBS Lett. *346*, 304-306.

Laloraya, S., Gambill, B. D., and Craig, E. A. (1994). A role for a eukaryotic GrpE-related protein, Mge1p, in protein translocation. Proc. Natl. Acad. Sci. USA *91*, 6481-6485.

Laloraya S, D. P. V. W. C. E. P. N. (1995). Mitochondrial Grpe Modulates the Function Of Matrix Hsp70 In Translocation and Maturation Of Preproteins. Mol. Cell. Biol. *15*, 7098-7105.

Lancelin, J. M., Bally, I., Arlaud, G. J., Blackledge, M., Gans, P., Stein, M., and Jacquot, J. P. (1994). NMR structures of ferredoxin chloroplastic transit peptide from Chlamydomonas reinhardtii promoted by trifluoroethanol in aqueous solution. FEBS Lett. *343*, 261-266.

Levchenko, I., Smith, C. K., Walsh, N. P., Sauer, R. T., and Baker, T. A. (1997). PDZ-like domains mediate binding specificity in the Clp/Hsp100 family of chaperones and protease regulatory subunits. Cell *91*, 939-947.

Liberek, K., Marszalek, J., Ang, D., Georgopoulos, C., and Zylicz, M. (1991). *E. coli* DnaJ and GrpE Heat Shock Proteins Jointly Stimulate ATPase Activity of DnaK. Proc. Natl. Acad. Sci. USA *88*, 2874-2878.

Liberek, K., Skowyra, D., Zylicz, M., Johnson, C., and Georgopoulos, C. (1991). The *E. coli* DnaK chaperone, the 70-kDa heat shock protein eukaryotic equivalent, changes conformation upon ATP hydrolysis, thus triggering its dissociation from a bound target protein. J. Biol. Chem. *266*, 14491-14496.

Lindquist, S. (1986). The heat-shock response. Ann. Rev. Biochem. *55*, 1151-1191.

Liu, X. Q., and Jagendorf, A. T. (1984). ATP-dependent proteolysis in pea chloroplsts. FEBS Lett. *166*, 248-252.

Lubeck, J., Soll, J., Akita, M., Nielsen, E., and Keegstra, K. (1996). Topology of IEP110, a component of the chloroplastic protein import machinery present in the inner envelope membrane. EMBO J. *15*, 4230-4238.

Lund, P. A. (1995). The roles of molecular chaperones in vivo. Essays Biochem. *29*, 113-123.

Lyman, S. K., and Schekman, R. (1997). Binding of secretory precursor polypeptides to a translocon subcomplex is regulated by BiP. Cell *88*, 85-96.

Ma, Y., Kouranov, A., LaSala, S. E., and Schnell, D. J. (1996). Two components of the chloroplast protein import apparatus, IAP86 and IAP75, interact with the transit sequence during the recognition and translocation of precursor proteins at the outer envelope. J. Cell Biol. *134*, 315-327.

Macejak, D., Rayfield, M., and Luftig, R. (1990). Isolation and characterization of human HSP70 expressed in *E. coli*. Arch. Biochem. Biophys. *280*, 53-60.

Madueno, F., Napier, J. A., and Gray, J. C. (1989). Newly imported Rieske iron-sulfur protein associates with both Cpn60 and Hsp70 in the chloroplast stroma. Plant Cell *5*, 1865-1876.

Malek, L., Bogorad, L., Ayers, A. R., and Goldberg, A. L. (1984). Newly synthesized proteins are degraded by an ATP-stimulated proteolytic process in isolated pea chloroplasts. FEBS Lett. *166*, 253-257.

Mallouk, Y., Vayssier-Taussat, M., Bonventre, J. V., and Polla, B. S. (1999). Heat shock protein 70 and ATP as partners in cell homeostasis (Review). Int. J. Mol. Med. *4*, 463-474.

Marshall, J. S., DeRocher, A. E., Keegstra, K., and Vierling, E. (1990). Identification of heat shock protein Hsp70 homologues in chloroplasts. Proc. Natl. Acad. Sci. USA *87*, 374-378.

Marshall, J. S., and Keegstra, K. (1992). Isolation and Characterization of a cDNA Clone Encoding the Major Hsp70 of the Pea Chloroplastic Stroma. Plant Physiol. *100*, 1048-1054.

Martin, J., Mahlke, K., and Pfanner, N. (1991). Role of an energized inner membrane in mitochondrial protein import. Delta psi drives the movement of presequences. J. Biol. Chem. *266*, 18051-18057.

Matlack, K. E., Misselwitz, B., Plath, K., and Rapoport, T. A. (1999). BiP acts as a molecular ratchet during posttranslational transport of prepro-alpha factor across the ER membrane. Cell *97*, 553-564.

May, T., and Soll, J. (2000). 14-3-3 proteins form a guidance complex with chloroplast precursor proteins in plants. Plant Cell *12*, 53-64.

McCarty, J. S., Buchberger, A., Reinstein, J., and Bukau, B. (1995). The role of ATP in the functional cycle of the DnaK chaperone system. J. Mol. Biol. *249*, 126-137.

McCarty, J. S., and Walker, G. C. (1991). DnaK as a thermometer: threonine-199 is site of autophosphorylation and is critical for ATPase activity. Proc. Natl. Acad. Sci. USA *88*, 9513-9517.

Miao, B., Davis, J. E., and Craig, E. A. (1997). Mge1 functions as a nucleotide release factor for Ssc1, a mitochondrial Hsp70 of Saccharomyces cerevisiae. J. Mol. Biol. *265*, 541-552.

Miao, Z. H., and Lam, E. (1995). Targeted disruption of the TGA3 locus in Arabidopsis thaliana. Plant J. *7*, 359-365.

Miernyk, J. (1997). The 70 kDa stress-related proteins as molecular chaperones. Trends Plant Sci. *2*, 180-187.

Miernyk, J. A., Duck, N. B., Shatters, R. G., and Folk, W. R. (1992). The 70-Kilodalton Heat Shock Cognate Can Act as a Molecular Chaperone During the Membrane Translocation of a Plant Secretory Protein Precursor. Plant Cell *4*, 821-829.

Moore, T., and Keegstra, K. (1993). Characterization of a cDNA clone encoding a chloroplast-targeted Clp homologue. Plant Mol. Biol. *21*, 525-537.

Murakami, K., and Mori, M. (1990). Purified presequence binding factor (PBF) forms an import-competent complex with a purified mitochondrial precursor protein. EMBO J. *9*, 3201-3208.

Nairn, A. C., and Greengard, P. (1987). Purification and characterization of Ca2+/calmodulin-dependent protein kinase I from bovine brain. J. Biol. Chem. *262*, 7273-7281.

Nielsen, E., Akita, M., Davila-Aponte, J., and Keegstra, K. (1997). Stable association of chloroplastic precursors with protein translocation complexes that contain proteins from both envelope membranes and a stromal Hsp100 molecular chaperone. EMBO J. *16*, 935-946.

Ostermann, J., Voos, W., Kang, P. J., Craig, E. A., Neupert, W., and Pfanner, N. (1990). Precursor proteins in transit through mitochondrial contact sites interact with Hsp70 in the matrix. FEBS Lett. *277*, 281-284.

Palleros, D. R., Reid, K. L., McCarty, J. S., Walker, G. C., and Fink, A. L. (1992). DnaK, hsp73, and their molten globules. Two different ways heat shock proteins respond to heat. J. Biol. Chem. *267*, 5279-5285.

Palleros, D. R., Reid, K. L., Shi, L., and Fink, A. L. (1993). DnaK ATPase activity revisited. FEBS Lett. *336*, 124-128.

Palleros, D. R., Reid, K. L., Shi, L., Welch, W. J., and Fink, A. L. (1993). ATP-induced protein-Hsp70 complex dissociation requires K+ but not ATP hydrolysis. Nature *365*, 664-666.

Palleros, D. R., Welch, W. J., and Fink, A. L. (1991). Interaction of Hsp70 with unfolded proteins: effects of temperature and nucleotides on the kinetics of binding. Proc. Natl. Acad. Sci. USA *88*, 5719-5723.

Panagiotidis, C. A., Burkholder, W. F., Gaitanaris, G. A., Gragerov, A., Gottesman, M. E., and Silverstein, S. J. (1994). Inhibition of DnaK autophosphorylation by heat shock proteins and polypeptide substrates. J. Biol. Chem. *269*, 16643-16647.

Panzner, S., Dreier, L., Hartmann, E., Kostka, S., and Rapoport, T. A. (1995). Posttranslational protein transport in yeast reconstituted with a purified complex of Sec proteins and Kar2p. Cell *81*, 561-570.

Park, K., Flynn, G. C., Rothman, J. E., and Fasman, G. D. (1993). Conformational change of chaperone Hsc70 upon binding to a decapeptide: a circular dichroism study. Protein Sci. *2*, 325-330.

Peake, P., Basten, A., and Britton, W. J. (1991). Characterization of the functional properties of the 70-kDa protein of Mycobacterium bovis. J. Biol. Chem. *266*, 20828-20832.

Perry, S. E., and Keegstra, K. (1994). Envelope membrane proteins that interact with chloroplastic precursor proteins. Plant Cell *6*, 93-105.

Pilon, M., Rietveld, A. G., Weisbeek, P. J., and Dekruijff, B. (1992). Secondary Structure and Folding of a Functional Chloroplast Precursor Protein. J. Biol. Chem. *267*, 19907-19913.

Pilon, M., Wienk, H., Sips, W., de Swaaf, M., Talboom, I., van 't Hof, R., de Korte-Kool, G., Demel, R., Weisbeek, P., and de Kruijff, B. (1995). Functional domains of the ferredoxin transit sequence involved in chloroplast import. J. Biol. Chem. *270*, 3882-3893.

Pinnaduwage, P., and Bruce, B. D. (1996). In vitro interaction between a chloroplast transit peptide and chloroplast outer envelope lipids is sequence-specific and lipid class- dependent. J. Biol. Chem. *271*, 32907-32915.

Plath, K., Mothes, W., Wilkinson, B. M., Stirling, C. J., and Rapoport, T. A. (1998). Signal sequence recognition in posttranslational protein transport across the yeast ER membrane. Cell *94*, 795-807.

Prapapanich, V., Chen, S., Toran, E. J., Rimerman, R. A., and Smith, D. F. (1996). Mutational analysis of the Hsp70-interacting protein Hip. Mol. Cell Biol. *16*, 6200-6207.

Rassow, J., Maarse, A. C., Krainer, E., Kubrich, M., Muller, H., Meijer, M., Craig, E. A., and Pfanner, N. (1994). Mitochondrial protein import: biochemical and genetic evidence for interaction of matrix Hsp70 and the inner membrane protein MIM44. J. Cell Biol. *127*, 1547-1556.

Rensink, W. A., Pilon, M., and Weisbeek, P. (1998). Domains of a transit sequence required for in vivo import in Arabidopsis chloroplasts. Plant Physiol *118*, 691-699.

Richarme, G., and Kohiyama, M. (1993). Autostimulation of the DnaK (HSP 70) ATPase of *E. coli*. FEBS Lett. *322*, 277-279.

Rudiger, S., Germeroth, L., Schneider Mergener, J., and Bukau, B. (1997). Substrate specificity of the DnaK chaperone determined by screening cellulose-bound peptide libraries. EMBO J. *16*, 1501-1507.

Sadis, S., and Hightower, L. E. (1992). Unfolded Proteins Stimulate Molecular Chaperone Hsc70 ATPase by Accelerating ADP/ATP Exchange. Biochemistry *31*, 9406-9412.

Sanders, S. L., and Schekman, R. (1992). Polypeptide translocation across the endoplasmic reticulum membrane. J. Biol. Chem. *267*, 13791-13794.

Sanders, S. L., Whitfield, K. M., Vogel, J. P., Rose, M. D., and Schekman, R. W. (1992). Sec61p and BiP directly facilitate polypeptide translocation into the ER. Cell *69*, 353-365.

Schatz, G., and Dobberstein, B. (1996). Common principles of protein translocation across membranes. Science *271*, 1519-1526.

Scherer, P. E., Krieg, U. C., Hwang, S. T., Vestweber, D., and Schatz, G. (1990). A precursor protein partly translocated into yeast mitochondria is bound to a 70 kd mitochondrial stress protein. EMBO J *9*, 4315-4322.

Schleyer, M., Schmidt, B., and Neupert, W. (1982). Requirement of a membrane potential for the posttranslational transfer of proteins into mitochondria. Eur. J. Biochem. *125*, 109-116.

Schlicher, T., and Soll, J. (1997). Chloroplastic isoforms of DnaJ and GrpE in pea. Plant Mol. Biol. *33*, 181-185.

Schlicher, T., and Soll, J. (1996). Molecular chaperones are present in the thylakoid lumen of pea chloroplasts. FEBS Lett. *379*, 302-304.

Schlossman, D. M., Schmid, S. L., Braell, W. A., and Rothman, J. E. (1984). An enzyme that removes clathrin coats: purification of an uncoating ATPase. J. Cell Biol. *99*, 723-733.

Schmid, D., Baici, A., Gehring, H., and Christen, P. (1994). Kinetics of molecular chaperone action. Science *263*, 971-973.

Schmid, D., Jaussi, R., and Christen, P. (1992). Precursor of mitochondrial aspartate aminotransferase synthesized in *E. coli* is complexed with heat-shock protein DnaK. Eur J Biochem *208*, 699-704.

Schmidt, G. W., and Mishkind, M. L. (1983). Rapid degradation of unassembled rubisco small subunit in chloroplasts. Proc. Natl. Acad. Sci. USA *80*, 2623-2636.

Schmitt, M., Neupert, W., and Langer, T. (1995). Hsp78, a Clp homologue within mitochondria, can substitute for chaperone functions of mt-Hsp70. EMBO J. *14*, 3434-3444.

Schneider, H. C., Berthold, J., Bauer, M. F., Dietmeier, K., Guiard, B., Brunner, M., and Neupert, W. (1994). Mitochondrial Hsp70/MIM44 complex facilitates protein import. Nature *371*, 768-774.

Schnell, D. J., Blobel, G., Keegstra, K., Kessler, F., Ko, K., and Soll, J. (1997). A consensus nomenclature for the protein-import components of the chloroplast envelope. Trends Cell Biol. *7*, 303-304.

Schnell, D. J., Kessler, F., and Blobel, G. (1994). Isolation of components of the chloroplast protein import machinery. Science *266*, 1007-1012.

Schonfeld, H. J., Schmidt, D., Schroder, H., and Bukau, B. (1995). The DnaK chaperone system of *E. coli*: quaternary structures and interactions of the DnaK and GrpE components. J. Biol. Chem. *270*, 2183-2189.

Schroder, H., Langer, T., Hartl, F. U., and Bukau, B. (1993). DnaK, DnaJ and GrpE form a cellular chaperone machinery capable of repairing heat-induced protein damage. EMBO J. *12*, 4137-4144.

Schumacher, R. J., Hansen, W. J., Freeman, B. C., Alnemri, E., Litwack, G., and Toft, D. O. (1996). Cooperative action of Hsp70, Hsp90, and DnaJ proteins in protein renaturation. Biochemistry *35*, 14889-14898.

Schumacher, R. J., Hurst, R., Sullivan, W. P., McMahon, N. J., Toft, D. O., and Matts, R. L. (1994). ATP-dependent chaperoning activity of reticulocyte lysate. J. Biol. Chem. *269*, 9493-9499.

Scott, S. V., and Theg, S. M. (1996). A new chloroplast protein import intermediate reveals distinct translocation machineries in the two envelope membranes: energetics and mechanistic implications. J. Cell Biol. *132*, 63-75.

Seedorf, M., Waegemann, K., and Soll, J. (1995). A constituent of the chloroplast import complex represents a new type of GTP-binding protein. Plant J. *7235*, 401-411.

Shanklin, J., DeWitt, N. D., and Flanagan, J. M. (1995). The stroma of higher plant plastids contain ClpP and ClpC, functional homologs of *E. coli* ClpP and ClpA: an archetypal two-component ATP-dependent protease. Plant Cell *7*, 1713-1722.

Sherman, M. Y., and Goldberg, A. L. (1991). Formation in vitro of complexes between an abnormal fusion protein and the heat shock proteins from *E. coli* and yeast mitochondria. J. Bacteriol. *173*, 7249-7256.

Sherman, M. Y., and Goldberg, A. L. (1993). Heat shock of *E. coli* increases binding of DnaK (the Hsp70 homolog) to polypeptides by promoting its phosphorylation. Proc. Natl. Acad. Sci. U S A *90*, 8648-8652.

Simon, S. M., Peskin, C. S., and Oster, G. F. (1992). What Drives the Translocation of Proteins. Proc. Natl. Acad. Sci. USA *89*, 3770-3774.

Sohrt, K., and Soll, J. (2000). Toc64, a new component of the protein translocon of chloroplasts. J. Cell Biol. *148*, 1213-1221.

Soll, J., and Waegemann, K. (1992). A functionally active protein import complex from chloroplasts. Plant J. Oxford : Blackwell Scientific Publishers and BIOS Scientific Publishers. Mar 2, 253-256.

Squires, C., and Squires, C. L. (1992). The Clp proteins: proteolysis regulators or molecular chaperones? J. Bacteriol. *174*, 1081-1085.

Stahl, T., Glockmann, C., Soll, J., and Heins, L. (1999). Tic40, a new "old" subunit of the chloroplast protein import translocon. J. Biol. Chem. *274*, 37467-37472.

Szabo, A., Korszun, R., Hartl, F. U., and Flanagan, J. (1996). A zinc finger-like domain of the molecular chaperone DnaJ is involved in binding to denatured protein substrates. Embo J. *15*, 408-417.

Szabo, A., Langer, T., Schroder, H., Flanagan, J., Bukau, B., and Hartl, F. U. (1994). The ATP hydrolysis-dependent reaction cycle of the *E. coli* Hsp70 system DnaK, DnaJ, and GrpE. Proc. Natl. Acad. Sci. USA *91*, 10345-10349.

Tamm, L. K., and Bartoldus, I. (1990). Secondary structure of a mitochondrial signal peptide in lipid bilayer membranes. FEBS Lett. *272*, 29-33.

Theyssen, H., Schuster, H. P., Packschies, L., Bukau, B., and Reinstein, J. (1996). The second step of ATP binding to DnaK induces peptide release. J. Mol. Biol. *263*, 657-670.

Thompson, J. D., Higgins, D. G., and Gibson, T. J. (1994). CLUSTAL W: improving the sensitivity of progressive multiple sequence alignment through sequence weighting, position-specific gap penalties and weight matrix choice. Nucleic Acids Res. *22*, 4673-4680.

Todd, M. J., Lorimer, G. H., and Thirumalai, D. (1996). Chaperonin-facilitated protein folding: optimization of rate and yield by an iterative annealing mechanism. Proc. Natl. Acad. Sci. USA *93*, 4030-4035.

Tsugeki, R., and Nishimura, M. (1993). Interaction of homologues of Hsp70 and Cpn60 with ferredoxin-NADP+ reductase upon its import into chloroplasts. FEBS Lett. *320*, 198-202.

Tu, G. F., Reid, G. E., Zhang, J. G., Moritz, R. L., and Simpson, R. J. (1995). C-terminal extension of truncated recombinant proteins in *E. coli* with a 10Sa RNA decapeptide. J. Biol. Chem. *270*, 9322-9326.

Ungermann, C., Guiard, B., Neupert, W., and Cyr, D. M. (1996). The delta psi- and Hsp70/MIM44-dependent reaction cycle driving early steps of protein import into mitochondria. Embo J *15*, 735-44.

Ungermann, C., Neupert, W., and Cyr, D. M. (1994). The role of Hsp70 in conferring unidirectionality on protein translocation into mitochondria. Science *266*, 1250-1253.

van den Wijngaard, P. W., Dabney-Smith, C., Bruce, B. D., and Vredenberg, W. J. (1999). The mechanism of inactivation of a 50-pS envelope anion channel during chloroplast protein import. Biophys. J. *77*, 3156-3162.

van den Wijngaard, P. W., and Vredenberg, W. J. (1997). A 50-picosiemens anion channel of the chloroplast envelope is involved in chloroplast protein import. J. Biol. Chem. *272*, 29430-29433.

van den Wijngaard, P. W., and Vredenberg, W. J. (1999). The envelope anion channel involved in chloroplast protein import is associated with Tic110. J. Biol. Chem. *274*, 25201-25204.

van 't Hof, R., Demel, R. A., Keegstra, K., and de Kruijff, B. (1991). Lipid-peptide interactions between fragments of the transit peptide of ribulose-1,5-bisphosphate carboxylase/oxygenase and chloroplast membrane lipids. FEBS Lett. *291*, 350-354.

van't Hof, R., van Klompenburg, W., Pilon, M., Kozubek, A., de Korte-Kool, G., Demel, R. A., Weisbeek, P. J., and de Kruijff, B. (1993). The transit sequence mediates the specific interaction of the precursor of ferredoxin with chloroplast envelope membrane lipids. J. Biol. Chem. *268*, 4037-4042.

Vestweber, D., Brunner, J., Baker, A., and Schatz, G. (1989). A 42K outer-membrane protein is a component of the yeast mitochondrial protein import site. Nature *341*, 205-209.

Vestweber, D., and Schatz, G. (1988). A chimeric mitochondrial precursor protein with internal disulfide bridges blocks import of authentic precursors into mitochondria and allows quantitation of import sites. J. Cell Biol. *107*, 2037-2043.

Vogel, J. P., Misra, L. M., and Rose, M. D. (1990). Loss of BiP/GRP78 function blocks translocation of secretory proteins in yeast. J. Cell Biol. *110*, 1885-1895.

Voisine, C., Craig, E. A., Zufall, N., von Ahsen, O., Pfanner, N., and Voos, W. (1999). The protein import motor of mitochondria: unfolding and trapping of preproteins are distinct and separable functions of matrix Hsp70. Cell *97*, 565-574.

von Heijne, G. (1984). Analysis of the distribution of charged residues in the N-terminal region of signal sequences: implications for protein export in prokaryotic and eukaryotic cells. EMBO J. *3*, 2315-2318.

von Heijne, G. (1985). Signal sequences. The limits of variation. J. Mol. Biol. *184*, 99-105.

von Heijne, G., Hirai, T., Klösgen, R. B., Steppuhn, J., Bruce, B. D., Keegstra, K., and Herrmann, R. (1991). CHLPEP- A Database of Chloroplast Transit Peptides. Plant Mol. Biol. Rep. *9*, 104-126.

von Heijne, G., and Nishikawa, K. (1991). Chloroplast transit peptides: The perfect random coil? FEBS Lett. *278*, 1-3.

von Heijne, G., Steppuhn, J., and Herrmann, R. G. (1989). Domain structure of mitochondrial and chloroplast targeting peptides. Eur. J. Biochem. *180*, 535-545.

Voos, W., Gambill, B. D., Laloraya, S., Ang, D., Craig, E. A., and Pfanner, N. (1994). Mitochondrial GrpE is present in a complex with Hsp70 and preproteins in transit across membranes. Mol. Cell. Biol. *14*, 6627-6634.

Waegemann, K., Eichacker, S., and Soll, J. (1992). Outer Envelope Membranes from Chloroplasts Are Isolated as Right-Side-Out Vesicles. Planta *187*, 89-94.

Waegemann, K., Paulsen, H., and Soll, J. (1990). Translocation of proteins into isolated chloroplasts requires cytosolic factors to obtain import competence. FEBS Lett. *261*, 89-92.

Waegemann, K., and Soll, J. (1991). Characterization of the Protein Import Apparatus in Isolated Outer Envelopes of Chloroplasts. Plant J. *1*, 149-158.

Waegemann, K., and Soll, J. (1996). Phosphorylation of the transit sequence of chloroplast precursor proteins. J. Biol. Chem. *271*, 6545-6554.

Wall, D., Zylicz, M., and Georgopoulos, C. (1994). The NH2-terminal 108 amino acids of the *E. coli* DnaJ protein stimulate the ATPase activity of DnaK and are sufficient for lambda replication. J. Biol. Chem. *269*, 5446-5451.

Walsh, K. A., Ericsson, L. H., Parmelee, D. C., and Titani, K. (1981). Advances in protein sequencing. Ann. Rev. Biochem. *50*, 261-284.

Waters, M. G., Chirico, W. J., and Blobel, G. (1986). Protein translocation across the yeast microsomal membrane is stimulated by a soluble factor. J. Cell Biol. *103*, 2629-2636.

Wawrzynow, A., Banecki, B., and Zylicz, M. (1996). The Clp ATPases define a novel class of molecular chaperones. Mol. Microbiol. *21*, 895-899.

Wawrzynow, A., Wojtkowiak, D., Marszalek, J., Banecki, B., Jonsen, M., Graves, B., Georgopoulos, C., and Zylicz, M. (1995). The ClpX heat-shock protein of *E. coli*, the ATP-dependent substrate specificity component of the ClpP-ClpX protease, is a novel molecular chaperone. EMBO J. *14*, 1867-1877.

Weisbeek, P., Hageman, J., de Boer, D., Pilon, R., and Smeekens, S. (1989). Import of proteins into the chloroplast lumen. J. Cell Sci. Suppl. *11*, 199-223.

Westermann, B., Prip-Buus, C., Neupert, W., and Schwarz, E. (1995). The role of the GrpE homologue, Mge1p, in mediating protein import and protein folding in mitochondria. EMBO J. *14*, 3452-3460.

Wickner, S., Gottesman, S., Skowyra, D., Hoskins, J., McKenney, K., and Maurizi, M. R. (1994). A molecular chaperone, ClpA, functions like DnaK and DnaJ. Proc. Natl. Acad. Sci. USA. *91*, 12218-12222.

Wienhues, U., Becker, K., Schleyer, M., Guiard, B., Tropschug, M., Horwich, A. L., Pfanner, N., and Neupert, W. (1991). Protein folding causes an arrest of preprotein translocation into mitochondria in vivo. J. Cell Biol. *115*, 1601-1609.

Wienk, H. L., Czisch, M., and de Kruijff, B. (1999). The structural flexibility of the preferredoxin transit peptide. FEBS Lett. *453*, 318-326.

Wild, J., Altman, E., Yura, T., and Gross, C. A. (1992). DnaK and DnaJ Heat Shock Proteins Participate in Protein Export in *E. coli*. Gene Develop. *6*, 1165-1172.

Wu, C., Seibert, F. S., and Ko, K. (1994). Identification of chloroplast envelope proteins in close physical proximity to a partially translocated chimeric precursor protein. J. Biol. Chem. *269*, 32264-32271.

Zhang, X. P., Elofsson, A., Andreu, D., and Glaser, E. (1999). Interaction of mitochondrial presequences with DnaK and mitochondrial Hsp70. J. Mol. Biol. *288*, 177-190.

Zhu, X., Zhao, X., Burkholder, W. F., Gragerov, A., Ogata, C. M., Gottesman, M. E., and Hendrickson, W. A. (1996). Structural analysis of substrate binding by the molecular chaperone DnaK. Science *272*, 1606-1614.

Ziegelhoffer, T., Lopezbuesa, P., and Craig, E. A. (1995). The Dissociation Of Atp From Hsp70 Of Saccharomyces-Cerevisiae Is Stimulated By Both Ydj1p and Peptide-Substrates. J. Biol. Chem. *270*, 10412-10419.

Ziegelhoffer, T., Lopez-Buesa, P., and Craig, E. A. (1995). The dissociation of ATP from Hsp70 of Saccharomyces cerevisiae is stimulated by both Ydj1p and peptide substrates. J. Biol. Chem. *270*, 10412-10419.

Zylicz, M., and Georgopoulos, C. (1984). Purification and properties of the *E. coli* DnaK replication protein. J. Biol. Chem. *259*, 8820-8825.

Zylicz, M., LeBowitz, J. H., McMacken, R., and Georgopoulos, C. (1983). The DnaK protein of *E. coli* possesses an ATPase and autophosphorylating activity and is essential in an in vitro DNA replication system. Proc. Natl. Acad. Sci. USA *80*, 6431-6435.

VITA

Robert Alvin Ivey, III, was born in Columbia, South Carolina, on July 2, 1970. He attended Pelion High School, graduating Valedictorian in 1988. He matriculated to Clemson University in August of that year, where he majored in Biochemistry and conducted research under the mentorship of Dr. Jessup Shively. While attending Clemson University, Robert completed the Cooperative Education Program, working for two years at International Bio-Synthetics, Inc., under the tutelage of Jacque Dekker, Carl Miller, and Marsha Cummings. Robert was married to Shannon Rebecca Mellichamp Ivey in August, 1992, and was awarded his Bachelor of Science degree in May, 1993. After entering the Biochemistry Department at the University of Tennessee, Knoxville, in August of that year, Robert entered the laboratory of Dr. Barry Bruce. He completed the requirements for the Doctorate of Philosophy degree, with a major in Biochemistry, in May, 2000, and graduated in August of that year.